Dissertation

submitted to the
Combined Faculties for the Natural Sciences and for Mathematics
of the Ruperto-Carola University of Heidelberg, Germany
for the degree of
Doctor of Natural Sciences

Presented by

Diplom-Biotechnology Daria Vokhminova
born in Moscow, Russian Federation
Oral-examination 10.11.10

Regulation of MHC class I polypeptide related sequence B expression in melanoma cells under proteasome inhibition

Referees: Prof. Dr. Viktor Umansky

PD Dr. Annette Paschen

Content

1 Summary

1.1 English Summary

Malignant melanoma is a very aggressive tumor with a high metastatic potential and persistently increasing incidence rate. The low efficacy of conventional chemotherapy and radiation demands for the development of new approaches. Several new strategies take advantage of the strong intrinsic immunogenicity of the tumor that in principle allows autologous Natural killer (NK) cells and T cells to recognize and kill melanoma cells. One of the key receptors involved in the anti-tumor immunity is NKG2D, expressed on NK cells and CD8+ T cells. So far, eight surface ligands for this receptor have been identified in humans, belonging to the MIC and ULBP molecule families. Interaction of NKG2D with its surface ligands activates and costimulates the cytotoxic activity of NK cells and T cells, respectively. Expression of NKG2D ligands (NKG2DL) is known to be induced upon cell stress and moderate expression of NKG2DL can also be observed on tumor cells. Thus developing strategies that induce NKG2DL expression on tumor cells might be helpful to enhance anti-tumor immune responses, but as a prerequisite the mechanisms of NKG2DL regulation have to be elucidated.

Proteasome inhibition causes so-called proteotoxic stress by an accumulation of unfolded proteins in the cell. As proteasome inhibitors are currently tested in melanoma therapy, the aim of the present study was to identify the impact of proteasome inhibition on NKG2DL expression in human melanoma cells. It was observed that treatment with the proteasome inhibitor MG132 strongly up-regulated the surface expression of the NKG2DL MICB on melanoma cells. Inhibitor treated cells contained elevated levels of MICB mRNA. MICB promoter driven luciferase reporter gene assays demonstrated that this up-regulation was dependent on transcription. Mutation of a heat shock factor 1 (HSF1) binding site within the MICB promoter region abrogated induction of transcription by MG132. Indeed, an enhanced binding of HSF1 to the MICB promoter in MG132 treated cells was demonstrated by chromatin immunoprecipitation (ChIP). Moreover, transfection of melanoma cells with a constitutively active HSF1 variant strongly stimulated MICB promoter driven reporter gene expression, whereas siRNA-mediated down-regulation of HSF1 blocked MICB induction upon proteasome inhibition.

Interestingly, while over-expression of constitutive active HSF1 in the melanoma cells stimulated MICB promoter driven reporter gene expression, it did not enhance the transcription of endogenous MICB in melanoma cells, suggesting that under “normal

conditions" HSF1 could not efficiently access the MICB promoter. Ubiquitination of histone H2A is known as an epigenetic mechanism of gene silencing. ChIP experiments demonstrated that ubiquitinated histone H2A is associated with the MICB promoter and that treatment of melanoma cells with MG132 resulted in a loss of H2A ubiquitination. This leads to the conclusion that proteasome inhibition elicits MICB expression by two events: down-regulation of the ubiquitination level of H2A, which controls promoter accessibility, and activation of HSF1 which then binds the MICB promoter and induces its transcription.

1.2 Deutsche Zusammenfassung

Das maligne Melanom ist ein sehr aggressiver Tumor mit hohem Potential zur Metastasierung und stetig steigender Inzidenz. Die geringe Effizienz konventioneller Chemo- und Strahlentherapien verlangt nach der Entwicklung alternativer Behandlungsstrategien. Verschiedene neue Ansätze machen sich die hohe intrinsiche Immunogenität des Tumors zu Nutze, die es autologen Natürlichen Killer (NK) Zellen und T Zellen in Prinzip erlaubt, Melanomzellen zu erkennen und zu töten. Ein “Schüssel”-Rezeptor in der anti-Tumor Immunität ist NKG2D, der auf NK Zellen und CD8+ T Zellen exprimiert wird. Bislang wurden acht Oberflächenliganden dieses Rezeptors im Menschen identifiziert, die zur Familie der MIC oder ULBP Familie gehören. Die Interaktion von NKG2D mit seinen Oberflächenliganden aktiviert bzw. kostimuliert die zytotoxische Aktivität von NK Zellen und T Zellen. Die Expression von NKG2D Liganden (NKG2DL) wird bekanntermaßen durch Zellstress induziert und eine moderate NKG2DL Expression kann auch auf Tumorzellen beobachtet werden. Folglich könnten Strategien, welche die Expression der Liganden auf Tumorzellen induzieren, hilfreich sein, um anti-Tumor Immunantworten zu verstärken. Als Voraussetzung hierfür müssen jedoch die Mechanismen der NKG2DL Regulation aufgeklärt werden.

Die Inhibition des Proteasoms verursacht durch die Akkumulation von ungefalteten Proteinen sogenannten proteotoxischen Stress in der Zelle. Da Proteasominhibitoren derzeit in der Melanomtherapie getestet werden, war das Ziel der vorliegenden Arbeit den Einfluss der Proteasominhibition auf die NKG2DL Expression in humanen Melanomzellen zu untersuchen. Es wurde beobachtet, dass die Behandlung mit dem Proteasominhibitor MG132 zu einer starken Hochregulation der Oberflächenexpression des Liganden MICB auf Melanomzellen führte. Inhibitor behandelte Zellen enthielten erhöhte Mengen an MICB mRNA. MICB promoter-getriebene Luziferase-Reportergen Analysen ergaben, dass die Hochregulation in Abhängigkeit von der Transkription erfolgte. Durch die Mutation einer Hitzeschock Faktor 1 (HSF1) Bindungsstelle in der MICB Promoterregion wurde die Induktion der Transkription durch MG132 aufgehoben. Tatsächlich konnte eine verstärkte Bindung von HSF1 an den MICB Promoter in MG132 behandelten Zellen mittels Chromatin-Immunpräzipitation (ChIP) nachgewiesen werden. Zudem führte die Transfektion von Melanomzellen mit einer konstitutiv aktiven HSF1 Variante zur einer starken Stimulierung der MICB Promoter-getriebenen Reportergen Expression, wohingegen durch die siRNA-vermittelte Herabregulation von HSF1 die MICB Induktion unter Inhibition des Proteasoms aufgehoben wurde.

Während die Überexpression von konstitutiv aktivem HSF1 in Melanomzellen die ICB Promoter-getriebene Reportergen Expression stimuliert, konnte keine verstärkte Transkription von endogenem MICB in Melanomzellen beobachtet werden. Dies führte zu der Annahme, dass unter “normalen Bedingungen” ein effizienter Zugang von HSF1 zum MICB Promoter nicht möglich ist. Die Ubiquitinierung von Histon H2A ist bekannt als ein epigenetischer Mechanismus, der Gene abschaltet. ChIP Experimente zeigten, dass ubiquitiniertes Histon H2A mit dem MICB Promotor assoziiert ist und dass die Behandlung von Melanomzellen mit MG132 zu einem Verlust der H2A Ubiquitinierung führte. Dies führt zu der Schlussfolgerung, dass die Inhibition des Proteasoms die Expression von MICB über zwei Ereignisse steuert: die Herabregulation des Ubiquitinierung von H2A, welche den Zugang zum Promoter kontrolliert, und die Aktivierung von HSF1, welches dann an den MICB Promotor bindet und die Transkription induziert.

2 Introduction

2.1 Melanoma epidemiology and conventional treatment strategies

Malignant melanoma is a very aggressive metastatic tumor originating from melanocytes, the cells that produce the pigment melanin that colors skin, hair and eyes. Melanoma incidence has been growing rapidly in the last decades (Lee, 2010). The tumor is characterized by a high metastatic potential and according to Quintana et al. even a single melanoma cell is able to form a tumor in NOD/SCID mice (Quintana et al., 2008). The 5-year survival rate for patients with resectable melanoma is nearly 100 %. However, for patients diagnosed with advanced disease involving distant metastases only 10–15% can overcome the 5 year-survival (Agarwala et al., 2010). Treatment options for such patients are few and mostly ineffective. Although, most patients receive systemic chemotherapy for metastatic disease, no therapeutic regimen has been shown to prolong survival in large, randomized, phase III trials. Dacarbazine (DTIC) treatment induces partial response rates of 10–13 % and complete responses of only 5 %. It has been used as a single-agent chemotherapy treatment for advanced melanoma for over 20 years (Eigentler et al., 2003). Temozolomide (TMZ), a functional analogue of DTIC, is well tolerated and is capable to penetrate into the central nervous system, which is essential for patients with brain metastases. However TMZ shows response and survival rates equivalent to DITC (Danson et al., 2003). The generally poor efficacy of all current single-agent chemotherapeutic approaches prompted numerous new studies encompassing combinations of chemotherapy, biochemotherapy and tumor specific immunological therapy (Eigentler et al., 2003; Gogas et al., 2007).

2.2 Oncogenic signaling and targeted therapies in melanoma

Significant attention has recently been focused on the development of targeted therapies that aim to selectively shut down the aberrant signaling pathways caused by genetic alterations that promote tumor formation, proliferation and therapy resistance. A number of mutations causing or accompanying melanoma development have been described (Chin et al., 2006; Haluska et al., 2006; Dahl and Guldberg, 2007; Hocker et al., 2008). Mutations in the RAS-RAF-MEK-ERK signaling pathway are common for melanoma (Fig. 1). Of the tumors, 20 % show activating mutations in NRAS, a GTPase and upstream member of the mitogen activated protein kinase (MAPK) signaling pathway, which can also stimulate the phosphatidylinosytol 3-kinase (PI3K) signaling pathway. The most common mutation found in about 70 % of malignant melanoma is a single amino acid substitution (V600E) in the B-

RAF proto-oncogene, a serine/threonine-protein kinase, the downstream effector of RAS that activates the MEK kinase, which in turn activates ERK. Although, the targeting of the RAS-RAF-MEK-ERK signaling pathway *in vitro* led to significant reduction of cell proliferation, *in vivo* experiments did not yield rewarding results (Panka et al., 2006).

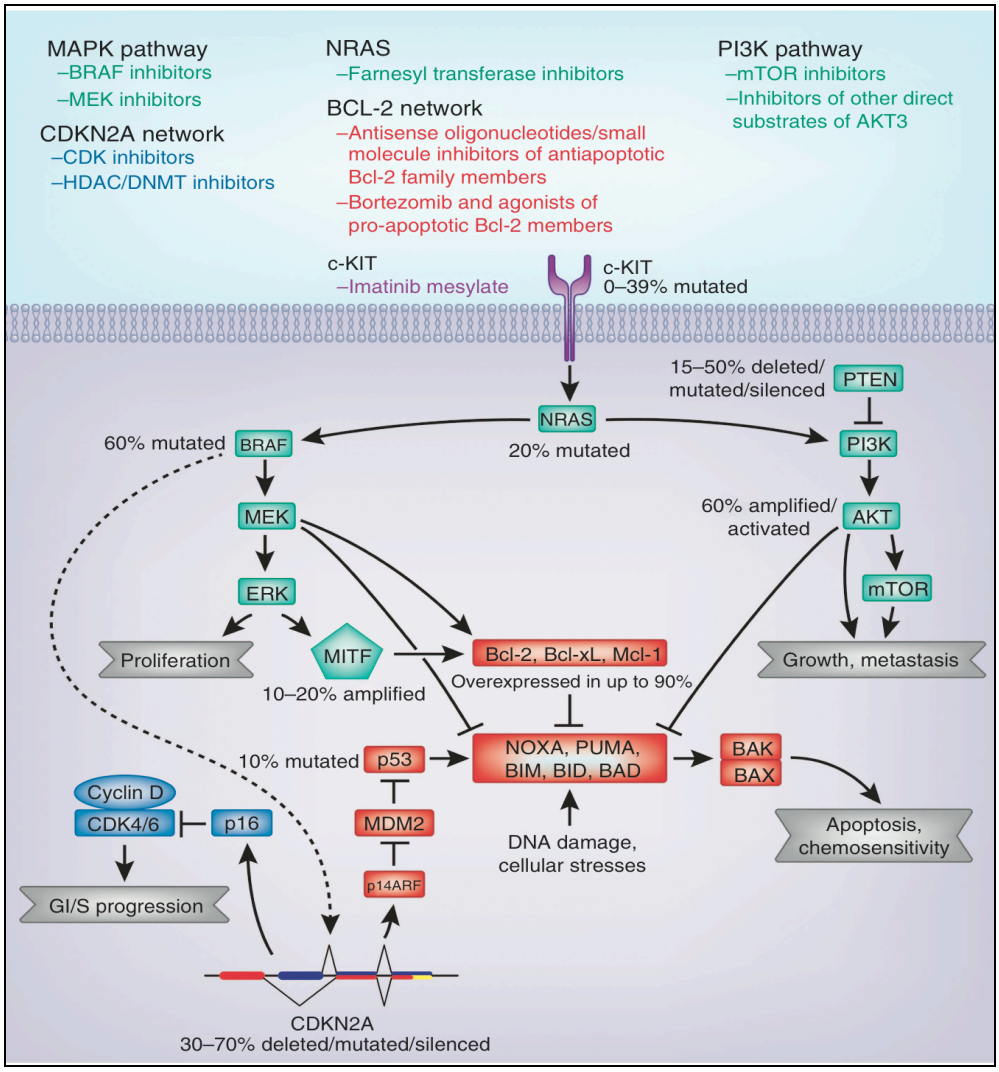

Figure 1. Melanoma signaling networks

Simplified presentation of three of the major genetic networks involved in melanoma tumorogenesis, survival, and senescence. Included in the NRAS signaling network (green) are the MAPK and the PI3K/AKT pathways, which have been implicated in melanoma proliferation, survival, and progression. The CDKN2A locus encodes two separate tumor suppressors, p16 and p14ARF; both are thought to contribute to senescence and tumor growth restriction. The p53/Bcl-2 signaling network (red) is a major contributor to melanoma apoptosis and chemosensitivity and is regulated by many of the oncogenic melanoma pathways. Shown at the top of the figure are selected therapeutic agents that target each of these genetic networks (obtained from Hocker et al., 2008).

Interestingly, the BRAF V600E mutation has been found frequently in benign and dysplastic nevi suggesting that this mutation represents an early event in melanocytic

neoplasia and alone is not sufficient for tumor formation. Thus, the full oncogenic potential depends on the presence of additional mutations leading to p53 inactivation or PTEN, INK4A deletion. MAPK signaling pathway has been found to be altered in about 90 % of melanoma, pointing out its essential role in melanocyte transformation (Bloethner et al., 2005; Chin et al., 2006).

The PI3K-AKT signaling pathway has been shown to be changed in up to 50 – 60 % of malignant melanoma (Aziz et al., 2007). It can be activated upstream by constitutively active NRAS, c-KIT or via inactivation of PTEN, which is known to block AKT activation (Fig. 1). The PI3K signaling pathway primarily acts via activation of the AKT kinase. Once activated, AKT has several different substrates, including Mdm2, procaspase 9, NF-κB, mammalian target of rapamycin (mTOR), and p27, many of which contribute to tumor proliferation and survival (Hocker et al., 2008).

For malignant transformation alterations of genes the products of which are involved in pathways controlling cell cycle and senescence such as $p16^{INK4A}$ and $p14^{ARF}$, both encoded by the major human melanoma genetic susceptibility locus CDKN2A via alternative reading frames, seem to be essential (Mooi and Peeper, 2006). Somatic alterations in cell cycle inhibitor genes in melanoma and some other tumors include mutations, homozygous deletions and promoter methylation. Germ-line mutations in the CDKN2A gene have been found to predispose carriers in melanoma-prone families to an increased risk of pancreatic cancer (Bloethner et al., 2006).

Inhibition of overlapping pathways by small therapeutic inhibitors, such as the MAPK and PI3K-AKT signaling pathway, might be a promising strategy for melanoma treatment (Molhoek et al., 2005; Meier et al., 2007). Besides, also inhibitors of the proteasome, the major proteolytic machinery of the cell, are currently tested for their therapeutic capacity in tumor patients. Due to their high protein turnover, survival and growth of the tumor cells are essentially dependent on the activity of the proteasome (see below).

2.3 The ubiquitin-proteasome system

In living cells a huge number of proteins have to be synthesized, processed and degraded to maintain the normal function of the cell. Protein degradation occurs in different cellular compartments such as the cytosol, lysosome and endoplasmic reticulum. The majority of cytosolic protein degradation in eukaryotes is performed via the ubiquitin-proteasome system (UPS). The proteasome is a giant cytosolic protease located in the cytoplasm and

nucleus of eukaryotic cells. For proteasome-dependent degradation proteins are tagged by multimers of an evolutionarily conserved protein known as ubiquitin (Nandi et al., 2006).

The functionally active 26S proteasome consists of a 20S core catalytic cylindrical complex capped at both ends by 19S regulatory subunits (Fig. 2). The 20S core proteasome is a complex of 28 protein subunits that are organized into four stacked rings and a cylindrical structure. The top and bottom rings of the 20S proteasome are formed by seven polypeptides, termed α-subunits. The two inner rings consist of seven β-subunits that form a central groove, which contains enzymatically active sites of the proteasome complex. Three (β1, β2 and β5) of the seven β-subunits have enzymatic activities, which have been characterized as chymotrypsin-like, trypsin-like and post-glutamyl peptidyl hydrolytic-like activities (Unno et al., 2002). A complex network of allosteric interactions regulates the sequence of enzymatic activities within the proteasome, which ultimately yields oligopeptides. The proteasome identifies proteins that have been targeted for degradation by their polyubiquitin “tag”, although ubiquitination is not a prerequisite for degradation of every protein (Pickart and Cohen, 2004). The 26S proteasome degrades proteins in an ATP-dependent manner. ATP hydrolysis is needed both for the formation of the 26S complex and for the unfolding and linearizing of large proteins to facilitate their entry into the catalytic inner core of the proteasome (Adams, 2004).

The UPS plays a key role in protein destruction, but it is also directly or indirectly implicated in many important cellular processes such as cell cycle control, DNA repair, regulation of transcription, signal transduction, antigen presentation, stress responses and apoptosis (Fig. 2; Adams et al., 2004). The UPS is known to control cell cycle progression via turnover of cyclins, ubiquitinated short lived regulators of cyclin-dependent kinase complexes. The UPS is also involved in the DNA damage response pathway by influencing p53 protein stability. The negative regulator of p53 MDM2 is an ubiquitin-ligase, which ubiquitinates p53, targeting it for the degradation by proteasome. Another important aspect of proteasome function, related to the immune system, is the generation of peptides upon protein degradation, which are further processed by cytoplasmic and ER-resident peptidases and loaded into MHC class I molecules for presentation on the cell surface (Borissenko and Groll, 2007).

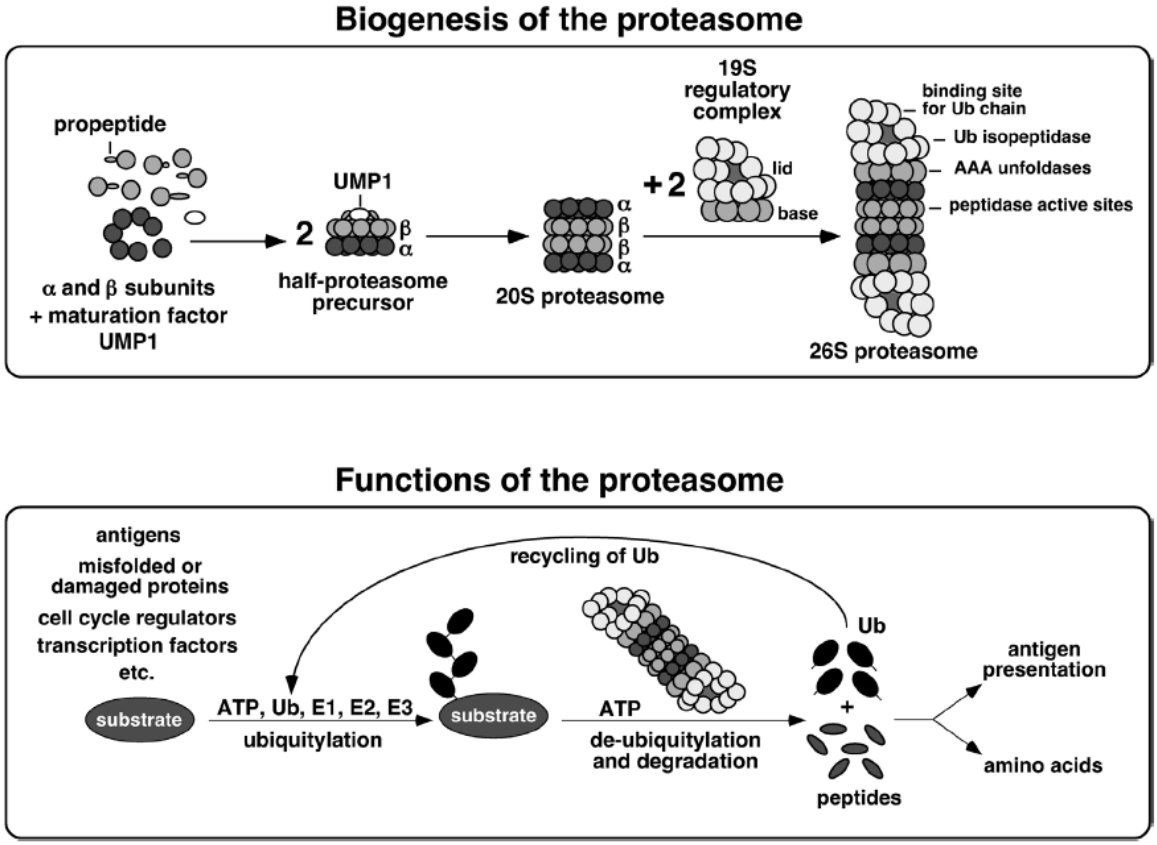

Figure 2. Proteasome biogenesis and function

Upper line: The seven α-subunits and seven β-subunits are assembled in one half-proteasome precursor. Dimerization of two precursor complexes leads to the formation of the 20S proteasome assisted by UMP1 a dedicated chaperone, which function is to "underpin the maturation of the proteasome" and is later degraded by the proteasome. To finalize the proteasome assembly the 19S lid is attached to the top and bottom of the 20S complex, forming the fully functional proteolytic complex.

Bottom line: Substrates dedicated to digestion such as misfolded, unfolded or damaged proteins, short lived proteins, undergo polyubiquitination interacting with ubiquitin ligases (E1-3), are degraded by the proteasome to small peptides and further processed for the presentation by MHC class I molecules or cut into amino acids for reuse in protein synthesis (obtained from Dohment R.J., Inst. for Genetics, University of Cologne).

2.4 Proteasome inhibitors in tumor therapy

Proteasome inhibitors originally used for the study of proteasome function appear to be cytotoxic for rapidly proliferating cells e.g. tumor cells, while less affecting quiescent cells. A possible explanation for this phenomenon could be that malignant cells due to their high proliferation rate accumulate damaged proteins, and therefore show a higher dependency on the proteasomal degradation processes (Almond and Cohen, 2002). Proteasome inhibitors tested *in vitro* on multiple myeloma, breast cancer and melanoma cells increased cell death (Chauhan et al., 2005; Ames et al., 2008; Młynarczuk-Biały et al., 2006; Lecis et al., 2010).

Nowadays proteasome inhibitors are intensively tested in the clinic in anti-cancer therapy either as monotherapy or in combination with other chemotherapeutic agents. Recently, the proteasome inhibitor bortezomib/PS-431 (Velcade) has been approved by the U.S. Food and Drug Administration (FDA) for the treatment of relapsed/refractory multiple myeloma. The mechanism of bortezomib action is still under the investigation, but it is known that bortezomib induces apoptosis in multiple myeloma cells via a number of different mechanisms (Chauhan et al., 2005; Obeng et al., 2006). *In vitro* studies have demonstrated that bortezomib attenuates NF-κB prosurvival activity by blocking proteasome degradation of IκB, an inhibitory subunit of the inactive NF-κB complex. Bortezomib-induced apoptosis has also been shown to be associated with following additional events: activation of stress response proteins such as heat shock proteins Hsp27, Hsp70, and Hsp90; up-regulation of the c-jun kinase; alteration of the mitochondrial membrane potential and production of reactive oxygen species; induction of the intrinsic cell death pathway and activation of extrinsic apoptotic signaling; impairment of the DNA repair machinery via inactivation of the DNA-dependent protein kinase; and down-regulation of mitogen-activated protein kinase and PI3K/Akt signaling pathways; phosphorylation and activation of p53. Taken together, these signaling events may collectively contribute to the overall anti-multiple myeloma activity of bortezomib against multiple myeloma (Chauhan et al., 2005).

In contrast to hematological malignancies, treatment of solid tumors with proteasome inhibitors as monotherapy was less successful, although *in vitro* tests showed promising results. bortezomib has been applied to non-small cell lung cancer and breast cancer patients in combination with other chemotherapeutical agents to sensitize tumor cells toward chemotherapeutic drugs (Lara et at., 2006; Ames et al., 2008). For melanoma, treatment with the combination of paclitaxel, carboplatin and proteasome inhibitor bortezomib showed limited efficacy in a phase II trial (Croghan et al., 2010). So far, proteasome inhibitors have only been considered as drugs to induce apoptosis. However, along with the inhibition of tumor cell proliferation may sensitize the cancer cells to the NK-mediated elimination, as demonstrated for multiple myeloma and hepatocellular carcinoma cells (Armeanu et al., 2008). Furthermore, *in vitro* treatment of melanoma cells with proteasome inhibitors has been demonstrated to increase the sensitivity of tumor cells to adoptive T-cell attack (Seeger et al., 2010). The immunological effects of proteasome inhibition might be exploited by immunotherapy.

2.5 Immunotherapy of malignant melanoma

Immunotherapy of malignant melanoma is aimed at increasing of the effectiveness of anti-tumor immune responses by a number of different approaches such as vaccination or adoptive cell transfer. However, strategies dedicated to abrogate immune-suppression are followed such as the therapy with monoclonal antibodies targeting the cytotoxic T-lymphocyte antigen 4 (CTLA-4), a molecule triggering T cell tolerance (Schadendorf et al., 2009).

During the last decade a number of melanoma vaccines have been developed based on the growing body of knowledge of tumor antigens and their peptide epitopes. So far, two main directions in therapeutic vaccination have been followed: vaccination with peptides and peptide-loaded dendritic cells. Unfortunately, these vaccination strategies have been shown to be ineffective in patients with distant metastatic melanoma (Schadendorf et al., 2009).

Adoptive cell transfer (ACT) exploits the observation that melanoma cells can be effectively recognized and eliminated by antigen-specific $CD8^+$ T cells. Over the last two decades a number of melanoma-associated T cell antigens have been identified. Via their T cell receptor $CD8^+$ T cells recognize peptide epitopes derived from these antigens in the complex with MHC class I molecules. The ACT approach is based on the *ex vivo* activation and expansion of autologous T lymphocytes and their re-infusion back to the patient (Yee et al., 2002; Dudley et al., 2002; Straten and Becker, 2009). Recently, ACT therapies based on the adoptive transfer of Melan-A/MART-1 or gp100 antigen-specific $CD8^+$ T cell clones obtained from peripheral blood of melanoma patients, have been tested (Khammari et al., 2009; Mackensen et al., 2006). In contrast to chemotherapy, ACT is well tolerated and the main adverse effects were mainly related to the injection of cytokines applied under the therapy. Significant clinical efficacy and diminished side effects make the ACT one of the most promising strategies in the melanoma therapy emerging recently (Straten and Becker, 2009). However, a main obstacle that may interfere with efficient melanoma cell recognition and eradication is the development of tumor immune escape variants. Down-regulation or complete loss of surface MHC class I molecules is a well-known mechanism of tumor cells to escape the MHC restricted T cell surveillance (Paschen et al., 2006). Nevertheless, such cells should still be recognized and eliminated by the innate immune system in particular by Natural Killer (NK) cells, as described below. Recently, some studies utilizing NK cells for metastatic melanoma treatment have been started (Burke et al., 2010).

2.6 NK cells and their receptors

Natural killer (NK) cells are lymphocytes of the innate immune system comprising about 10% of the peripheral blood lymphocytes. They monitor autologous cells for an aberrant expression of surface MHC class I molecules or stress markers. MHC class I positive "healthy" autologous cells are protected from NK cytotoxicity.

NK cells are characterized by a strong cytolytic activity against virus-infected cells and malignant cells. Upon activation NK cells can display an immunomodulating action via the production of cytokines such as TNF-α and IFN-γ or can directly kill target cells by releasing perforines and granzymes (Bryceson et al., 2006). The cytolytic activity of NK cells is tightly regulated by the balance of signals received from inhibitory and activating receptors. The NK inhibitory receptors fall into two main groups according to their structure and consist of immunoglobulin superfamily receptors including killer-cell immunoglobulin like receptors (KIR) and C-type lectin-domain receptors. Inhibitory receptors are sensors of "normal homeostasis" and bind to classical and non-classical MHC class I molecules (Vivier and Malissen, 2005), which in turn prevents the killing of normal cells. The down-regulation or the lack of MHC class I molecules on the target cell surface can serve as a signal of NK cell activation and is described by the "missing self" theory (Ljunggren et al., 1990). Recently it has been shown that for complete activation NK cells have to receive activating signals by receptors binding to corresponding surface ligands on the target cell (Mistry and O'Callaghan, 2007). Activating receptors expressed on NK cells are structurally related to the inhibitory KIR and C-type lectin-domain receptor families, but there are also many unrelated receptors such as the natural cytotoxicity receptor family. The ligands for activating NK receptors are commonly not expressed by normal cells. Viral infection, or malignant transformation, or the presence of other stress conditions can lead to the up-regulation of activating ligands on the cell surface that renders them susceptible to NK cell-mediated lysis as described by the "altered self or stressed self" theory (Malarkannan, 2006). The inhibitory and activatory NK cell receptors discovered so far and their ligands are listed in Table 1 (Empson et al., 2010).

One of the most well studied activating NK receptors is Natural-killer group 2, member D (NKG2D), which is known to be a key receptor in anti-tumor immunity. NKG2D is a dimeric, type II transmembrane protein, which in humans is constitutively expressed by natural killer (NK) cells, most NKT cells, subsets of γδ T cells, all $CD8^+$ T cells, and a subset of $CD4^+$ T cells (Champsaur and Lanier, 2010). This receptor directly activates NK cells and acts as a co-stimulatory receptor for T cells. The signaling activity of human NKG2D is

mediated through an exclusive interaction with the adaptor protein DAP10 (Coudert and Held, 2006).

Inhibitory receptors	*Ligands*
CEACAM1	CEACAM1
IRp60 (CD300a)	Unknown
KIR2DL1 (CD158a)	HLA-C group 2
KIR2DL2/3 (CD158b)	HLA-C group 1
KIR2DL5	Unknown
KIR3DL1	HLA-B alleles and Bw4
KIR3DL2	HLA-A alleles
KLRG1/MAFA	E/N/P-cadherin
NKG2A (CD94/CD159a)	HLA-E
NKR-P1A (CD161)	LLT1
LAIR1	Collagen
LIR-1/IL-T2 (CD85j)	Multiple HLA class I
Siglec-7 (CD328)	Sialic acid
Siglec-9 (CD329)	Sialic acid

Activating receptors	*Ligands*
2B4 (CD244)	CD48
BY55 (CD160)	HLA-C
CD2	LFA-3 (CD58)
CD7	SECTM1, Galectin
CD11c/18	ICAM-1, iC3b
CD16 (FcgRIIIA)	IgG
CD44	Hyaluronan
CD59	C8, C9
CRACC (CD319)	CRACC (CD319)
DNAM-1 (CD226)	PVR (CD155), CD112
KIR2DL4 (CD158d)	HLA-G (soluble)
KIR2DS1-2	HLA-C (low affinity)
KIR2DS3-6	Unknown
KIR3DS1	Unknown
LFA-1 (αLβ2, CD11a/18)	ICAM-1-5
MAC-1 (αMβ2, CD11b/18)	ICAM-1, iC3b, fibrinogen
NKG2C (CD94/159c)	HLA-E
NKG2D (CD314)	ULBPs, MICA, MICB
NKp30 (CD337)	BAT-3
NKG2E	HLA-E
NKp44	Viral hemaglutinin
NKp46 (CD335)	Viral hemaglutinin
NTBA	NTBA
VLA-4 (α4β1, CD49d/29)	VCAM-1, fibronectin
VLA-5 (α5β1, CD49e/29)	Fibronectin

Table 1. Inhibitory and activating NK cell receptors and their ligands

(Adapted from Empson et al., 2010)

2.6.1 The role of NKG2D and NKG2D ligands in tumor immune surveillance

The critical role of NKG2D in the tumor surveillance has been shown in different mouse tumor models. For example, mice inoculated with MHC class I positive RMA lymphoma cells developed tumors while mice transplanted with RMA cells, recombinantly expressing the murine NKG2D ligand Rae-1 did not show tumor formation (Cerwenka et al., 2001). The significance of NKG2D in early tumor immune surveillance has recently been demonstrated by Guerra et al. in the NKG2D-deficient mouse model (*Klrk1*$^{-/-}$) (Guerra et al., 2008). These mice do not show any disturbances in the embryonic development and exhibit no visible alterations in major organs. *Klrk1*$^{-/-}$ mice were further interbred with the well characterized mouse prostate adenocarcinoma model (TRAMP) in order to study the influence of the NKG2D knock-down on tumor development. The TRAMP-mice get mild to severe prostate hyperplasia by 12 weeks of age developing to the severe hyperplasia and adenocarcinoma by 18 weeks of age and metastatic disease by 30 weeks of age. NKG2D-deficient TRAMP mice (*Klrk1*$^{-/-}$ TRAMP) displayed early-arising, massive prostate tumors progressing rapidly to poorly differentiated lesions, while their NKG2D positive littermates (*Klrk1*$^{+/+}$ TRAMP) mostly developed late-arising carcinomas, which were classified as phylloides-like tumors, a

non malignant epithelial-stromal tumor. Moreover, early-arising large tumors in NKG2D$^{-/-}$ mice showed substantially higher amounts of NKG2D ligand transcripts and ligand surface expression as compared to large early-arising tumors of NKG2D$^{+/+}$ littermates, suggesting that NKG2D-dependent immunoediting can favor loss of NKG2D ligands at the early stages of malignant tumors formation and disease aggressiveness. In case transgenic mice developing mixed pre-B and B-lymphomas (Eμ-myc mice) were inbred with NKG2D$^{-/-}$ (*Klrk1*$^{-/-}$) mice, the onset of the disease occurred significantly earlier in the B6-*Klrk1*$^{-/-}$Eμ-myc mice than in B6-*Klrk1*$^{+/+}$Eμ-myc mice, suggesting that NKG2D deficiency accelerates the progression of Eμ-myc driven lymphomas (Guerra et al., 2008).

A.

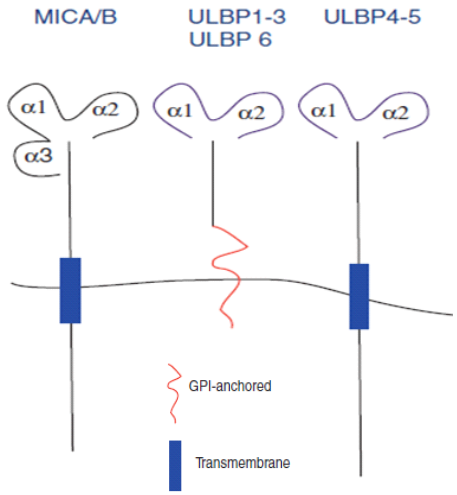

B.

Name	Alternate name	NKG2D affinity (K_D)	Chromosome
MICA	PERB11.1	0.6-1 x 10-7 M	6q21.3
MICB	PERB11.2	0.8 x 10^{-6} M	6q21.3
ULBP1	RAET1I	1.1 x 10^{-6} M	6q25
ULBP2	RAET1H	ND	6q25
ULBP3	RAET1N	ND	6q25
ULBP4	RAET1E, LETAL	ND	6q24.3
ULBP5	RAET1G	low	6q24.1-25.1
ULBP6	RAET1L	ND	6q24.2-25.3

Figure 3. Structures and affinities of human NKG2D ligands

A. MICA and MICB are the only NKG2DL known to contain a α3-like domain, similar to classical MHC class I molecules, while all other ligands contain only α1 and α2 domains. NKG2DL can either be transmembrane proteins or GPI-anchored proteins.

B. The affinities are expressed as the equilibrium dissociation constant (K_D) and given for interactions between NKG2D receptor and ligands of the same species (adapted from Champsaur and Lanier, 2010).

In humans eight ligands for the NKG2D receptor have been identified, which have a structure similar to classical MHC class I molecules (Fig.3). They fall into two families: the MHC class I chain related sequence A and B (MICA and MICB) group and the cytomegalovirus UL-16 binding protein (ULBP1 – 6) family (Champsaur and Lanier, 2010). All NKG2D ligands (NKG2DL) show structural similarity in their α1 and α2 extracellular domains to those of classical MHC class I molecules. However, the differences between the

two groups of NKG2DLs are rather significant. MICA and MICB are transmembrane proteins consisting of three extracellular domains, while ULBP molecules have two extracellular domains and are GPI-anchored in the cell membrane, except for ULBP4 and 5, which have been described to be transmembrane proteins (Mistry and O'Callaghan, 2007; Champsaur and Lanier, 2010).

NKG2DL are highly polymorphic, particularly the MICA and MICB genes of which 70 and 31 alleles have been described, respectively. In the last decade growing interest has been displayed to the regulation of NKG2DL expression. It has been demonstrated that viral infection induces expression of NKG2DL on the cell surface. Viral products could directly affect the transcription of NKG2DL or infection could indirectly promote ligand expression through the induction of cytokines. On the other hand, viruses such as human and mouse cytomegalovirus, HCMV and MCMV, respectively, evolved numerous mechanisms to evade NK cell recognition and in particular NKG2D-mediated immune surveillance via retention of activating ligands in the virus-infected cell (Champsaur and Lanier, 2010).

Numerous studies revealed NKG2DL expression by different human tumor cell lines and freshly extracted primary tumors and demonstrated that expression of NKG2DL on tumors renders them susceptible to killing by NK cells *in vitro*. Although, surface expression of NKG2DL has been detected on a wide variety of tumors, the profile of the expressed molecules has been reported to be various. Jinushi et al. detected MICA and MICB expression on a subset of human hepatocellular carcinoma tissues. They also found that MIC molecules are involved in hepatoma cell sensitivity to NK cells (Jinushi[1] et al., 2003). Hematological tumors such as different types of leukemia, including acute myeloid leukemia (AML), acute lymphatic leukemia (ALL), chronic myeloid leukemia (CML), and chronic lymphatic leukemia (CLL) have been shown to express heterogeneous levels both MIC and ULBP molecules, though a predominant expression of ULBP2 has been reported (Pende et al., 2002). Salih et al. demonstrated that expression of NKG2DL accounted for the NK cell-mediated lysis of AML and CML cells (Salih et al., 2003).

2.6.2 Regulation of NKG2D ligand expression

NKG2DL are rarely expressed on the surface of normal healthy cells (Eagle et al., 2009) and their expression is associated with cellular stress caused among others by tumorogenesis, though the transforming activity of tumor oncogenes like N-ras, c-myc, Akt, c-kit or their combinations, was not found to directly force NKG2DL expression (Nausch and Cerwenka, 2008). At present, several stresses influencing NKG2DL expression both in normal and in

malignant cells have been identified. Studying the molecular mechanisms it has been shown that different stresses affect different signaling pathways and stimulate various NKG2DL expression pattern. NKG2DL have been shown to be regulated transcriptionally, post-transcriptionally and post-translationally. The promoter region of *MICA* and *MICB* genes has been characterized and similar regulatory elements controlling their expression have been found (Eagle et al., 2006; Venkataraman et al., 2007). In tumor cells lines expressing MICs constitutively occupied GC boxes (Sp1 binding sites) and an inverted CCAAT box have been shown to control MIC expression, though these elements are also believed to be responsible for stress-induced expression of MIC molecules in normal cells. A key element found both onto MICA and MICB promoter sequence, regulating MIC expression under heat shock and oxidative stress, is a heat shock responsive element (HSE) (Venkataraman et al., 2007). For ULBP molecules the main stress-responsive element has been found to be a NFκB binding site, while their expression in tumor cells is considered to be regulated by a complex of Sp1 and Sp3 transcription factors (Eagle et al., 2006).

NKG2DL have been shown to be regulated not only transcriptionally but also post-transcriptionally. Stern-Ginossar et al. identified a group of endogenous cellular microRNAs (miRNAs) that bind to the 3'-UTR (untranslated region) of MICA and MICB and repress their translation thereby limiting the expression of the stress ligands under normal conditions (Stern-Ginossar et al., 2008). Tumor cells can also benefit from the down-regulation of stress ligands by onco-microRNAs and escape from the NK cell surveillance.

A role of the BCR/ABL oncogene in the regulation of NKG2DL expression was discovered by Boissel et al. (Boissel et al., 2006). Constitutively active BCR/ABL fusion kinase in CML cells activates the PI3K/mTOR pathway, which in turn has been shown to affect MICA translation. Also the DNA damage pathway has been found to induce NKG2DL expression. Double strand brakes and stalled DNA replication are sensed by the PI3K-related protein kinases ATM (ataxia telangiectasia, mutated) and ATR (ATM and Rad3-related), respectively, which results in cell cycle arrest and DNA repair or in apoptosis if the DNA damage is too extensive to be repaired. DNA damage pathway has been shown to be constitutively active in certain human cancer cells. Gasser et al. demonstrated that both mouse and human cells up-regulate NKG2DL following treatment with DNA-damaging agents (Gasser et al., 2005). They proposed that this effect was dependent on ATR / ATM function, as inhibitors of ATR and ATM kinases prevented ligand up-regulation in a dose-dependent fashion. Moreover, ATR and ATM have been shown to stimulate NKG2DL expression independently of p53, though the exact molecular mechanism remains to be elucidated.

Furthermore, it has been shown that treatment with histone deacetylase (HDAC) inhibitors led to an up-regulation of MICA and MICB in hepatoma cells and in leukemic cells. This suggests that hypoacetylation of MIC promoters, associated with transcriptional silencing, was abrogated by the HDAC inhibitors Trichostatin A and Sodium valproate and resulted in an accumulation of hyperacetylated histones and an up-regulation of the repressed genes (Armeanu et al., 2005; Andersen et al., 2007; Kato et al., 2007). Besides, treatment of myeloma cells with proteasome inhibitors has been demonstrated to induce NKG2DL expression, however, the detailed underlying molecular mechanisms are still unknown (Jinushi et al., 2008).

Toll-like receptor (TLR) signaling has been also shown to stimulate NKG2DL transcription. Peritoneal macrophages treated either with TLR agonists *in vitro*, or *in vivo* after the injection of LPS, exhibited surface expression of Rae-1, the murine NKG2DL (Hamerman et al., 2004). Poly(I:C) and LPS, which induced TLR signaling on dendritic cells (DC), also resulted in ULBP1 and ULBP2 ligand expression (Ebihara et al., 2007). Certain cytokines are also known to influence NKG2DL expression. IFN-α in humans leads to the expression of MICA on DC (Jinushi[2] et al., 2003). However, other cytokines have been demonstrated to down-regulate NKG2DL expression. For instance, treatment of human melanoma cells with IFN-γ resulted in a decreased MICA expression (Schwinn et al., 2009). Interestingly, IFN-γ-regulated miRNAs have been discovered that can suppress MICA expression (Yadav et al., 2009). Transforming growth factor-β (TGF-β) has been also described to decrease the transcription of MICA, ULBP2 and ULPB4 in human malignant gliomas (Eisele et al., 2006). Thus, different signals exist that down-regulate NKG2DL expression thereby allowing tumor cells to escape from NKG2D-mediated immune surveillance.

2.6.3 NKG2D ligands and immune escape

Several mechanisms have been described by which tumors evade from NKG2D mediated immune surveillance (Champsaur and Lanier, 2010). One of the mechanisms is based on the shedding of NKG2DL from the cell surface. This impairs the recognition of the tumor cells by NK cells and decreases cell lysis (Salih et al., 2003; Waldauer et al., 2008). Moreover, shed soluble NKG2DL (sNKG2DL) which are detectable in the sera of tumor patients, are still able to bind to the NKG2D receptor on lymphocytes thereby inducing its internalization. Thus, sNKG2DL contribute to tumor immune escape. Our group demonstrated that elevated levels of soluble ULBP2 in the sera of melanoma patients correlate

with poor survival (Paschen et al., 2009). Therefore, understanding the regulation of NKG2DL expression in tumor cells will allow the design of novel therapeutical strategies to improve immune response in the patient.

2.7 Aims of the study

Metastatic melanoma is one of the most aggressive tumors, characterized by an increasing incidence. The low efficacy of the conventional therapies demands for the development of new treatment approaches. Several strategies take advantage of the strong intrinsic immunogenicity of the tumor that in principle allows autologous NK cells and T cells to recognize and kill melanoma cells. An important lymphocyte receptor involved in tumor immune surveillance is NKG2D. Expression of its surface ligands the MIC and ULBP molecules is induced upon cell stress but can also be detected on tumor cells. Binding of NKG2D to the ligands on tumor cells strongly stimulates the cytotoxic anti-tumor activity of NK cells and co-stimulates T cell activity. Thus developing strategies to enhance NKG2D ligand expression on melanoma cells might be helpful to enhance tumor immunogenicity.

Proteasome inhibition causes an accumulation of unfolded proteins in the cell, which should increase the expression of NKG2DL. As proteasome inhibitors are currently tested in melanoma therapy, the aim of the present study was to identify the impact of proteasome inhibition on NKG2DL expression in melanoma cells and to elucidate the underlying molecular mechanisms.

3 Materials and methods

3.1 Materials

Lab equipment	Company
Autoclave	Syntec
Balance	Kern
Blotting cells	BioRad
Cassette for film development	BioRad
CO_2 incubator	Binder
Cooling microcentrifuge	Hermle
Dark Hood	BioStep
Fastpette V-2	Labnet
Gallios Cytometer	Beckman Coulter
Gradient thermocycler	BioRad
High speed Cooling centrifuge Rotanta 460R	Hettich
Horizontal electrophoresis System for agarose gels	BioRad
Infinite M200	Tecan
Laminar flow hood	ThermoScientific
Microcentrifuge	Biofuge
Magnetstirrer	IKA-Combimag RCT
Microscope	Leica
Mini-PROTEAN Vertical electrophoresis System	BioRad
Mixer Ususio VTX-3000L	Oehmen Lab Technik
Multichannel pipette	Rainin
pH-meter 510	EUTECH Instruments
Pipette set: 1000, 100 and 10 µl	Rainin
Rotamax 120 (Thermoblock)	Heidolph Instruments
Refrigerators: +4; -20; -80°C	
Shaker Rotamax 120	Heidolph Instruments
Step One Plus real-time PCR system	Applied Biosystems
Waterbath	Fischer & Rintelen

Disposable and re-usable materials	Company
6 well Plates TC	TPP
8er Strips PCR-tubes with single caps 0,2 ml	Biozym
96 Well Suspension culture Plate with lid sterile	Greiner/Oehmen
96 Well Plate flat bottom white	Costar
96 Well Multiply Fast PCR Platte	Sarstedt

96 Well Half Area Microplatte UV-Star Transparent µclear	Tecan
Amersham Hyperfilm ECL 18x24 cm	GE Healthcare
Amersham Hybond ECL	GE Healthcare
Cell count chamber	Neubauer
Cell culture flasks 25 cm3; 75 cm3; 175 cm3	Greiner Bio-One
Cell scraper 28 cm	Greiner Bio-One
Cover glass	Neubauer
Falcon tubes 15 ml; 50 ml	Oehmen
Filter 0,2 µm sterile	Sartorin
Foam Pads 8x11 cm	BioRad
Freezing Tubes 2 ml, Greiner	Oehmen
High speed centrifuge plastic tubes 50 ml	Nalgene
Optical adhesive covers	Applied Biosystems
Petri dish m.N. 100/20mm TC Greiner	Greiner Bio-One
Petri dish m.N. 60/15mm TC Greiner	Greiner Bio-One
Pipette tips 10, 100, 1000 µl	Rainin
Reaction tubes, Safe lock 0,5; 1,5; 2,0 ml safe-lock	Eppendorf
Syringe 5, 10, 50 ml sterile	Terumo
Tissue culture plates uncoated	Greiner Bio-One
Whatman-Papier 3MM Chr sheets 46x57 cm	GE Healthcare

Cell culture / media	**Company**
FCS Charge A10108-2367	PAA
OptiMem	Gibco
PBS w/o Ca Mg (1x)	Invitrogen
Penicillin/Streptomycin 100x	PAA
RPMI 1640 mit L-Glutamin	PAA
Trypsin-EDTA (10x)	PAA

Kits	**Company**
ChIP IT Express Enzymatic	Active Motif
ChIP IT Express HT	Active Motif
ChIP IT Control Kit Human	Active Motif
DuaL-Glo Luciferase Assay System	Promega
GeneJet Plasmid Miniprep Kit	Fermentas
One Shot TOP10 Chemically Competent E.coli	Invitrogen
pcDNA 3.1 V5-His TOPO TA Expression Kit	Invitrogen
Plasmid Maxiprep Kit	Qiagen
QiaAmpDNA Blood Mini Kit	Qiagen

Quick Change Lightning Mutagenesis Kit	Stratagene
QIAQuick Nucleotide Removal Kit	Qiagen
QiaQuick PCR Purification Kit	Qiagen
Qiashredder	Qiagen
Reporter Lysis Buffer 5x	Promega
Rnase-Free DNase Set	Qiagen
Rneasy Plus Mini Kit	Qiagen

Reagents / Chemicals	Company
Inhibitors	
Actinomycin D	Sigma-Aldrich
Brefeldin A	Sigma-Aldrich
Chloroquine	Sigma-Aldrich
Cycloheximide	Sigma-Aldrich
MG132(Z-leu-leu-leu-al)	Sigma-Aldrich
General	
Agarose	Sigma-Aldrich
Agar-agar	Invitrogen
Ampicillin	Sigma-Aldrich
Aqua ad iniectabilia	Braun
Calcium chloride	Sigma-Aldrich
DMSO	Sigma-Aldrich
EDTA	Sigma-Aldrich
Ethanol p.A absolut	Sigma-Aldrich
Ethidiumbromid 1%	Roth
Formaldehyde 37%	Merck
Hepes	Biochrom
Isopropanol p.A.	Sigma-Aldrich
Kalium chlorid	Merck
PMSF	Biochemica
Sodium chlorid p.A	Merck
Sodium hydroxyde	Fluka
Trypanblue 0,5%	Biochrom
Trypton/Pepton from Casein	Roth
Yeast extract	Gerbu
FACS	
APC-Annexin V	BD Biosciences
Propidium iodid	BD Biosciences
Flow Check	Beckman Coulter
COULTER CLENZ Cleaning Agent	Beckman Coulter

IsoFlow Sheath Fluid	Beckman Coulter
Western blot	
30% Acrylamid Bis solution	BioRad
β-mercaptoethanol	Sigma-Aldrich
Ammoniumperoxidsulfat	Sigma-Aldrich
Bradford Reagent	Sigma-Aldrich
Bromphenolblue	Sigma-Aldrich
BSA Type H1	Gerbu
BSA Standard solution	BioRad
Complete Protease inhibitor tablet	Roche
Glycin	Gerbu
Glycerol	Roth
H_2O_2 p.A	Merck
Luminol	Sigma-Aldrich
Methanol	Sigma-Aldrich
Non fat dry milk	Gerbu
p-Coumarine acid	Sigma-Aldrich
PageRuler™ Prestained Protein Ladder	Fermentas
Puanceou Solution	Sigma-Aldrich
SDS	Gerbu
Sodium deoxycholate	Gerbu
Tris Base	AppliChem
Triton-x-100	Sigma-Aldrich
Temed	Sigma-Aldrich
Tween 20	Gerbu
RT-PCR / quantitative RT-PCR / cloning	
Deoxynucleotide Mix 10mM	Stratagene
DNA loading dye (6 x)	Fermentas
DSF-Taq DNA polymerase 500u	Bioron
Expand High Fidelity PCR System	Roche
GeneRuler™ 100 bp DNA Ladder Plus	Fermentas
GeneRuler ™ 1 kb DNA Ladder	Fermentas
High-Capacity cDNA Reverse Transcription Kits	Applied Biosystems
Hind III	Fermentas
Nco I	Fermentas
T4 DNA Ligase	Promega
TaqMan Universal PCR Master Mix, no AmpErase UNG	Applied Biosystems
Taqman Gene Expression Assay GAPDH (4352934E)	Applied Biosystems
Taqman Gene Expression Assay HSP70 (Assay ID HS00271229-s1)	Applied Biosystems

Thermoprime Plus	ThermoScientific
Yellow Tango buffer (10 x)	Fermentas
Transfection	
Fugene HD	Roche
X-Treme Gene siRNA transfection reagent	Roche
Chromatin immunoprecipitation	
Acid Phenol Chloroform	Applied Biosystem
Ethanol	Sigma-Aldrich
Sodium acetate	Sigma-Aldrich

Buffers and solutions

Flow Cytometry:

1) FACS buffer:	PBS (1 x)	500 ml
	FCS	50 ml
	NaN_3	0.5g
2) 10 x Binding buffer	Hepes	0.1 M (pH 7.4)
	NaCl	1.4 M
	$CaCl_2$	25 mM
3) Fixation solution (PFA):	4 % Formaldehyde in PBS	

Western blot:

1) 10% SDS:	50 g SDS in 500 ml H_2O	
2) 10% Ammoniumperoxidsulfat:	1 g in 10 ml H_2O	
3) 0,25% Bromphenolblue:	50 mg in 202 ml H_2O	
4) RIPA buffer for protein extraction	Tris	50 mM
	NaCl	150 mM
	SDS	0.1 %
	Na Deoxycholate	0.5 %
	Triton X 100	1 %
	PMSF	1 mM
	Roche Complete Protease inhibitor tablet	

5) 5 x Sample buffer:	Glycerol (99%)	5 ml
	SDS	1.5 g
	0.25 % BPB	1 ml
	adjust with H_2O up to	7.5 ml
	mercaptoethanol	2.5 ml
6) 4 x low buffer:	Trisma Base 1,5M	90.85 g
	10 % SDS	20 ml
	adjust with H_2O up to	500 ml
	pH 8.8	
7) 4 x upper buffer:	Trisma Base 0,5M	15.15 g
	10 % SDS	10 ml
	adjust with H_2O up to	250 ml
	pH 6.8	
8) 10 x running buffer:	Trisma Base	75 g
(electrophoresis buffer)	SDS	25 g
	Glycin	360 g
	adjust with H_2O up to	2500 ml
9) 10 x transfer buffer:	Trisma Base	75 g
	SDS	9.35 g
	Glycin	362.5 g
	adjust with H_2O up to	2500 ml
10) PBS/Tween (TBS):	2 ml Tween dissolve in 2000 ml PBS	
11) ECL-blots development:		
Solution A	TRIS-HCl 0.1 M (pH 8.6)	200 ml
	Luminol	50 mg
Solution B	p-Coumarin acid	11 mg
	DMSO	10 ml

Mix immediately before use:

For 1 miniblot membrane (8 x 11 cm) 4 ml SA + 1.2 µl H_2O_2 + 400 µl SB

Bacterial cultures

1) LB-Medium:	Trypton/Pepton from Casein	10 g
	Yeast extract	5 g
	NaCl	10 g

Adjust with water up to 1 l, autoclave

$LB_{Ampicillin}$-Medium: LB-Medium plus sterile Ampicillin solution (150 µg/ml)

2) Agar-plates:

Agar-Agar	12-14 g
Trypton/Pepton from Casein	10 g
Yeast extract	5 g
NaCl	10 g

Adjust with water up to 1 l, autoclave

Chromatin immunoprecipitation

1) Ethanol 70%

2) Sodium acetate 3M, pH 5.2

Plasmid	Characteristics	Source
pGL4.10	Basic promoterless Firefly luciferase reporter gene plasmid, for insertion of promoter fragments	Promega
pGL4.74	Renilla luciferase gene under HSV-TK promoter	Promega
pGL4.13	Firefly luciferase gene under SV40 promoter	Promega
pMICB-470	MICB promoter region 470 bp in pGL4.10	generated within this study
pMICB-470-HSE*mut	MICB promoter region 470 bp in pGL4.10, promoter mutated in HSE	synthesized by MWG
pMICB-470-NRF*mut	MICB promoter region 470 bp in pGL4.10, promoter mutated in predicted NRF1 binding site	generated within this study
pMICB 225	MICB promoter region 225 bp in pGL4.10	generated within this study
pMICB 115	MICB promoter region 115 bp in pGL4.10	generated within this study
pMICA 455	MICA promoter region 455 bp in pGL4.10	generated within this study
pHβAPr-hHSF1ΔRD	expression vector for a constitutive active form of human HSF1 (hHSF1ΔRD) driven by β-actin promoter	kindly provided by A. Nakai (Nakai et al., 2000; Gunnung et al., 1987)
pHβAPr-1-neo	expression vector containing β-actin promoter	generated within this study by excision of hHSF1ΔRD
pLNCX2-hHSF1ΔRD	expression vector for a constitutive active form of human HSF1 (hHSF1ΔRD) driven by CMV promoter	kindly provided by W. Widlak
pLNCX2	expression vector containing CMV promoter	generated within this study by excision of hHSF1ΔRD

Primers, siRNA		Sequence: 5' → 3'
Real-time RT-PCR primers and probes		
MICA	Fw	CGATATCTAAAATCCGGCGTAGTC
	Rev	TGCGGGTGACATTCACCAT
	Probe	FAM-AGGAGAACAGTGCCC-MGB
MICB	Fw	TGCAGAAACTACAGCGATATCTGAA
	Rev	TGCATGTCACGGTGATGTTG
	Probe	FAM-CCATGGTGAATGTCAC-MGB
Primer for MIC promoter regions (Cloning)		
MICA-455 bp	Fw	ATAAGACTCGAGACTCTACAGCCAGG
	Rev	ATAAGACCATGGTGCCAGCCAGAAGCAGGAAGACC
MICB-470 bp	Fw	ATAAGAAAGCTTACGCGTTGTCTGTCCCGGAAG
	Rev	ATAAGACCATGGAGGCGACGGCCAGAAACAGCAG
MICB-225 bp	Fw	ATAAGAAAGCTTTCCCGCCTTCTAAATTTCCCC
	Rev	ATAAGACCATGGAGGCGACGGCCAGAAACAGCAG
MICB-115 bp	Fw	ATAAGAAAGCTTACTGGATAAGCGGTCGCTGAGC
	Rev	ATAAGACCATGGAGGCGACGGCCAGAAACAGCAG
Site-directed mutagenesis		(nucleotide substitutions shown in bold, wild type in parentheses)
MICB-470 NRF1*mut	Fw	ATTTTGGCTGCGCTCG**TA**(CG)CACGCTCCCCCTTTTC
	Rev	GAAAAGGGGGAGCGTG**TA**(CG)CGAGCGCAGCCAAAAT
Chromatin immunoprecipitation		
MICB-ChIP1	Fw	TCCCGCCTTCTAAATTTCCCC
	Rev	TGAATGAAACCGGTGAGAAGAC
MICB-ChIP2	Fw	ACTGGATAAGCGGTCGCTGAGC
	Rev	AGGCGACGGCCAGAAACAGCAG
siRNA duplexes		*5' → 3'* (Source: Page et al., 2006)
Human HSF1		GUCGUCAACCCGCUCAUUAUU
	sense	GUCGUCAACCCGCUCAUUA
	antisense	GAAUGAGCUUGUUGACGAC
Luciferase (contr)		CGUACGCGGAAUACUUCGCDTDT
	sense	CGUACGCGGAAUACUUCGC
	antisense	UCGAAGUAUUCCGCGUACG

Antibodies

Non-coupled antibodies

Antibody (clone)	Specificity	Application	Conc /ml	Working conc	Source
MICA (AMO1)	Monoclonal mouse anti-human, IgG_1	FACS	1 mg	0.2 µg /sample	BAMOMAB
MICB (BMO2)	Monoclonal mouse anti-human, IgG_{2a}	FACS	1 mg	0.2 µg /sample	BAMOMAB
ULBP1 (170818)	Monoclonal mouse anti-human, IgG_{2a}	FACS	500 µg	0.1 µg /sample	R&D systems
ULBP2 (BUMO1)	Monoclonal mouse anti-human, IgG_1	FACS	1 mg	0.2 µg /sample	BAMOMAB
ULBP3 (166510)	Monoclonal mouse anti-human, IgG_{2a}	FACS	500 µg	0.1 µg /sample	R&D systems
HLA class I (-A, -B; -C) (W6/32)	Monoclonal mouse anti-human, IgG_{2a}	FACS	hybridoma	5 µl /sample	ATCC
MICA/B (BAMO1)	Monoclonal mouse anti-human, IgG_1	WB	1 mg	1 µg /ml	BAMOMAB
MICB	Polyclonal gat anti-human	WB	0.2 mg	1 µg /ml	R&D systems
HSF1	Polyclonal rabbit anti-mouse	WB CHIP	1 mg	1 µg/ml 10 µg	Stressgen
Ubiquitin (FK2)	Monoclonal mouse anti-human, IgG_1	WB	1 mg	1 µg/ml	Stressgen
H2A	Polyclonal rabbit anti-human	WB CHIP	500 µg	1 µg/ml 5 µg	Active Motif
uH2A (E6C5)	Monoclonal mouse anti-human IgM	WB CHIP	—	1:1000	Millipore
GAPDH (14C10)	Polyclonal rabbit anti-human	WB	—	1:5000	Cell Signaling
IgG	Rabbit anti-mouse IgM, µ chain	CHIP	2.4 mg	5 µg	Dianova

Coupled secondary antibodies

Antibody (clone)	Specificity	Application	Conc /ml	Working conc	Source
R-Phycerythrin (PE)	Goat anti-mouse $F(ab')_2$ fragment, IgG	FACS	0.5 mg	0.25 µg /sample	Dianova
IgG, Horseradish peroxidase linked (HRP)	ECL, polyclonal donkey anti-rabbit	WB	—	1:10000	GE Health care
IgG, HRP	ECL, polyclonal rabbit anti-goat	WB	—	1:2000	DakoCytomation
IgG, HRP	ECL, goat anti-mouse IgG_{2a}	WB	—	1:5000	Biozol
IgG, HRP	ECL, polyclonal goat anti-mouse IgM, µ Chain specific	WB	0.8 mg	1:1000	Dianova

3.2 Methods

3.2.1 Cell culture and treatment

Human melanoma cell lines UKRV-Mel-02, MA-Mel-47, MA-Mel-86b, MA-Mel-103, MA-Mel-107, established in our laboratory from tumor metastasis, human cervical carcinoma HeLa cells and human colon carcinoma HCT116 cell line were cultivated in RPMI 1640/2mmol/L glutamine supplemented with 10 % FCS, 100 U/ml penicillin and 100 µg/ml streptomycin at 37°C in a humidified atmosphere with 5 % CO_2. Cells were seeded at 50 – 60 % confluence 24 hrs before treatment.

MG132, Cycloheximide, Chloroquine, Brefeldin A and Actinomycin D were resuspended as recommended by the manufacturer and used at the indicated concentrations. Control cells were treated with solvent.

3.2.2 Flow cytometry

To determine the surface expression of NKG2DL and classical human MHC class I molecules (HLA-A, -B, -C), tumor cells were harvested, washed with PBS, counted and resuspended in in FASC buffer at concentration 1 x 10^6 cells/ml. Of each sample 2 x 10^5 cells (200 µl) were used for the staining, transferred in 96 well plates. Primary antibodies were added and samples were incubated on ice for 30 min, than centrifuged at 1500 rpm for 5 min and washed twice with 200 µl FACS buffer. Then a secondary antibody conjugated with phycoerythrin (PE) was added. The suspension was incubated in the dark on ice for 30 min, than centrifuged at 1500 rpm for 5 min and washed twice with 200 µl FACS buffer. Finally cells were fixed in 4 % PFA and stored at 4°C or immediately measured using Gallios Cytometer and analysed by FlowJo 7.2.2 software.

3.2.3 Annexin V / PI staining

To determine the basal and induced apoptosis level, melanoma cell lines were incubated with MG132 or with solvent contol DMSO for 8 hrs, then harvested and washed twice with ice-cold PBS followed by the centrifugation steps at 1200 rpm for 7 min at 4°C. Washed cells were resuspended in 1 x Binding buffer at concentrations of 1 x 10^6 cells/ml. Of each sample 1 x 10^5 cells (100 µl) were used for the staining and transferred in a 5 ml culture tube. 5 µl of APC Annexin V (for one or two color analysis) and 1 µl of PI (for two color analysis only) were added to the probe, gently vortexed and incubated in the dark for 15 min at RT. After incubation 400 µl of 1 x Binding buffer was added to each tube. The measurement was

perforemed within 1 hr after staining using Gallios Cytometer and analyzed by FlowJo 7.2.2 software; the samples during measurement were kept on ice.

3.2.4 Western blot

To prepare cell lysates, cells were trypsinized, washed with PBS followed by a centrifugation step at 1200 rpm for 7 min. Cells were resuspended in 1 ml PBS and the cell number was determined and cells were transferred into 1.5 ml microcentrifuge tubes, centrifuged at 2000 rpm for 10 min at 4°C. The supernatant was discarded; the undisturbed cell pellet was immediately placed into liquid nitrogen. Cell pellets were either stored at –80°C or immediately used for protein isolation. Cell pellets were lysed by RIPA buffer supplemented with complete protease inhibitor (Roche) in the ratio 100 µl to 4 µl (10 x), respectively. 50 µl of completed RIPA buffer was used for lysis of 10^6 cells. After 15 min incubation on ice samples were clarified by centrifugation at 13000 rpm for 15 min at 4°C, supernatants containing proteins were collected and either stored at –80°C or used immediately for SDS-PAGE electrophoresis. Protein concentrations of the lysates were determined with the Bradford method in 96 well plates in triplicates according to manufacturer protocol for micro volumes (Sigma). BSA (2 mg/ml; BioRad) was used for a standard curve, to determine the concentration in the lysats. Equal amounts of protein (µg) were supplemented with 5 µl of sample buffer and adjusted with electrophoresis buffer to 20 µl. The mixtures were heated at 99°C for 5 min, chilled on ice and loaded onto a SDS polyacrylamide gel. After separation proteins were transferred onto a nitrocellulose membrane. The membranes were blocked for 1 hour with 5 % non fat dry milk in TBS, washed with TBS and incubated with the primary antibodies anti-MICB, -MICA/B, -HSF1, -Ub, -H2A, uH2A in 1 % TBS-milk and anti-GAPDH in 5 % TBS-bovine serum albumin overnight at 4°C, followed by three washing steps in TBS. Membranes were then incubated for 1 hr at RT with the horseradish peroxidase (HPR)-coupled secondary antibodies dissolved in 1 % TBS-milk, followed by three washing steps in TBS and a last washing with PBS (1 x). Antibody binding to membranes was visualized using ECL developing solution incubated with the membranes for a maximum of 2 min in the dark.

3.2.5 Histone extraction

Cells were trypsinized and washed twice with ice-cold PBS followed by centrifugation steps at 1200 rpm for 7 min. The cell pellet was resuspended in Triton Extraction Buffer (TEB: PBS containing 0.5 % Triton X 100 (v/v), 2 mM phenylmethylsulfonyl fluoride

(PMSF), 0.02 % (w/v) NaN_3) at a density of 10^7 cells/ml and incubated (10 min) on ice with gentle stirring. The lysate was centrifuged at 6500 x g for 10 min at 4°C to spin down the nuclei. The nuclei pellet was washed in half of the TEB volume and centrifuged at 6500 x g for 10 min at 4°C. The pellet was resuspended in 0.2 N HCl at a density of $4x10^7$ nuclei/ml and left overnight at 4°C for acid extraction. The extracts were then centrifuged at 6500 x g for 10 min at 4°C to pellet the debris. The supernatant was collected and the protein content was determined, performing the Bradford assay. The histone extracts were used for Western blot and resolved by SDS-PAGE as described before, or stored at -80°C.

3.2.6 Quantitative RT-PCR

For RT-RCR, total RNA (free of genomic DNA) was isolated from tumor cells using the RNeasy Mini Plus Kit according to the manufacturer protocol. To ensure that genomic DNA is not present in the samples an additional step of purification was performed as follows: 80µl of DNase I mix (10 µl DNase I Stock solution and 70 µl RDD buffer, supplied) (DNase I, RNase-free Set; Qiagen) was added to each sample after the first washing step of the column with RW1 buffer (RNeasy Mini Plus Kit, Qiagen) and left to penetrate for 15 min at RT. Next proceed to the manufacturer protocol (RNeasy Mini Plus Kit; Qiagen). The concentration of total RNA, was measured with Infinite M200 (Tecan). The concentration of a sample containing RNA may be calculated following Equation: 40 x $OD_{(260\ nm)}$ of the sample = concentration of RNA (µg/ml). 1 µg RNA was used for reverse transcription. The reverse transcription reaction was performed using high-capacity cDNA reverse transcription kit (Applied Biosystems) with reverse transcription random primers. DNA was quantified with Infinite M200. The concentration of a sample containing DNA may be calculated following Equation: 50 x $OD_{(260\ nm)}$ of the sample = concentration of DNA (µg/ml).

cDNA was amplified with specific primers and probes for MICA and MICB, or using predesigned TaqMan gene expression assay kits for HSP70 and GAPDH (endogenous control) (Applied Biosystems). For real-time PCR reaction 2 x TaqMan Universal PCR Master Mix (no AmpErase UNG) was used. The reaction mixtures were composed as follows:

for MICA and MICB	for HSP70 and GAPDH
5 µl (2x) TaqMan master mix	5 µl (2x) TaqMan master mix
0.3 µl forward primer (1:10; 300 nM)	0.5 µl of primer and probe mix
0.3 µl reverse primer (1:10; 300 nM)	50 ng cDNA
1 µl probe (1:100; 100 nM)	adjust to 10 µl with Aqua Braun
50 ng cDNA	
adjust to 10 µl with Aqua Braun	

TaqMan PCR amplification was performed using an Applied Biosystems sequencer detection system. The cycling conditions were 10 min at 95°C followed by 35 cycles: 20 sec at 95°C, 90 sec at 60°C. The final extension was performed at 72°C 10 min. Reactions were performed in triplicates. Changes in MICA, MICB and HSP70 expression levels, normalized to GAPDH mRNA levels, were calculated by the $2^{-\Delta\Delta CT}$ method (Livak, Schmittgen, 2001).

3.2.7 Amplification of promoter fragments, cloning and site-directed mutagenesis

UKRV-Mel-02 cells were trypsinized, washed with PBS followed by centrifugation steps at 1200 rpm for 7 min. Washed cells were resuspended in 1 ml PBS and centrifuged at 2000 rpm (10 min, 4°C). The supernatant was discarded; the undisturbed cell pellet was used for the isolation of genomic DNA by the QiaAmpDNA Blood Mini Kit (Qiagen). MICA and MICB promoter regions were amplified from genomic DNA with PCR using the Expand High Fidelity polymerase (Roche) and specific primers following the manufacturer protocol.

The thermocycling program was as follows: 94°C – 2 min; 94°C – 15 sec; 69°C – 30 sec; 72°C – 45 sec, 39 cycles from step 2; 72°C – 10 min; 4°C. PCR products were purified with the QIAquick PCR purification kit (Qiagen) according to the manufacturer protocol.

For cloning of the PCR products into pGL4.10 the following reaction mixtures generated:

MICB promoter constructs			*pGL4.10 restriction (1 µg/µl)*	
purified PCR product	12 µl or	30 µl	pGL4.10	1 µg
Nco I (10 u/µl)	2 µl	5 µl	Nco I (10 u/µl)	2 µl
Hind III (10 u/µl)	2 µl	5 µl	Hind III (10 u/µl)	2 µl
2 x (10 x Yellow Tango buffer)	4 µl	10 µl	2 x (10 x Yellow Tango buffer)	4 µl
			H_2O	add to 20 µl
	V = 20 µl	V = 50 µl		V = 20 µl

The DNA was incubated with restriction enzymes at 37°C for 4 hrs, enzymes were subsequently inactivated at 80°C for 20 min. The products of the restriction reaction were purified with the QIAquick nucleotide removal kit following the manufacturer instructions. DNA concentration was measured. For ligation, PCR product and linearized vector were mixed in the ratio determined by the following equation: Amount of insert [ng] = 5 x amount of vector [ng] x (size of insert [bp] / size of vector [bp]). Ligation was performed at RT overnight followed by an inactivation step at 65°C – 10 min.

Vector, Insert	calculated amount
10 x Ligase buffer	2 µl
T4 Ligase	1.5 µl
H_2O	add. to 20 µl

3.2.8 Transformation and DNA isolation

One Shot TOP10 chemically competent *Escherichia Coli* (Invitrogen) were transformed with the ligation product as follows: 50 µl of TOP10 cells were mixed with 20 µl ligation product and incubated 30 min on ice; the suspension was then incubated for 45 sec in a water bath at 42°C for heat shock and chilled on ice for 3 min. SOC medium (300 µl) was added to the bacteria and the suspension was incubated for 1 hr at 37 °C, 250 rpm. Then 100-150 µl of the *E. coli* suspension was spread onto the agar dishes containing ampicillin (100 µg/ml) and incubated overnight at 37 °C.

For DNA isolation bacterial colonies were picked, placed into a glass tube with 5 ml sterile LB medium supplemented with ampicillin (100 µg/ml) and incubated overnight at 37°C in a shaker (200 rpm). Of the bacterial suspension 4 ml were collected to isolate plasmid DNA using the GeneJet Plasmid Miniprep Kit (Fermentas), 1 ml was left at 4°C to use for maxi-prep. Concentration of the isolated DNA was measured and restriction of 0.5 µg DNA was performed to confirm the presence of the insert in the plasmid.

Following constructs were generated: pMICA-455 bp, pMICB-470 bp, pMICB-225 bp, pMICB-115 bp. MICB promoter element mutation in HSE was synthesized by MWG Operon Eurofins. The mutation in the NRF1 binding site was made by mutagenic megaprimer NRF1* PCR (34) using the pMICB-470 construct and QuikChange-II site-directed mutagenesis methodology (Stratagene). All DNA fragments in pGL4.10 were verified by sequencing.

The correct constructs confirmed by sequencing were amplified in 100 ml of LB medium supplemented with ampicillin (100 µg/ml) (for high copy plasmids) and incubated

overnight at 37°C, 200 rpm. Plasmid DNA was isolated with Plasmid Maxiprep Kit (Qiagen) according to the manufacturer protocol.

3.2.9 Transfection and luciferase assay

Melanoma cells were seeded in 6-well plates at 1.5 x 10^5 cells/well. After 24 hrs cells were transiently transfected with luciferase reporter gene expression plasmid DNA (1 µg/well) together with the internal control plasmid pGL4.74, encoding Renilla luciferase (200 ng/well), used for normalisation. As negative control the luciferase promoterless pGL4.10 vector was used (mock), as positive control pGL4.13 containing the Firefly luciferase gene driven by SV40 promoter was used. For DNA transfection the Fugene transfection reagent (Roche) was used. Transfected melanoma cells were incubated for 24 hrs, then 10 µM MG132 or solvent (DMSO) were added. Cells were incubated for 8 hrs, then washed twice with PBS. 500 µl (1 x) Reporter lysis buffer (Promega) was added to each well, plates were immediately placed at -80°C and incubated there for 10 min. Frozen plates were placed at 37°C for thawing, then lysates were harvested, transferred into 1.5 ml microcentrifuge tubes and then placed into liquid nitrogen. The lysates were either stored at -80°C or immediately used for measurement of luciferase activity. For the luciferease assay the lysates were thawed at 37°C in a water bath. Of the lysate 75 µl were used to measure Firefly and Renilla luciferase activities in triplicates using the DuaL-Glo Luciferase Assay System (Promega) in 96-well white flat bottom luminometer plates (Costar) using the Infinite 2000 system (Tecan) and the IControl software. Promoter construct activities were determined by normalizing Firefly luciferase activities to Renilla luciferase activities.

In some assays, an HSF1 expression plasmid and a corresponding control plasmid were transfected in addition.

Statistic analysis was done by GraphPad Prism program using standard paired t-test.

3.2.10 Transfection of siRNA

For HSF1 knock-down, cells were seeded in 6-well plates at 1.5 x 10^5 cells/well. After 24 hrs cells were transfected with HSF1-specific siRNA or luciferase-specific siRNA (negative control) at 2 µg/well using the X-treme Gene Transfection Reagent (Roche). siRNA transfection reagent and si RNA were mixed at a ratio 1:5. The cells were incubated for 72 hrs followed by treatment with proteasome inhibitor.

3.2.11 Chromatin immunoprecipitation (ChIP) assay

Melanoma cells, either treated with the proteasome inhibitor MG132 (10 μg/ml) for 4 hrs or left untreated, were harvested and processed for ChIP using the ChIP-IT Enzymatic kit following the protocol of the manufacturer (Active Motif, USA). Antibodies for immunoprecipitation were used as recommended by the manufacturer: mouse IgG control 2 μg/ChIP reaction and anti-HSF1, anti-uH2A 5 μg/ChIP reaction. For mouse anti-human uH2A (IgM) mAb the preincubation of 25 μl G-protein magnetic beads with rabbit anti-mouse IgM (4 μg) Ab adjusted with water up to 100 μl was nessesary for 1 hr at 4°C, by shaking. Then beads were washed with 100 μl of ChIP buffer 1 and proceed to the immunoprecipitation with uH2A mAb according to the manufacturer protocol. As an additional control rabbit anti-mouse IgM (4 μg) Ab were immunoprecipitated without adding uH2A to confirm the specificity of the bands in the immunoprecipitates with uH2A. Immunocomplexes were collected with G-protein magnetic beads and sequentially washed. Chromatin was eluted, digested with proteinase K and the cross-linking was reversed, as detailed in the kit protocol. Purified DNA was further used for PCR with Thermoprime Taq DNA polymerase. Fractions of chromatin were processed similar to immunoprecipitated chromatin for input DNA controls. The forward and reverse primers for PCR amplification are listed above. Thermocycling procedure was as follows: 95°C – 2 min; 35 cycles: 95°C – 25 sec; 59°C (for ChIP1) or 66°C (for ChIP2) – 35 sec; 72°C – 65 sec. The final extension was performed at 72°C – 5 min.

4 Results

Ligands of the NKG2D receptor, the MIC and ULBP molecules, sensitize melanoma cells for recognition by NK cells (Schwinn*, Vokhminova* et al., 2009; *shared first authorship), suggesting that therapeutic upregulation of these molecules should be supportive in terms of an effective anti-tumor immune response. Small molecule inhibitors that induce stress in tumor cells like inhibitors of the proteasome have been demonstrated to up-regulate NKG2DL expression on myeloma and hepatocellular carcinoma (Salih et al., 2003; Jinushi[1] et al., 2003), but the molecular mechanisms behind remain unknown. The aim of this study was to determine the impact of proteasome inhibition on NKG2DL expression in melanoma cells and to elucidate the underlying molecular mechanisms.

4.1 Proteasome inhibition up-regulates surface expression of NKG2D ligands

4.1.1 Short-term proteotoxic stress exclusively induces MICB surface expression

To test the influence of proteasome inhibition on NKG2DL expression, the two melanoma cell lines UKRV-Mel-02 and MA-Mel-86b, already known to express NKG2DL (Schwinn, Vokhminova et al., 2009), as well as three additional metastatic cell lines MA-Mel-47, MA-Mel-103 and MA-Mel-107 were selected for this study. Furthermore the cervix carcinoma cell line HeLa and the colon carcinoma cell line HCT116 were included in some experiments in order to compare melanoma cells to tumor cells from other entities. Analysis of the indicated cell lines for the surface expression of individual NKG2DL by flow cytometry revealed different patterns (Fig. 1). The ligand most prominently expressed on all melanoma cells was MICA, while MICB was present only on 4 out of the 5 melanoma cell lines and its basal expression was quite low. In contrast to melanoma, the cell lines HeLa and HCT116 showed much stronger MICA and MICB surface expression. Of the ULBP family the ligand ULBP2 was most prominently expressed, with modest expression on MA-Mel-47 and HeLa to relatively strong levels on MA-Mel-86b, Ma-Mel-103 and HCT116. All cell lines were negative for ULBP1 and ULBP3 (data not shown), with the exception of MA-Mel-47, which expressed low amounts of ULBP1 on the surface (data not shown). To analyse if induction of proteoxic stress elicited by proteasome inhibition influences NKG2DL expression, the tumor cell lines were treated with proteasome inhibitor MG132 and analyzed for NKG2DL surface expression (Fig. 1).

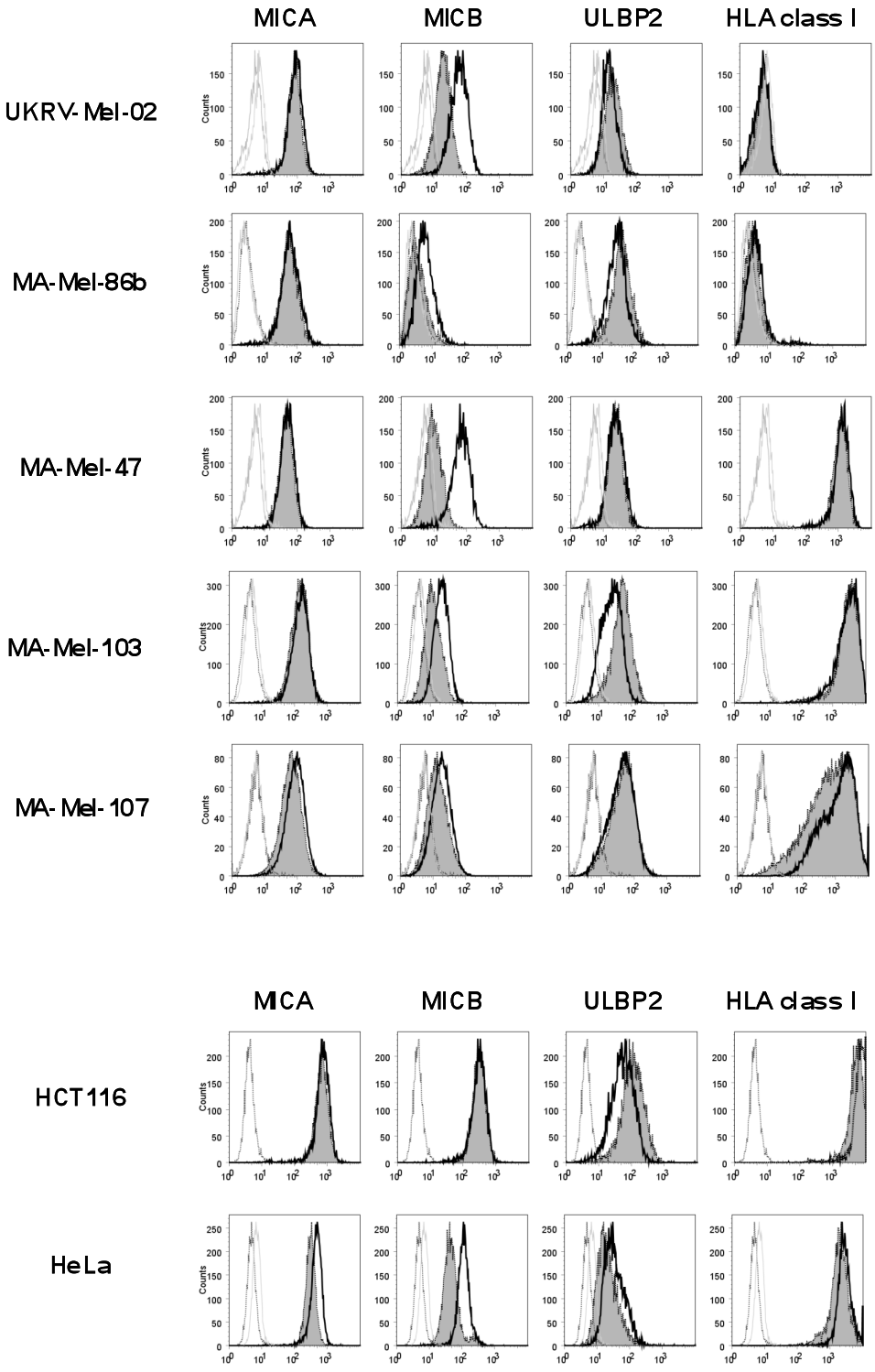

Figure 1. Surface expression of NKG2DL on tumor cells

The indicated human tumor cell lines were treated either with MG132 (10 μM) (solid black line histograms) or with DMSO (solvent, gray shaded histograms) for 8 hrs, then washed and incubated with unconjugated mouse anti-human MICA, MICB, ULBP2 or HLA class I specific mAb, followed by staining with PE-conjugated goat F(ab')2 anti-mouse IgG. Cells were then analyzed by flow cytometry. Representative data from one of at least two independent experiments are presented.

Already after 8 hrs, 4 out of 5 melanoma cell lines showed an up-regulation of MICB expression, though to different extent. Similarly, HeLa cells upregulated MICB, while no NKG2DL modulation could be observed for HCT116. In contrast to MICB, expression of MICA and ULBP2 was not up-regulated, noteworthy, even the level of classical HLA class I molecules remained constant. The induction of MICB was not caused by apoptosis as shown by a control Annexin V / PI staining (see Appendix, Fig. A1).

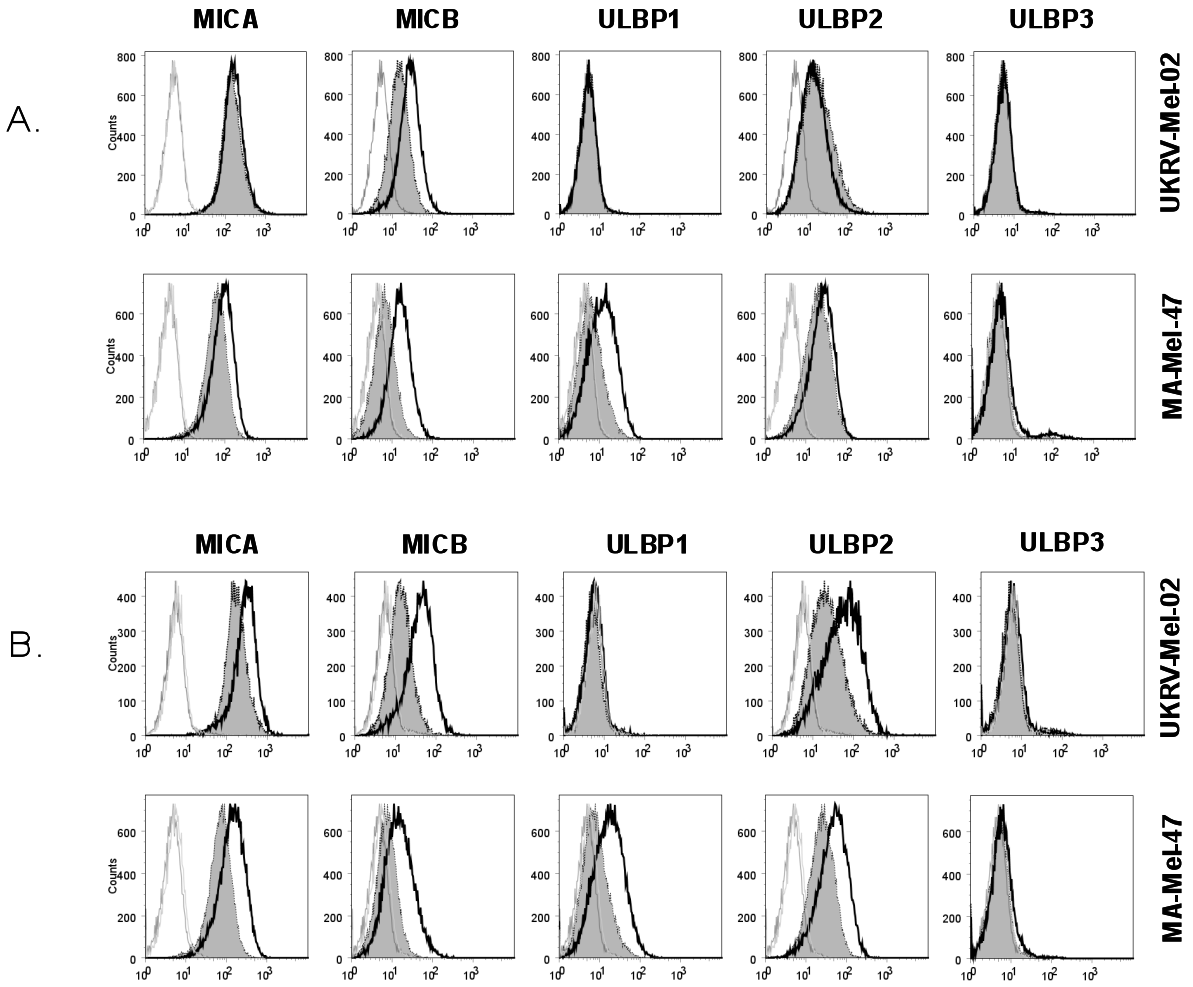

Figure 2. Up-regulation of NKG2DL surface expression on melanoma cells upon proteasome inhibition

Human melanoma cell lines UKRV-Mel-02 and MA-Mel-47 were stained with unconjugated mouse anti-MICA, MICB, ULBP1, ULBP2, ULBP3 mAb followed by PE-conjugated goat F (ab')2 anti-mouse IgG and analyzed by flow cytometry for NKG2DL surface expression. Gray lines – background staining with secondary PE–conjugated antibody only.

A. UKRV-Mel-02 or MA-Mel-47 cells were incubated with MG132 (10 µM) (black lines) or with DMSO (solvent, gray shaded histograms) for 8 hrs.

B. UKRV-Mel-02 or MA-Mel-47 cells were treated either with MG132 (10 µM) (black lines) or with DMSO (solvent, gray shaded histograms) for 8 hrs then washed and incubated in the absence of MG132 for additional 24 hrs. Data are representative from one of four independent experiments.

4.1.2 Prolonged proteotoxic stress induces expression of multiple NKG2D ligands on melanoma cell lines

Among the melanoma cell lines UKRV-Mel-02 and MA-Mel-47 were most sensitive to proteasome inhibitor treatment in terms of MICB up-regulation. These cells were chosen for further experiments to study the underlying molecular mechanisms. Since MG132 is a potent but reversible inhibitor of the proteasome, it was determined, whether increased MICB expression on melanoma cells persisted in the absence of MG132. Therefore, UKVR-Mel-02 and Ma-Mel-47 cells were treated with MG132 for 8 hrs and either harvested for direct analysis (Fig. 2A) or washed and incubated for additional 24 hrs in medium without inhibitor and then studied for NKG2DL surface expression by flow cytometry (Fig. 2B). Again treatment of melanoma cells with MG132 for 8 hrs and subsequent analysis revealed a clear induction of MICB expression on both melanoma cell lines. In case cells were cultured in medium alone for additional 24 hrs after proteasome inhibition, elevated levels of MICB were still detectable. Interestingly, under these conditions melanoma cells showed increased surface expression also of MICA and ULBP2, suggesting that the delayed induction was a secondary event. MA-Mel-47 and UKRV-Mel-02 cells showed similar pattern of NKG2DL regulation regarding MICA, MICB, ULBP2-3, only for Ma-Mel-47 an increased expression of ULBP1 was observed in addition. Taken together, MG132 induces NKG2DL expression on melanoma cells and this study focused on the analysis of the early response of MICB, in comparison to MICA.

4.1.3 Up-regulation of MICB protein under MG132 treatment is time-dependent

As demonstrated above, melanoma cells rapidly increased the expression of MICB upon proteasome inhibition. To examine the kinetic of this response melanoma cells were treated with MG132 for 2, 4, 6 and 8 hrs and analyzed for the surface expression of MICA and MICB (Fig. 3A). While MICA levels remained constant, MICB surface expression increased already after the 6 hrs of treatment.

The increase of MICB surface expression could just be due to an enhanced transport of intracellularly stored protein to the cell surface not associated with an increase in the amount of total MICB protein. To analyse this whole cell lysates from melanoma cells treated with MG132 were prepared and analyzed for total MICB protein levels by Western blot (Fig. 3B). A slight but clearly detectable enrichment of total MICB protein was observed already after 2 hrs of proteasome blockade while a strong increase was detectable after 6 hrs, suggesting that

the enhanced MICB surface expression was due to an increase in total specific protein. Visualizing of MICB revealed different bands with molecular weights of lower than 40 kD and around 55 kD. The diffuse bands around 55 kD represent differently glycosylated forms of MICB, while the lowest band about 40 kD represents non-glycosylated MIC (Eleme et al., 2004).

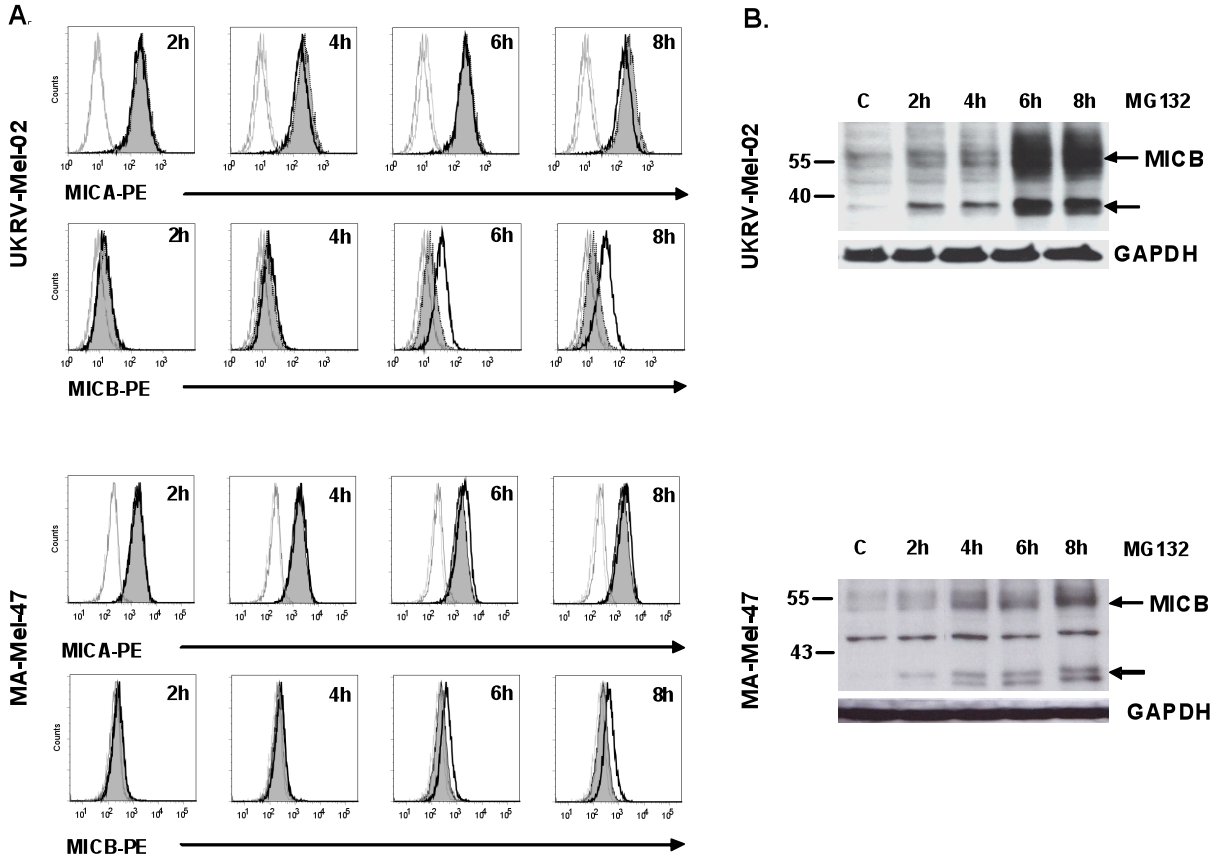

Figure 3. MG132 rapidly up-regulates MICB expression in melanoma cells

Human melanoma cell lines UKRV-Mel-02 and MA-Mel-47 were treated with MG132 (10μM) for 2, 4, 6 or 8 hrs and analyzed for MICA and MICB surface expression and for the total level of MICB protein. Data are representative of three independent experiments for UKRV-Mel-02 and of two experiments for MA-Mel-47.

A. UKRV-Mel-02 (top) and MA-Mel-47 cells (bottom) were treated with MG132 (black lines) or with DMSO (gray shaded histograms) as the solvent control for 8 hrs and subsequently stained with unconjugated mouse anti-MICA or anti-MICB mAb followed by PE-conjugated goat F (ab')2 anti-mouse IgG. Cells were analyzed by flow cytometry for MICA and MICB surface expression. Gray lines, background staining with the secondary PE–conjugated antibody only. Logarithmic scale of histograms: 10^0-10^3 for UKRV-Mel-02, 10^1-10^5 for MA-Mel-47.

B. UKRV-Mel-02 (top) or MA-Mel-47 cells (bottom), after the treatment with MG132 for the indicated time periods, were harvested and whole cell lysates were analyzed by Western blot for MICB total protein expression. The protein samples were separated by SDS-PAGE and probed with a polycloncal anti-MICB antibody (R&D). The arrows show the unglycosylated MICB (about 38 kD) and the glycosylated form of MICB protein (about 55 kD). C, indicates control cells treated with DMSO for 8 hrs. GAPDH was used as the loading control.

4.2 Upregulation of MICB upon proteasome inhibition is dependent on translation

Inhibition of the proteasome blocks protein degradation. To determine if stabilization of the MICB protein is responsible for the up-regulation of its surface presentation on melanoma, cells were treated with a combination of MG132 and Cycloheximide (CHX). The latter is known as an inhibitor of translation in eukaryotic cells. In cells treated with MG132 a strong induction of MICB was observed as shown by Western blot analysis. This upregulation was abrogated in the presence of CHX, indicating that translation is essentially required for the induction of MICB expression on melanoma cells.

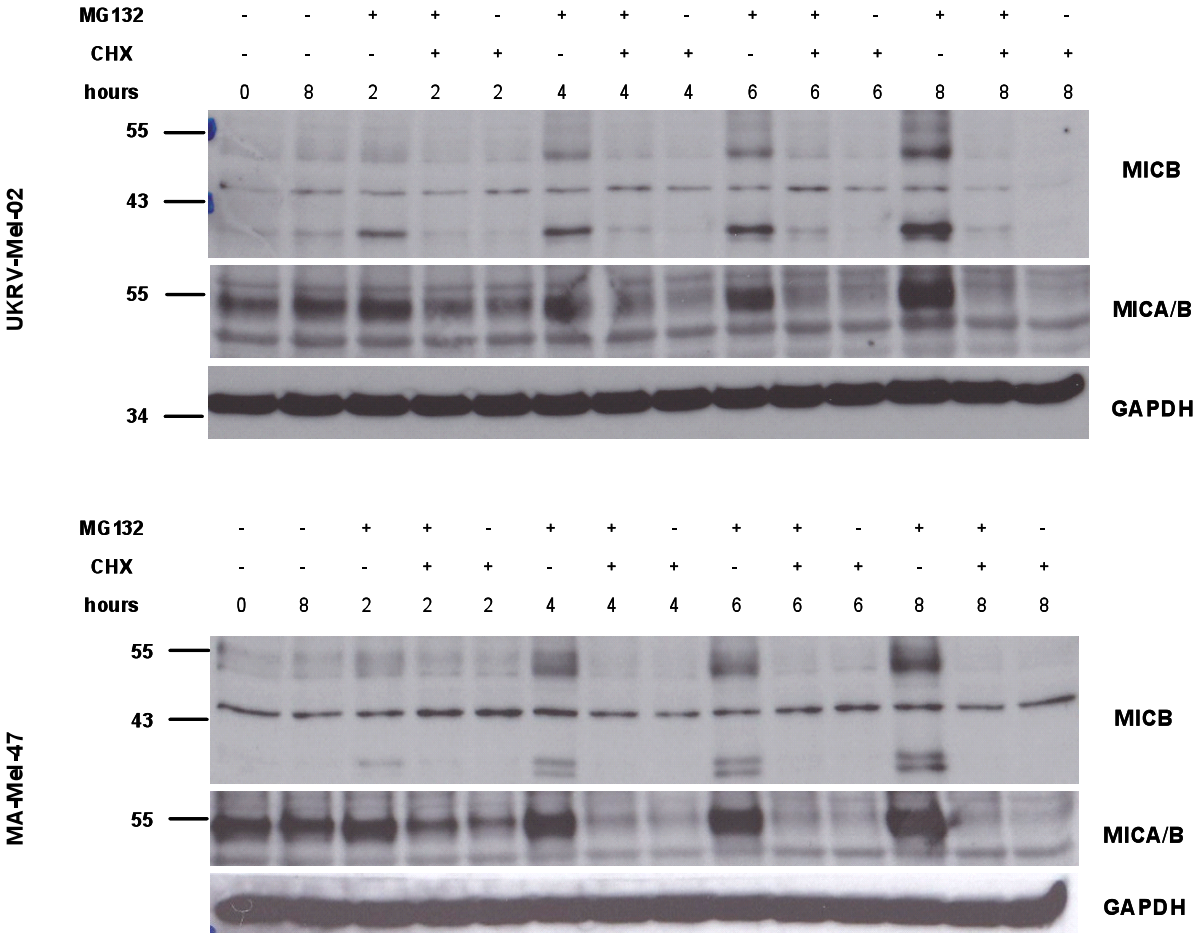

Figure 4. Induction of MICB by MG132 is abrogated in the presence of cycloheximide

UKRV-Mel-02 (top) and MA-Mel-47 cells (bottom) were treated either with MG132 (10 µM), or with Cycloheximide (100 µg/ml), or with both simultaneously for 2, 4, 6 and 8 hrs. Control cells were left untreated or DMSO as solvent control was added. Whole cell lysates were analyzed by Western blot for MICB total protein. Anti-MICA/B mAb recognized both MICA and MICB proteins in the tested lysates. GAPDH was used as a loading control. The blots are representative of three independent experiments.

Cells treated with MG132 and CHX showed slightly higher levels of MICB protein in comparison to cells treated with CHX alone (Fig. 4). This suggests that upon MG132 treatment there is a certain increase in MICB stability that, however, does not play the major role in MG132-induced MICB upregulation.

4.3 MICB up-regulation is caused by proteasome inhibition but not by blockade of lysosomal degradation

Proteasome inhibitor MG132 can effectively block proteosomal degradation of polyubiquitinated proteins. Moreover, MG132 was also described to be able to block the lysosomal degradation of proteins (Nice et al., 2009). To determine the role of lysosomal degradation in MICB induction, melanoma cell lines were treated with chloroquine, which inhibits lysosomal degradation without affecting proteasomal degradation. Unlike MG132, chloroquine did not change surface expression of MICB within 8 hrs of treatment (Fig. 5). Thus, the inhibition of lysosomal degradation did not contribute to the rapid MICB induction under MG132 treatment.

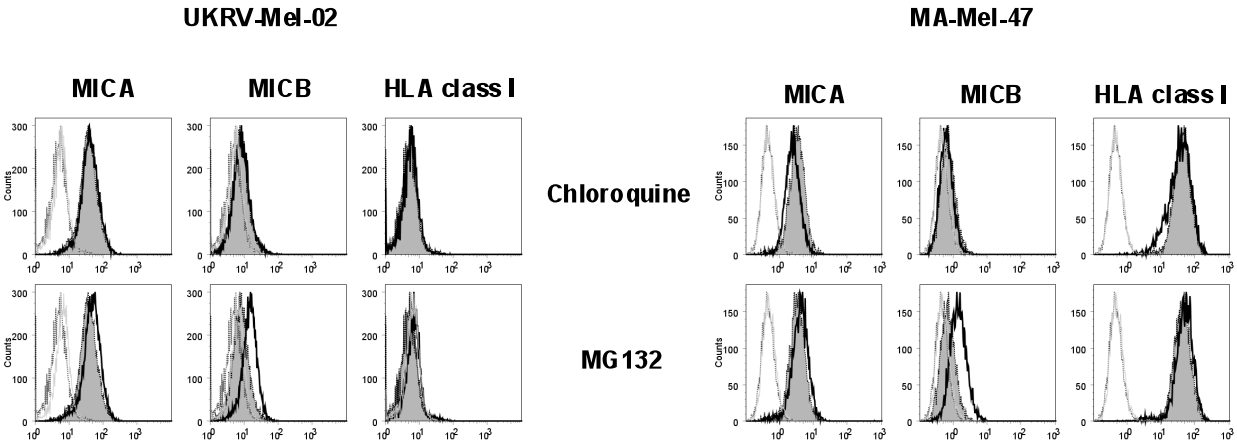

Figure 5. Inhibiton of lysosomal proteases does not induce MICB expression

UKRV-Mel-02 and MA-Mel-47 cells were treated either with Chloroquine (50 µM, top), or with MG132 (10 µM, bottom) or with DMSO (solvent control) for 8 hrs and then analyzed for MICA, MICB and HLA class I surface expression by flow cytometry. Solid black line historgrams represent inhibitor treated cells, gray shaded histograms indicate control cells treated with DMSO (solvent). Gray line histograms – background staining with the secondary PE–conjugated antibody only. Representative data from one of two independent experiments are shown.

4.4 Transcriptional up-regulation of MICB expression under proteasome inhibition

To elucidate the underlying molecular mechanism of MICB upregulation, the influence of proteasome inhibition on MICB specific mRNA levels was determined. Upon MG132

treatment MICB mRNA levels in UKRV-Mel-02 and Ma-Mel-47 cells were strongly induced (Fig. 6), whereas MICA specific mRNA levels were hardly affected. Up-regulation of MICB mRNA was time-dependent. Compared to untreated cells the specific mRNA levels were around three fold increased in UKRV-Mel-02 and more that six fold in MA-Mel-47 cells after 8 hrs of proteasome inhibition.

To determine if the increase in MICB mRNA levels was due to an enhanced mRNA stabilization or an activation of transcription, melanoma cells were treated with MG132 or with MG132 in combination with Actinomycin D, which is known as a potent inhibitor of transcription. Control cells were treated either with DMSO as solvent control or with Actinomycin D alone. As shown in Figure 6, the addition of Actinomycin D completely blocked the induction of MICB mRNA by proteosomal stress, which suggests that MG132 indeed potentiates MICB transcription.

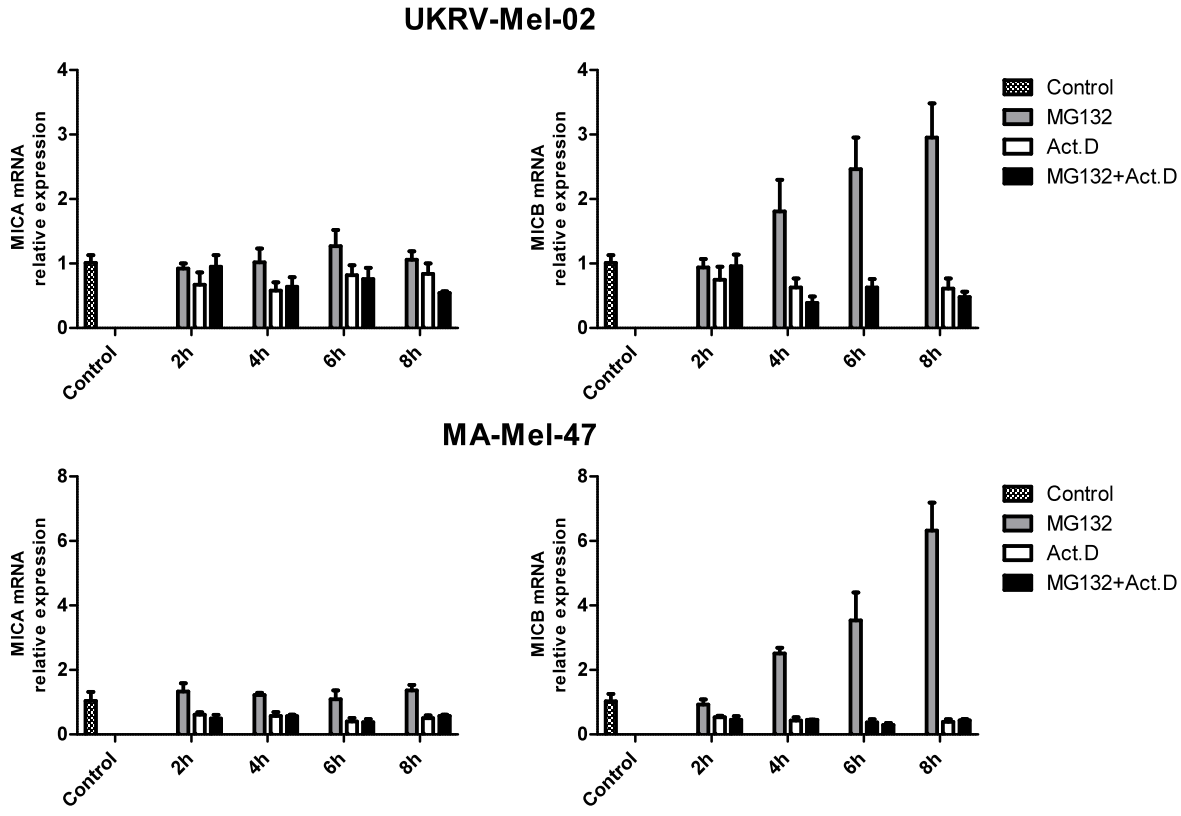

Figure 6. Proteasome inhibition transcriptionally regulates MICB expression in melanoma cells

Quantitative real time PCR analysis of MICA (left) and MICB (right) mRNA expression in melanoma cells UKRV-Mel-02 (top row) and MA-Mel-47 (bottom row) after treatment either with MG132 (10µM) alone, with Actinomycin D (1µg/ml) alone or with a combination of both drugs for the indicated period of time. Control cells were treated with DMSO for 8 hrs and set to one. MIC mRNA levels were normalized to endogenous GAPDH levels. PCR reactions were performed in triplicates, error bars indicate standard deviation (SD). One representative experiment of two experiments for each cell line is shown.

Again the influence of chloroquine on MICB mRNA levels was tested. Corresponding to the surface expression, no changes in MICA and MICB mRNA expression level were detected in melanoma cells after chloroquine treatment for 8 hrs, while cells treated with MG132 strongly increased MICB mRNA levels (Fig. 7).

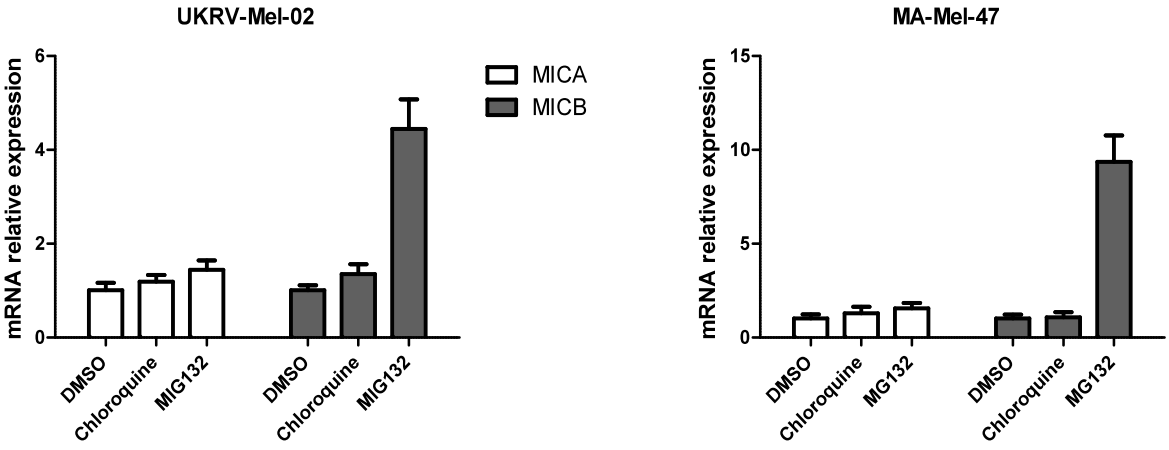

Figure 7. Proteasome blockade but not lysosome inhibition stimulates MICB mRNA up-regulation

UKRV-Mel-02 and MA-Mel-47 cells were treated either with Chloroquine (50 µM), or with MG132 (10 µM) for 8 hrs and analyzed by qRT-PCR for MICA and MICB mRNA expression. Control cells were treated with DMSO (solvent) for 8 hrs and set to one. MIC mRNA levels were normalized to endogenous GAPDH levels. PCR reactions were performed in triplicates, error bars indicate SD.

4.4.1 Activation of the MICB promoter under proteasome blockage

Recently, promoter regions of the MICA and MICB genes, cloned from colon carcinoma cells HCT116, were described (Venkataraman et al., 2007, Rodríguez-Rodero et al., 2007), which comprised about 500 bp upstream of the translational start side (nucleotide position +1). To determine putative transcription factor binding sites (TFBS) within this region, that are involved in the induction of MICB transcription by MG132, the corresponding nucleotide sequence was analyzed using the MatInspector (Genomatix) database, which predicts potential TFBS based on a weighted matrix approach (Fig. 8A). For both MIC molecules heat shock responsive elements (HSE) were predicted at –200 and –185 bp upstream of the start codon for MICA and MICB, respectively. The HSE sites were shown to be relevant for the up-regulation of MIC expression under heat shock and oxidative stress (Venkataraman et al., 2007). Interestingly, the activation of HSF1 in MG132 treated cells has been indirectly demonstrated via activation of HSP70 a direct target of HSF1 (Bush et al.,

1997). Moreover, a putative binding site for Nuclear respiratory factor 1 (NRF1) was predicted about 60 bp upstream of the HSE within the MICB promoter, which could play a role in the expression regulation of MIC molecules under the oxidative stress.

To study the MIC promoter activity under proteotoxic stress a number of MICB and one control MICA promoter constructs were generated by cloning fragments into the promoterless pGL4.10 vector: pMICB–470; pMICB–225; pMICB–115 and pMICA–455, encompassing 470 bp, 225 bp and 115 bp and 455 bp upstream of the start codon, respectively (Fig. 8B). These constructs were tested for their ability to drive the Firefly luciferase reporter gene in transiently transfected melanoma cells (Fig. 9). For normalization the pGL4.10 derivatives were co-transfected with the pGL4.74 plasmid, containing the Renilla luciferase gene under control of the HSV-TK promoter.

The transfection experiments revealed that the strength of the luciferase signal in cells transfected with the pMICB-225 construct was at least two fold lower compared to cells transfected with the pMICB-470 plasmid. The pMICB-115 construct did not yeld any detectable luciferase signal. To study the effect of proteasome inhibition on MICB promoter activity, UKRV-Mel-02 and MA-Mel-47 cells treated with MG132 24 hrs after transfection (Fig. 9). The luminescent signal obtained for proteasome-inhibitor treated cells transfected with pMICB–470 and pMICB–225 constructs were about three fold stronger for UKRV-Mel-02 and ten fold and five fold stronger in MA-Mel-47 cells compared to untreated controls. No induction in luciferase activity after proteasome inhibition was detected for cells transfected with the pMICB–115 plasmid, which does not contain any HSE. Cells transfected with pMICA-455 showed three (UKRV-Mel-02) to five fold (MA-Mel-47) higher luciferase expression under MG132 treatment. Mock-transfected cells displayed similar luciferase activities under all conditions. In contrast activity of the positive control plasmid pGL4.13 containing the firefly luciferase under control of the SV40 early enhancer/promoter region, which provides strong luciferase expression was down-regulated under MG132 treatment. The same was true for the Renilla luciferase expression plasmid pGL4.74, used for normalization. Therefore, the Renilla luciferase values from DMSO-treated cells were used for normalization of Firefly luciferase signals of both DMSO-treated and proteasome inhibitor treated cells.

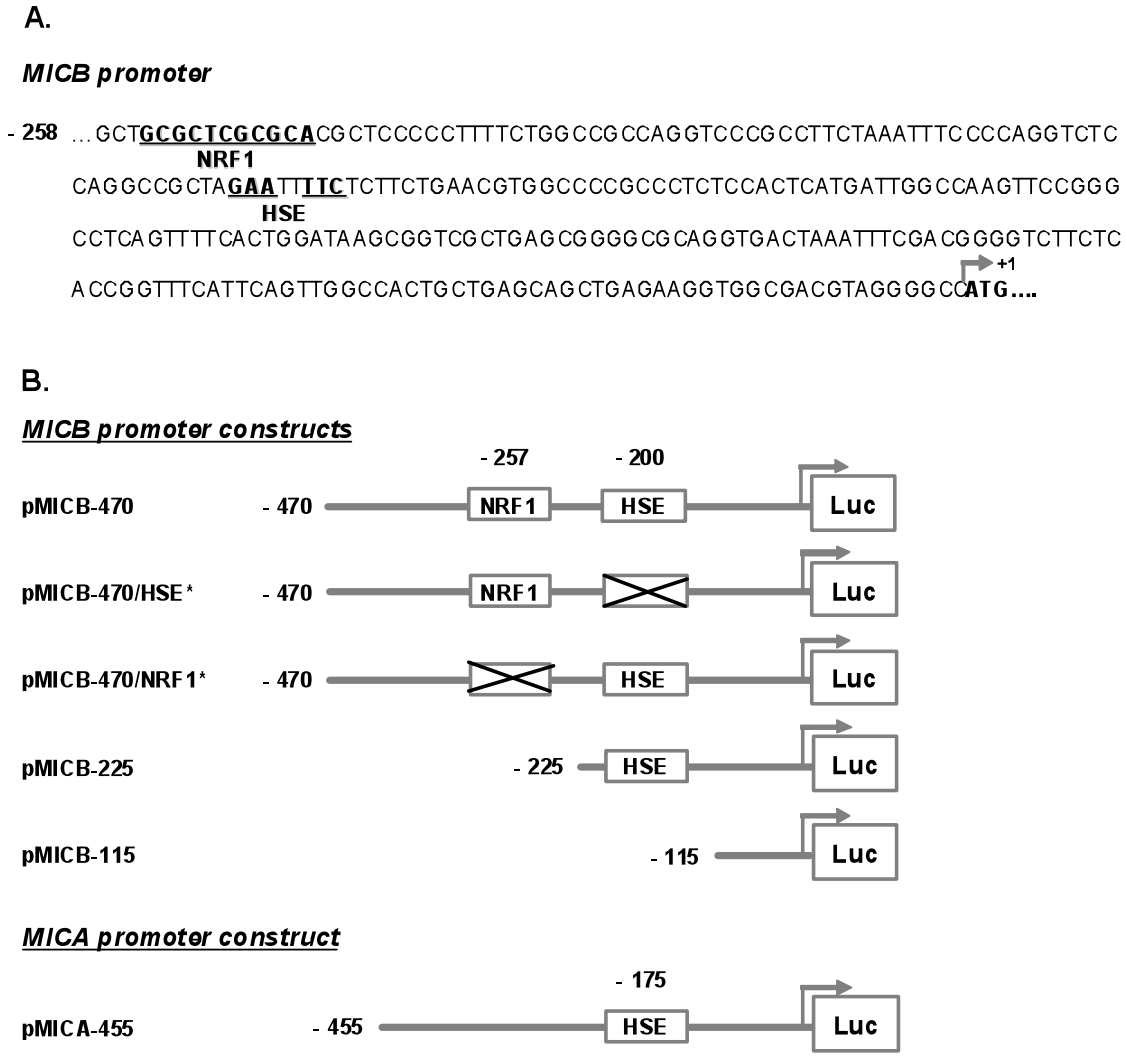

Figure 8. MICB and MICA promoter constructs

A. Sequence of the MICB promoter region. The arrow indicates the start codon, marked by +1. Predicted binding sites for transcription factors are given in bold and underlined.

B. Schematic presentation of the MICB and MICA promoter fragments cloned into the pGL4.10 vector and used for the studies on MIC promoter activity under proteotoxic stress. HSE – heat shock responsive element; NRF1 – nuclear respiratory factor 1 binding site. For analysis of the MICB promoter activity five different constructs were generated, containing fragments of the following size/characteristics: –470 bp; –470 bp/HSE* with mutated binding site for HSF1; –470 bp/NRF1* with mutated predicted NRF1 binding site; –225 bp; –115 bp for MICB and –455 bp for MICA.

Thus, proteotoxic stress significantly stimulates MICB promoter activity and the presence of heat shock responsive element located about 200 bp upstream the translation start seems to be essential for enhancing MICB transcription.

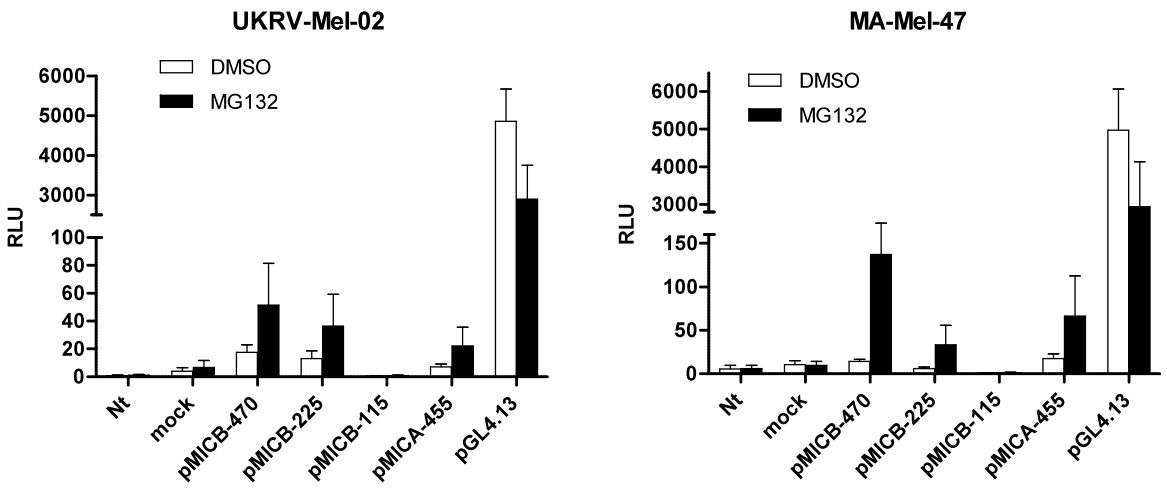

Figure 9. Influence of the proteotoxic stress on MIC promoters in melanoma cells

Indicated are the Firefly luciferase reporter gene activities driven by MICB and MICA promoter fragments of the indicated length. The MICB and MICA promoter constructs were transiently transfected in UKRV-Mel-02 and MA-Mel-47 cells. Control cells were transfected either with the promoterless pGL4.10-basic vector (mock), the pGL4.13 positive control plasmid or left untransfected. For normalization Renilla luciferase expression plasmid pGL4.74 was co-transfected. After 24 hrs, 10 µM MG132 or DMSO (solvent control) were added, cells were incubated for 8 hrs, then harvested and analyzed for Firefly and Renilla luciferase activities. Assays were done in triplicates. Data are means of at least five independent experiments. Error bars indicate SD.

4.4.2 The HSF1 and the potential NRF1 binding sites are relevant for MICB promoter activity

In order to analyze the functional significance of the HSF1 and the predicted NRF1 binding sites for MICB transcription under proteotoxic stress, pMICB–470 derivatives with specific mutations in the corresponding DNA elements were generated yielding pMICB-470/HSE* and pMICB-470/NRF1*. In transfected melanoma cells the pMICB-470/HSE* constructs mediated a slightly decreased luciferease activity compared to pMICB-470. More important, under MG132 treatment the induction of luciferase activity for the pMICB-470/HSE* constructs was almost completely abrogated (Fig. 10), indicating that binding of HSF1 to HSE is essential for MICB promoter activation by proteotoxic stress. The cells transfected with pMICB-470/NRF1* showed diminished luciferase activity pointing out the relevance of this element for MICB expression in melanoma cells. The response of this construct to proteasome inhibition was also impaired.

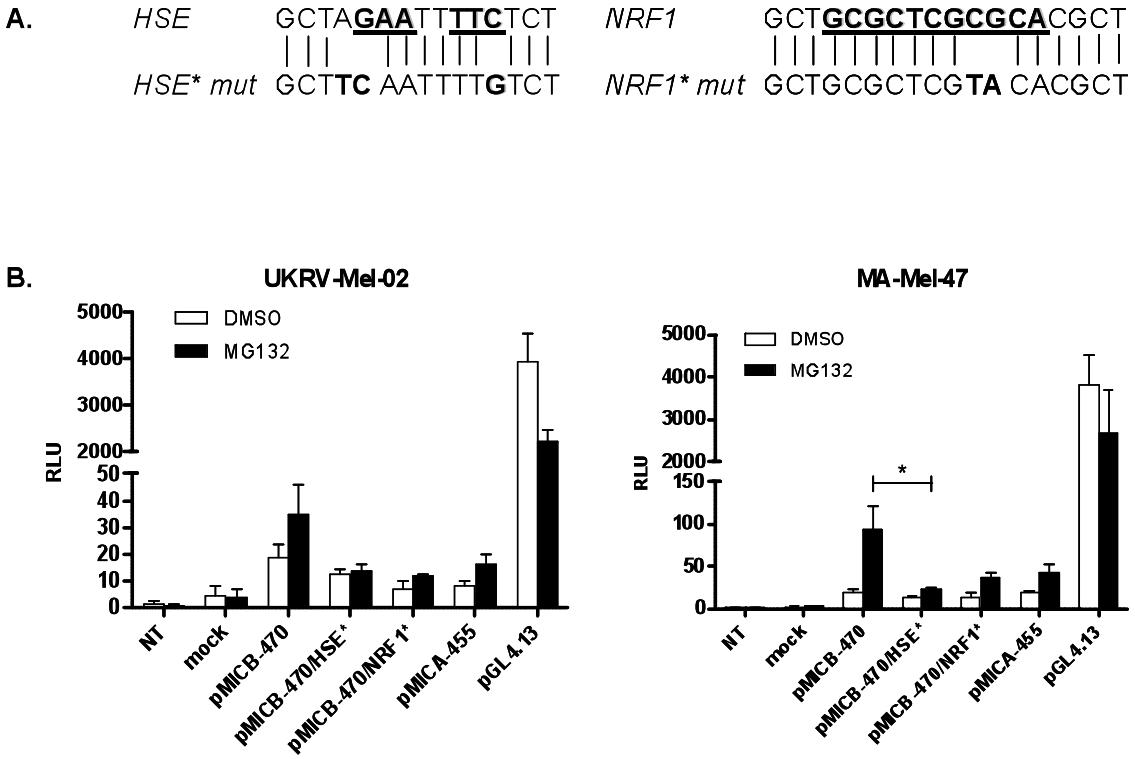

Figure 10. Effect of mutations in HSF1 and putative NRF1 binding sites on MICB promoter activity

A. Part of promoter region sequences around the known shock responsive element (HSE) and the putative nuclear respiratory factor 1 binding site (NRF1). Conserved nucleotides of the binding sites are underlined. The nucleotides in bold were exchanged by site-directed mutagenesis.

B. pMICB-470, pMICB-470/HSE*, pMICB-470/NRF1* and pMICA-455 were transiently transfected in UKRV-Mel-02 and MA-Mel-47 cells. Control cells were transfected either with pGL4.10 (mock), or with pGL4.13 (positive control) or left untransfected. 24 hrs after the transfection 10 µM MG132 or DMSO as the solvent control were added, cells were incubated for 8 hrs, then harvested and analyzed for luciferase activity. Assays were done in triplicates. Data are representative of at least three independent experiments with pMICB-470/HSE*, only the pMICB-470/NRF1* construct was tested in two independent experiments. (*, p = 0.0372).

Statistic analysis was done by GraphPad Prism program using standard paired t-test.

4.5 Proteotoxic stress mediated MICB induction is controlled by HSF1

4.5.1 Expression of a constitutive active HSF1 variant stimulates MICB reporter gene activity

Both, the MICA and MICB promoter region contain a HSE sequence about –200 bp upstream of the ATG start codon. As described above, the mutation of the HSF1 binding site within the MICB promoter interfered with the induction of promoter activity by MG132 treatment and suggests that, indeed, HSF1 stimulates MICB transcription under proteotoxic stress. To further examine the role of HSF1, a constitutively active form of HSF1 was expressed in melanoma cells. The constitutively active HSF1 variant is deleted of a regulatory

domain that normally suppresses the C-terminal activation domain of HSF1. The active HSF1 variant was encoded by the two different expression plasmids pHβAPr-hHSF1ΔRD and pLNCX2-hHSF1ΔRD. The construct pHβAPr-hHSF1ΔRD mediates expression of HSF1 by the human β-actin promoter, while on pLNCX2-hHSF1ΔRD the human cytomegalovirus promoter activates HSF1 expression. As controls the empty vectors, deleted of the inserts, were used. To analyze the effect of active HSF1 on MICB promoter activity melanoma cells were co-transfected with the HSF1 expressing plasmids and the different pMICB and pMICA reporter gene constructs (Fig. 11).

Co-transfection of pMICB–470 and pMICB–225 with pHβAPr-hHSF1ΔRD led to a ten fold up-regulation of luciferase reporter gene activity, while co-transfection with the control vector pHβAPr-1-neo yielded signals comparable to those obtained for transfection of pMICB constructs alone. Similar to pHβAPr-hHSF1ΔRD also the HSF1 expression plasmid pLNCX2-hHSF1ΔRD induced reporter gene expression. Co-transfection of the HSF1 expression plasmids with pMICB–115 or pGL4.10 did not lead to any reporter gene expression. Constitutive active HSF1 also induced activity of the MICA promoter on pMICA-455, similar to pMICB–470.

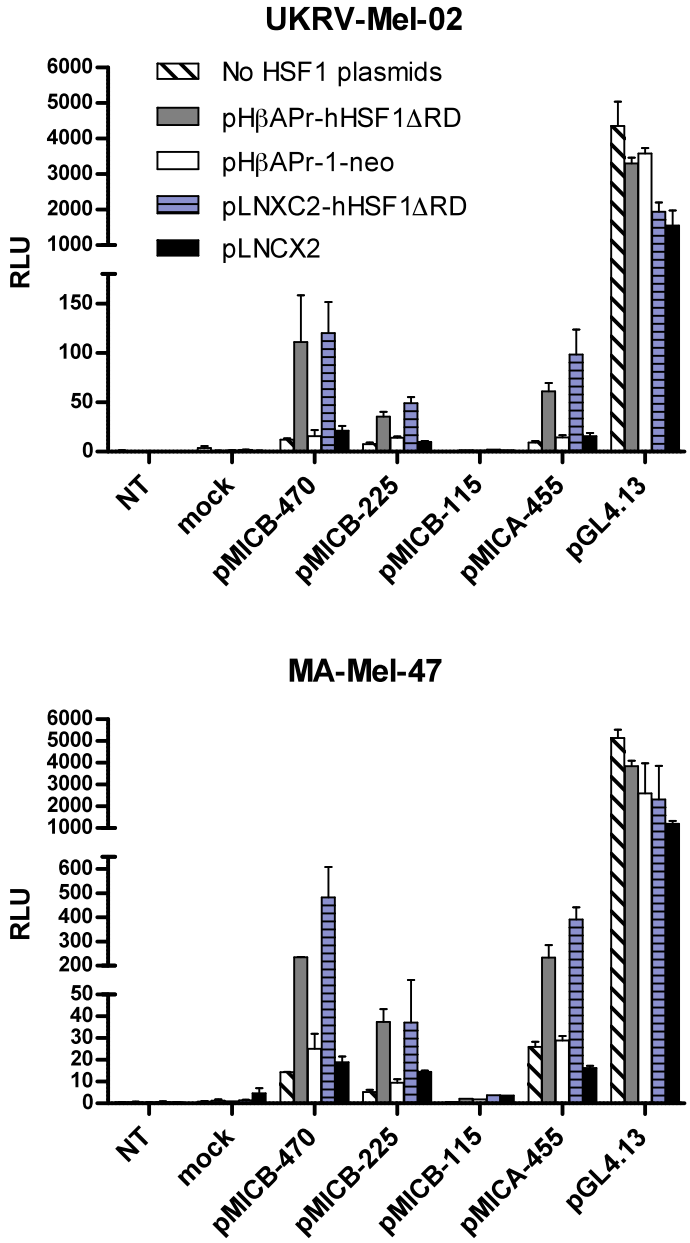

Figure 11. Influence of constitutive active HSF1 on the activity of the MIC promoters

The different MICB (pMICB–470, pMICB–225, pMICB–115) and MICA (pMICA–455) promoter constructs were transiently transfected into UKRV-Mel-02 and MA-Mel-47 cells. Control cells were transfected with pGL4.10 (mock, neg. control) or with pGL4.13 (positive control). Where indicated, cells were cotransfected with expression plasmids (pHβAPr-hHSF1ΔRD, pLNCX2-hHSF1ΔRD) for constitutive active HSF1 (HSF1ΔRD), or with empty control plasmids (pHβAPr-1-neo, pLNCX2). NT – cells transfected with HSF1 plasmids (or control plasmids) without pGL4 luciferase bearing vectors only. Twenty-four hrs after transfection cells were harvested and analyzed for luciferase activity. Assays were done in triplicate. Data are representative of at least three independent experiments. Error bars indicate SD.

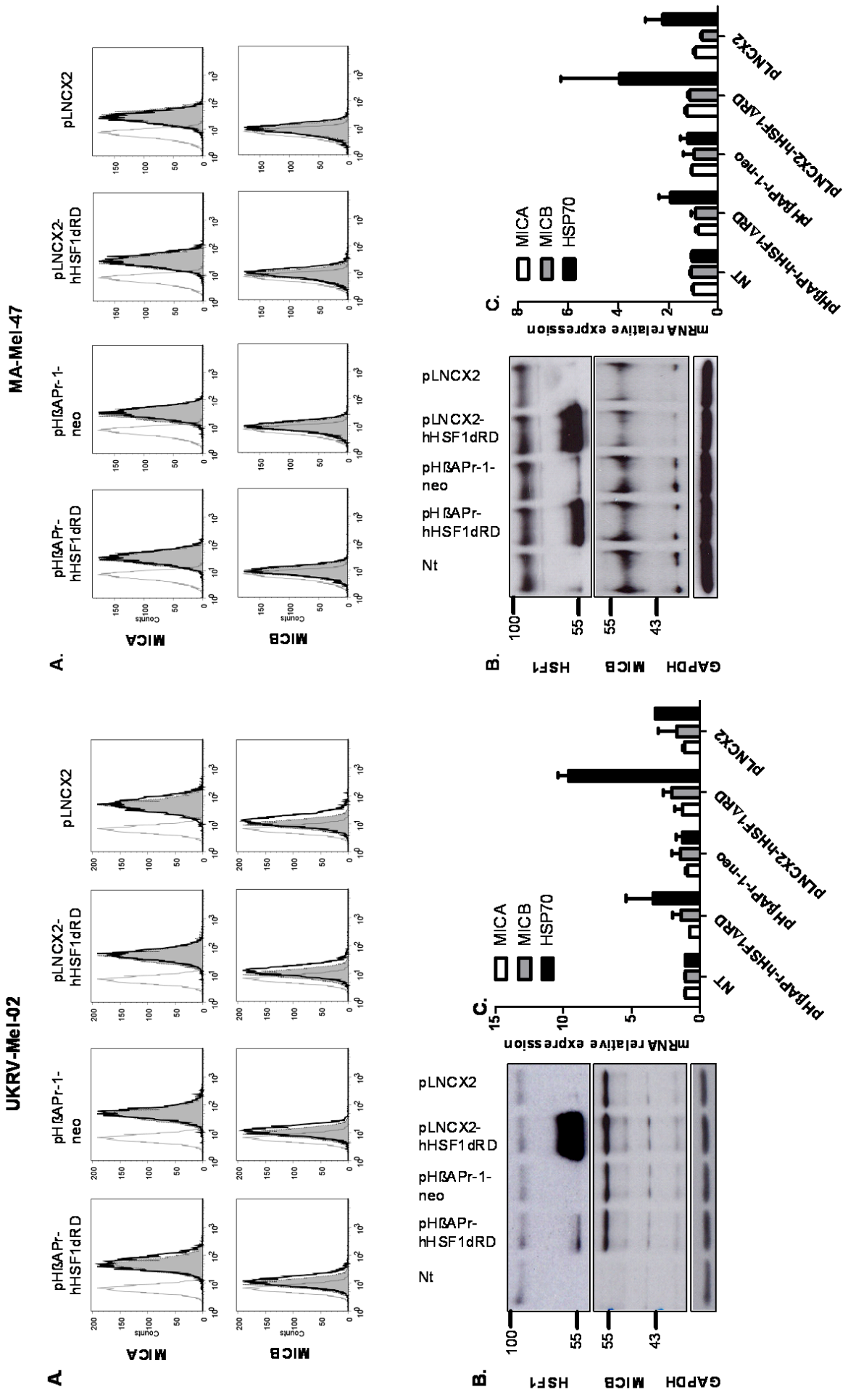

Figure 12. Influence of constitutive active HSF1 on the expression of endogenous MIC molecules

*** Figure 12. Influence of active HSF1 on the expression of endogenous MIC molecules**

Melanoma cell lines UKRV-Mel-02 and MA-Mel-47 were transfected either with HSF1 expression plasmids (pHβAPr-hHSF1ΔRD, pLNCX2-hHSF1ΔRD) or empty control plasmids (pHβAPr-1-neo, pLNCX2), or left untreated. Twenty-four hrs after transfection, cells were harvested and analyzed for the surface expression of MIC molecules, total MICB protein and MICA, MICB and HSP70 mRNA levels. Representative results from one of two independent experiments are depicted.

A. Cells transfected with HSF1 expression plasmids or with control plasmids (black lines) or left untransfected (gray shaded histograms) were stained with unconjugated mouse anti-MICA and anti-MICB mAb followed by PE-conjugated goat F(ab')2 anti-mouse IgG and analyzed by flow cytometry for MIC surface expression. Light gray lines – background staining with the secondary PE–conjugated antibody only.

B. Cells were harvested for whole cell lysate preparation. Proteins were analyzed by Western blot for the expression of total MICB protein. Control cells were left untransfected (first line – Nt). GAPDH was used as the loading control.

C. Quantitative RT-PCR analysis of MICA, MICB and HSP70 mRNA expression in total RNA isolated from transfected cells. Expression levels form nontransfected control cells (NT) is set to one. Ct values of MICA and MICB were normalized to GAPDH Ct values. PCR reactions were performed in triplicates, error bars indicate SD. One representative experiment of two experiments for each cell line is presented.

4.5.3 HSF1 silencing interferes with MICB induction under proteasome inhibition

Site-directed mutagenesis of the HSE sequence within the MICB promoter region led to the loss of MICB promoter responsiveness to proteotoxic stress induced by MG132 treatment of the cells. As HSE is the conserved binding site for activated HSF1 this suggests that HSF1 is essential for MICB up-regulation under proteasome inhibition. Although, expression of constitutive active HSF1 failed to induce endogenous MICB it strongly stimulated plasmid-based reporter gene expression driven by the MICB promoter. In order to demonstrate the functional relevance of HSF1 for MICB up-regulation under proteasome inhibition a transient knock-down of HSF1 in melanoma cells with specific siRNA was performed.

As shown at the Fig. 13, in both cell lines HSF1 was effectively silenced by siRNA HSF1 while control siRNA LUC did not affect HSF1 expression. Followed by siRNA transfection, cells were treated with MG132 and whole cell lysates were analyzed by Western blot for total MICB expression. In untransfected control cells as well as in cells transfected with siRNA LUC, treatment with proteasome inhibitor MG132 strongly enhanced MICB protein levels as compared to the untreated cells. Silencing of HSF1 led to a complete abrogation of MICB induction in UKRV-Mel-02 cells and strongly impaired MICB increase in MA-Mel-47 cells upon proteasome inhibition. The deregulated MICB response to MG132 treatment in cells with an HSF1 knock-down clearly demonstrates the requirement of this transcription factor for the induction of MICB expression under this kind of stress.

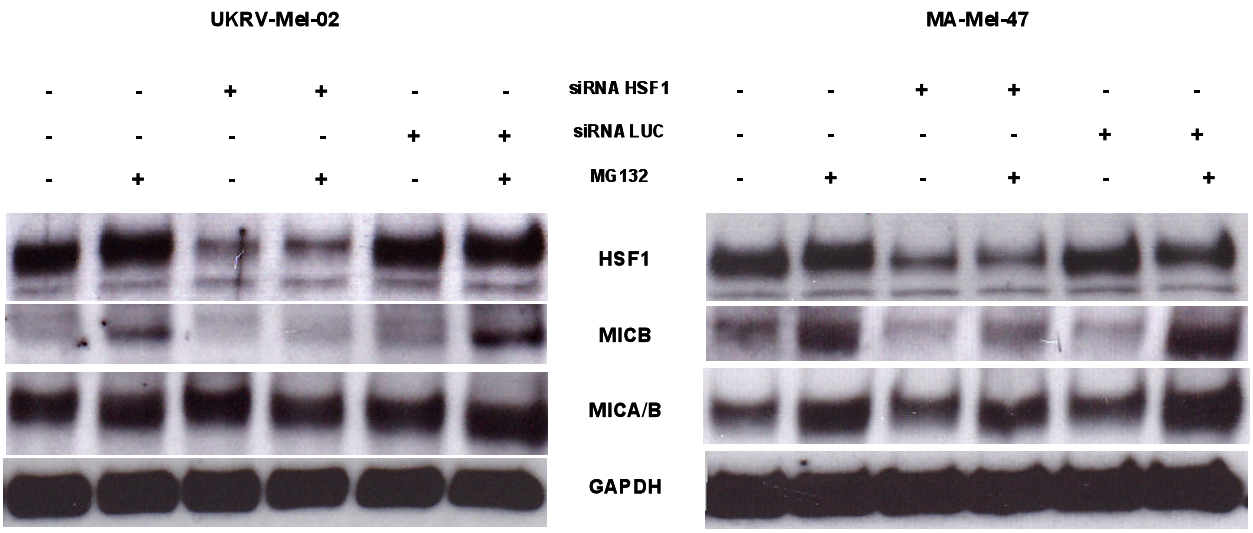

Figure 13. Influence of HSF1 silencing on MICB expression

Melanoma cell lines UKRV-Mel-02 and MA-Mel-47 were transfected with siRNA against HSF1, or with control siRNA LUC, or left untransfected. Fourty-eight hrs after transfection, cells were treated with 10 µM MG132, or with DMSO (solvent control) for 8 hrs, then harvested and used for whole cell lysate preparations. Lysates were analyzed by Western blot for the level of HSF1 and MICB protein. GAPDH served as loading control. The results are from one representative of three independent experiments.

4.5.4 Interaction of HSF1 with the MICB promoter is epigenetically regulated

Our results show that HSF1 is essential for MICB upregulation in melanoma cells under MG132 treatment. However, expression of a constitutive active HSF1 variant in melanoma cells only stimulated the activity of the plasmid-located but not of the endogenous cellular MICB promoter. This suggest that induction of MICB expression under proteasome inhibition is more complex and not just dependent on the activation of HSF1. Furthermore it suggests that the endogenous MICB promoter might be epigenetically closed. Ubiquitinated histone H2A (uH2A) has been described to act as a repressor of transcription. This repression is released upon deubiquitination of H2A (Zhou et al., 2008). Interestingly, inhibition of the proteasome has been described to elicit a very fast uH2A deubiquitination by depletion of the pool of free ubiquitin in the cell (Dantuma et al., 2006).

Inhibition of the proteasome in UKRV-Mel-02 and Ma-Mel-47 cells led to the enrichment of polyubiquitinated proteins, as demonstrated by a Western blot (Fig. 14). Importantly, MG132 treatment of melanoma cells was also found to rapidly deplete uH2A (25 kD), already 0.5 hrs after the onset of proteasome inhibition. No uH2A was detectable after 4 hrs of treatment (Fig. 14).

These results suggest that deubiquitination of uH2A upon proteasome inhibition might allow active HSF1 to access the MICB promoter and to enhance MICB transcription. To confirm that the MICB promoter is indeed regulated by uH2A, chromatin immunoprecipitation (ChIP) assays were performed. Chromatin from nuclear pellets of MA-Mel-47 cells, previously showing the strongest response to proteasome inhibitor treatment, was immunoprecipitated by anti-uH2A and anti-HSF1 antibodies and bound DNA was further analyzed by PCR using primer sets flanking different regions of the MICB promoter (Fig.15A). The ChIP analysis demonstrated an enhanced HSF1 recruitment to the MICB promoter under MG132 treatment. At the same time, proteasome inhibition decreased the level of uH2A at the MICB promoter, caused by the deubiquitination of the latter (Fig. 14).

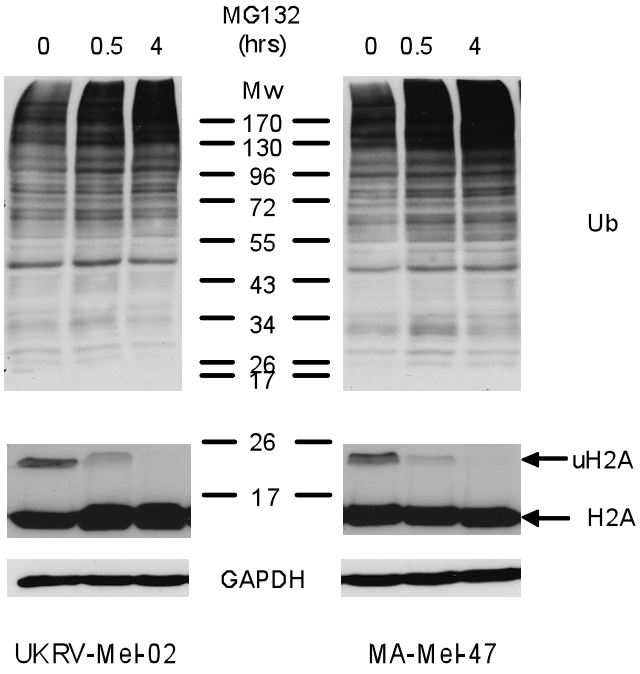

Figure 14. Proteasome inhibition leads to a rapid depletion of free ubiquitin and deubiquitination of monoubiquitinated H2A

UKRV-Mel-02 and MA-Mel-47 cells were treated with MG132 (20 μM) for 0.5 and 4 hrs, or with DMSO (solvent control) for 4 hrs, then harvested and used either for total protein isolation or for histone acid extraction. Total protein was separated by SDS-PAGE and probed with anti-ubiquitin polyclonal Ab (FK2) recognising both monoubiquitin and polyubiquitin chains (top). Acid histone extracts were separated by SDS-PAGE and probed with anti-H2A polyclonal Ab, recognising both uH2A and H2A, yielding the bands of 25 and 14 kD, respectively (middle). GAPDH was used as the loading control (bottom). The results are representative on of two independent experiments.

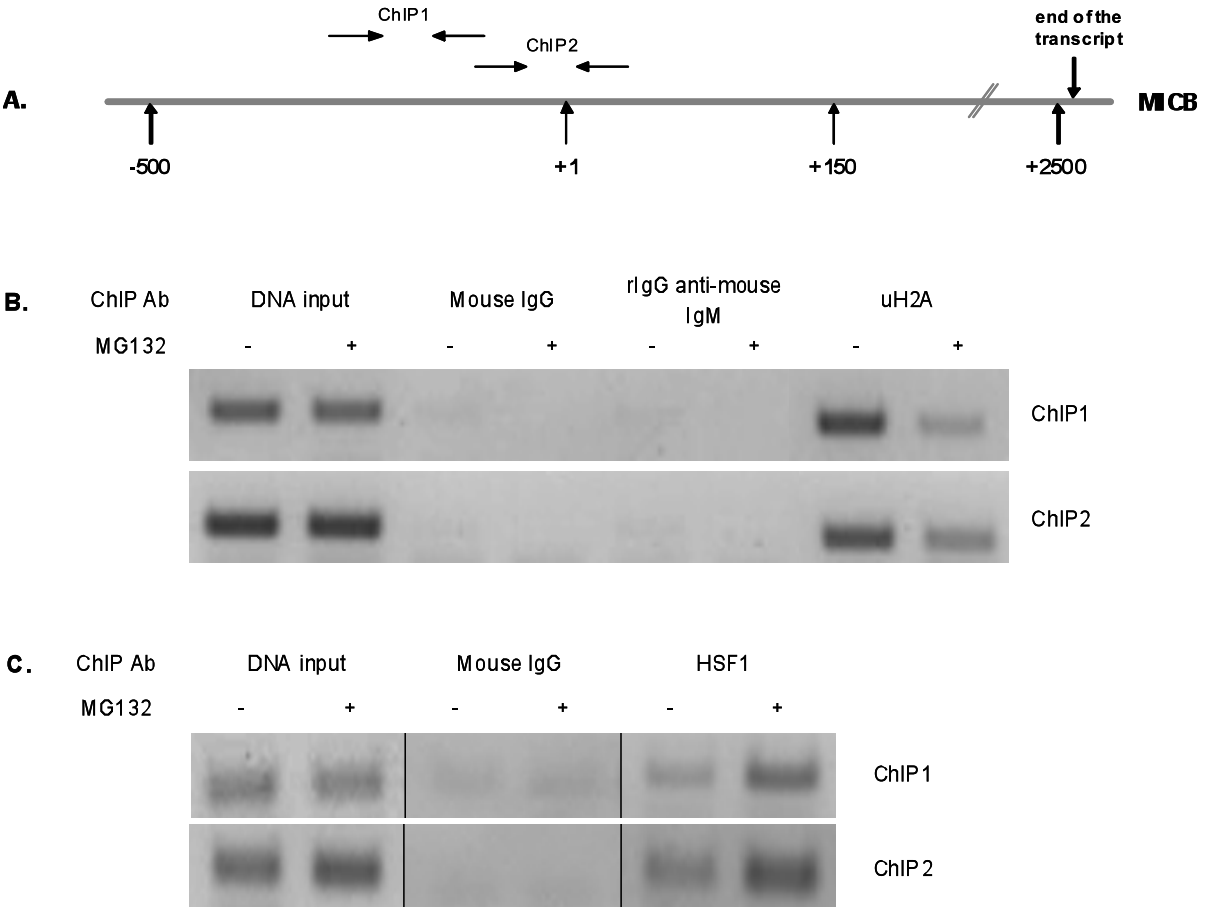

Figure 15. Decrease of uH2A but increase of HSF1 levels at the MICB promoter under proteasome inhibition

A. Schematic representation of the MICB promoter region and the primers used in ChIP experiments.

B–C. MA-Mel-47 cells were treated with MG132 (20 μM) for 4 hrs or with DMSO (solvent control), then fixed, harvested and used for isolation of chromatin. Chromatin was immunoprecipitated by (**B**) anti-human uH2A and (**C**) anti-human HSF1 antibodies. Control antibodies used in ChIP experiments: mouse IgG; rabbit IgG anti-mouse IgM. Immunoprecipitated DNA was amplified by PCR using the indicated primer pairs, yielding the fragments ChIP1 and ChIP2. DNA input corresponds to non-immunoprecipitated chromatin. The data are representative from one of two independent experiments.

Taken together, the MICB promoter is bound to uH2A under normal conditions restricting MICB transcription. Proteotoxic stress facilitates uH2A deubiquitination which increases the accessibility of the MICB promoter for transcription factors. The released promoter in turn can be bound by transcription factors such as HSF1, which subsequently leads to an enhancement of transcription. This represents another aspect in the complexity of the MICB regulation.

4.6 Proteasome inhibition stabilizes the surface expression of MIC molecules

Monoubiquitination of transmembrane proteins is also known as a signal that controls endocytosis. MIC molecules are transmembrane proteins, of which most alleles contain three lysine residues in their cytoplasmic domain. It has been demonstrated that viral ubiquitin ligases mediate ubiquitination of these lysine residues thereby inducing the internalization of MIC molecules (Thomas et al., 2008). Similar to viral ligases also cellular ligases might be involved in the control of MIC internalization and their activity might also be influenced by depletion of free ubiquitin under proteasome inhibition. On the other hand, proteasome inhibition might prolong the membrane residence time of the MIC molecules by blocking the degradation of endocytosed proteins which then recycle back to the membrane. To investigate the stabilizing effect of MG132 on MIC surface expression, melanoma cells were treated with Brefeldin A (BFA), a potent inhibitor of protein transport from the ER to the Golgi. The treatment of melanoma cells with BFA alone led to a tremendous down-regulation of MICA surface expression within 8 hrs, also MICB was no longer detectable on the cell surface (Fig. 16). The presence of MG132 rescued the surface expression of MICA and MICB in both melanoma cell lines. This indicates that proteasome inhibition also influence the surface expression of MIC molecules. The underlying mechanism remains to be elucidated and was beyond the scope of the thesis.

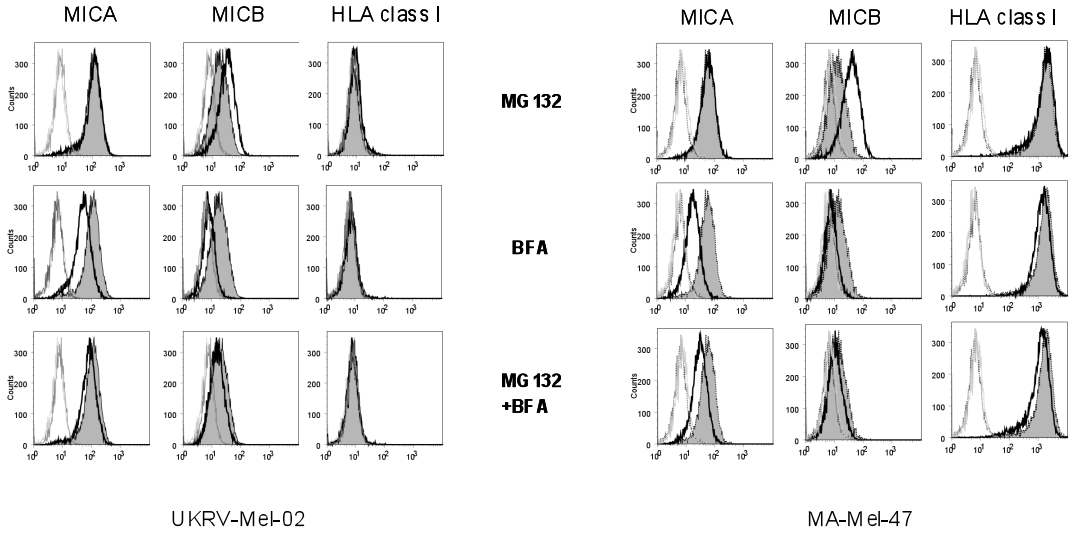

Figure 16. MG132 stabilizes MIC molecules on the cell surface

UKRV-Mel-02 and MA-Mel-47 cells were incubated with 10 µM MG132 (black lines – top), 5 µg/ml BFA (black lines – middle), or with MG132 and BFA (black lines – bottom) simultaneously for 8 hrs and then analyzed for MICA, MICB and HLA class I surface expression by flow cytometry. Control cells were treated with the solvent DMSO (shaded histograms). Gray lines – background staining with the secondary PE–conjugated antibody only. The results are representative from one of the three independent experiments.

5 Discussion

Malignant melanoma is one of the most aggressive tumors, with a persistently rising incidence rate over the last decades. The metastatic tumor displays a marked resistance to conventional cytotoxic drugs resulting in disappointing clinical outcomes when currently available chemotherapeutic treatment strategies are used (Soengas et al., 2003; Chin et al., 2006). In principle, the patient's immune system has the capability to recognize and kill tumor cells. Several melanoma-associated antigens have been characterized which are recognized by cytotoxic $CD8^+$ T cells in the complex with surface MHC class I molecules. Recently, a number of clinical studies have demonstrated specific interaction and effective eradication of melanoma cells by adoptively transferred T cells (Straten and Becker, 2009). Thus, immunotherapy might be a promising alternative strategy for the treatment of malignant melanoma.

However, during progression melanoma cells can down-regulate or completely loose MHC class I expression, which interferes with the effective recognition and eradication of the tumor cells by T cells. In our lab it was demonstrated that the loss of MHC class I expression in melanoma metastases is generally due to mutations in the gene encoding β2-microglobulin, which is part of the MHC class I complex (Paschen et al., 2003; 2006). Loss of MHC class I molecules allows melanoma cells to escape immune surveillance by T cells, but at the same time, according to the "missing self" theory, those tumor cells become targets for NK cells, given that they express ligands for activating receptors of NK cells on their surface. If activatory ligands are not present on the tumor cell, effective recognition and elimination by NK cells cannot take place. Recently, a number of activating receptors on NK cells have been described (reviewed by Eagle and Trowsdale, 2007; López-Larrea et al., 2008). One of the key receptors in the anti-tumor activity of NK cells is the C-type lectin-like molecule NKG2D triggering cytokine as well as perforine and granzyme release. In fact, it has been shown that NKG2D contributes to the early recognition and elimination of tumors by NK cells and knock-down of the expression of this receptor in mice yielded an increased incidence of spontaneous tumors (Guerra et al., 2008).

In humans, NKG2D is expressed on NK cells, some NKT cells and $CD8^+$ T cells (Champsaur and Lanier, 2010). On activated NK cells it functions as a main activating receptor, while on T cells NKG2D mostly plays a co-stimulatory role. Once bound to its surface ligand on a target cell the NKG2D receptor delivers activating signals into an effector cell. So far eight NKG2DL have been identified in human: MICA, MICB, ULBP1-6. The

present study focused on the analysis of MICA and MICB expression and the differences in their regulation under proteotoxic stress caused by proteasome inhibition.

5.1 *In situ* expression and shedding of NKG2D ligands

NKG2DL are stress molecules, which are commonly found to be restricted under normal conditions *in vivo*, thereby preserving normal cells from the recognition and elimination by NK cells and certain T cells. However, NKG2DL expression has also been reported on some cells that could not be described as stressed or damaged. For example activated T cells can express NKG2DL, and constitutive expression of NKG2DL has been reported on normal myelomonocytic cells, dendritic cells, and epithelial cells of the gut mucosa (reviewed by Eagle et al, 2009), suggesting that NK cells can play a role in the regulation of inflammatory responses preventing the persistent over-activation of $CD8^+$ T cells via their direct killing, or killing of helper cells, such as antigen-presenting cells. T regulatory cells (Tregs) have also been shown to be targets for NK cells, though their elimination by NK cells might be regulated via NKG2DL-independent mechanism. NKG2DL expression on epithelial cells in the gut or airways might be explained by the fact that these cells have to be often renewed due to their guardian function as a barrier for pathogens (Eagle et al., 2009).

Many tumor cell lines and freshly isolated primary tumors express NKG2DL. Tumor cells extracted from patients with different types of leukemia, including AML, ALL, CML, and CLL, express heterogeneous levels of NKG2DL (Salih et al., 2003). In addition, using the human NK cell line NKL as effector cells it was shown that expression of NKG2DL on patient AML and CML cells rendered them susceptible to NK cell mediated lysis in an NKG2D-dependent manner. MICA and MICB are expressed in a subset of human hepatocellular carcinoma tissues and are involved in hepatoma cell sensitivity to NK cell killing *in vitro* (Armeanu et al., 2008). Primary glioma cultures as well as glioma cell lines display surface NKG2DL expression (Friese et al., 2003). In colorectal cancer high levels of MICA *in situ* are associated with a good prognosis (Watson et al., 2006).

Human melanoma cells can express NKG2DL *in situ* (Vetter et al., 2002; Paschen et al., 2009), but NKG2DL expression has been described to be lost during the progression of uveal melanoma (Vetter et al., 2004). In our lab it was shown that melanoma cells cultured *in vitro* as well as tumors *in situ* show expression of MICA and ULBP2, though expression of the ligands within metastatic tumors was often very heterogeneous. Melanoma cells were effectively recognized and lysed by NKL cells in an NKG2D-dependent manner. Blocking of the NKG2D receptor led to an impaired lysis of melanoma cells *in vitro* (Paschen et al., 2009;

Schwinn et al., 2009). Immunohistochemistry analyses on tumor metastases, controlled by staining against HMB-45 a melanoma-associated antigen, demonstrated that expression of NKG2DL within the lesions varied and in some tumors MIC-positive cells were primarily located at the periphery of the tumor. This suggests that *in situ* expression of NKG2DL in the melanoma could be influenced by the microenvironment, by cell-cell contacts as well as by soluble factors like cytokines (Paschen et al., 2009; Schwinn et al., 2009). Another explanation for the low level of NKG2DL expression *is situ* might has been suggested to be their proteolytic shedding (Salih et al., 2002). It has been shown that decreased levels of MICA on gastrointestinal tumor cell lines were due to the activity of extracellular matrix metalloproteinases (MMPs). The blocking of proteinases by MMP inhibitors resulted in a reduced ligand release and sustained surface expression of MICA. NKG2DL shed by tumor cells become detectable in patient sera, thus, the levels of soluble MICA were significantly higher in sera of patients with gastrointestinal malignancies as compared to sera of healthy donors (Salih et al., 2002). Recently it has been shown that NKG2DL shedding in advanced diseases also has "clinical significance". Our group has demonstrated that enhanced levels of sNKG2DL can be detected in sera of melanoma patients which were associated with poor prognosis (Paschen et al., 2009). The soluble forms of NKG2DL are still able to bind to the NKG2D receptor thereby causing persistent activation of NK cells, which in turn leads to the internalization of NKG2D and reduced reactivity of NK cells against the tumor cells. Hence, the poor prognosis associated with NKG2D ligand release might on the one hand be due to a decrease in melanoma immunogenicity but on the other hand, might also be supported by an impaired NK cell activity. These observations suggest that therapeutic up-regulation of NKG2DL expression might be a promising strategy to increase immunogenicity of melanoma.

5.2 Signals controlling expression of NKG2D ligands

At present the regulation of NKG2DL is intensively studied. A number of different stresses inducing NKG2DL expression on the cell surface have been described. It has been also shown that depending on the type of the stress, different ligands are induced. Viral infection induces expression of NKG2DL, but exact mechanism of this induction is for most part unknown. Viral proteins can either directly affect NKG2DL transcription (Venkataraman et al., 2007), or the release of cytokines upon infection can indirectly control NKG2DL expression (Cerwenka and Lanier, 2001; Champsaur and Lainier, 2010). Some viruses like mouse and human CMV evolved mechanisms to retain NKG2DL in the cell and to prevent their surface expression (Dunn et al., 2003; Thomas et al., 2008).

Different cytokines, in particular interferons, have been described to control NKG2DL expression. Our own studies revealed a STAT1-dependent down-regulation of MICA in human melanoma under IFN-γ treatment (Schwinn et al., 2009), while on monocytes IFN-γ has been demonstrated to induce MIC expression (Wang et al., 2009), suggesting that the cellular context might influence the outcome of NKG2DL expression.

Up-regulation of MICA and MICB ligands has been reported under oxidative stress and heat shock stress in human colon carcinoma cells HCT116 (Venkataraman et al., 2007), Oxidative stress can induce DNA damage. Indeed, DNA damage has been described to cause an up-regulation of NKG2DL via ATM and ATR dependent mechanisms. Gasser et al. demonstrated that ionizing irradiation of secondary human foreskin fibroblasts stimulated ULBP1, 2 and 3 as well as MICA expression via ATM/ATR, which sense DNA double-strand breaks and stalled DNA replication, respectively, resulting in cell cycle arrest, DNA repair or apoptosis (Gasser et al., 2005).

5.3 Proteasome inhibiton induces expression of NKG2D ligands on tumor cells

Within the present study the influence of proteasome inhibition on NKG2DL expression in melanoma cells was analyzed. Proteasome inhibitors are currently tested as small therapeutic molecules for the treatment of different tumor entities, including melanoma (Russo et al., 2010; Su et al., 2010). As the proteasome is the major cellular proteolytic machinery, drugs blocking its activity cause an accumulation of polyubiquitinated proteins in the cytosol, the nucleus and induce an ER associated degradation stop (Adams, 2004). The signals elicited by proteasome inhibitors in tumor cells are multifaceted. Proteasome inhibitors are shown to induce apoptosis in highly proliferating tumor cells, which have a robust protein turn-over, while less affecting normal, quiescent cells (Almond and Cohen, 2002). Proteasome blockade suppresses the NF-κB pathway preventing digestion of the inhibitory subunit IκB, leading to cell cycle arrest. (Chauhan et al., 2005). Moreover, blockade of proteasome function activates caspases as well as pro-apoptotic proteins such as BH3-only proteins and PUMA triggering apoptosis via the p53/PUMA pathway (Concannon et al., 2006).

In the present study we demonstrated that treatment of human melanoma cells with proteasome inhibitors led to an up-regulation of NKG2DL expression. We found that proteotoxic stress induced upon proteasome inhibition strongly stimulated MICB expression in melanoma cells via direct activation of the MICB promoter. In addition to that prolonged proteotoxic stress was able to induce surface expression of MICA and ULBP2, though, this

up-regulation was considered to be the result of complex secondary effects. Under the conditions tested we observed an induction of NKG2DL on MHC class I-negative and MHC class I-positive tumor cells, while the surface expression of MHC class I molecules, as measured by flow cytometry, was not affected. Thus, by inducing NKG2DL expression on MHC class I-negative and MHC class I-positive melanoma cells, proteasome inhibitors may facilitate target cell recognition and killing by NK cells and $CD8^+$ T cells, respectively. Indeed, Armeanu et al. demonstrated an increased recognition of proteasome inhibitor treated HCC cells by NK cells that was mediated by the NKG2D receptor (Armeanu et al., 2008). They observed that low-dose bortezomib and other proteasome inhibitor drugs caused human hepatocellular carcinoma cell lines to produce increased amounts of MICA and MICB, while ULBP1–3 remained uninfluenced. Butler et al., 2009 studied the influence of proteasome inhibition on HNSCC cells and observed that the cells responded via up-regulation of ULBP1 surface expression, which increased tumor cell recognition by NK cells. The authors demonstrated that this upregulation occurs via an ATM/ATR independent pathway. In contrast, Valés-Gómez et al. reported that exposure of Jurkat cells to very low concentrations of MG132 selectively induced expression ULBP2 (Valés-Gómez et al., 2008). They suggested that ATM and ATR, which are normally described to be involved in the DNA damage pathway, are required for ULBP2 expression after proteasome inhibition. Taken together, these studies demonstrate that proteasome inhibitors act differently on NKG2DL, most probably dependent on the cell type, on the dose and time of the treatment.

Besides killing by NK cells, proteasome inhibition has also been demonstrated to increase the sensitivity of melanoma cells to lysis by T cells by enhancing the mitochondrial apoptotic response, which causes mitochondrial accumulation of NOXA. As a consequence the release of the second mitochondria-derived activator of caspase (SMAC) occurs, which is suggested to be responsible for the sensitization (Seeger et al., 2010).

5.4 Transcriptional and post-transcriptional regulation of MIC expression

Within this study and previous work, it was demonstrated that of the MIC molecules, MICA was predominantly expressed on the surface of melanoma cell lines, while MICB expression was frequently undetectable or occurred only at very low levels (Schwinn et al., 2009). The disparity in MICA and MICB expression may be accounted for by diverse regulatory mechanisms acting on different levels of expression such as transcription, mRNA stability or translation. Recently, the promoter region of both the MICA and MICB gene was analyzed and binding sites of specific transcription factors were defined (Eagle et al., 2006; Venkataraman et al., 2007; Rodriges-Rodero et al., 2007). A number of DNA elements

essential for MIC transcription and stress-mediated activation of the promoter were described, such as TATA-like elements, Sp1 sites and a heat shock responsive element (HSE). Sp1 binding sites (GC-islands) and TATA-box have been shown to be essential for expression of MICA and MICB in HCT 116 cells (Venkataraman et al., 2007).

One of the possible reasons for the differences in MICB expression levels between cell lines might be the fact that the MICB promoter is highly polymorphic. In some alleles single nucleotide polymorphisms within or in close proximity of binding sites have been identified, which may interfere with an efficient Sp1 binding, thereby influencing MICB expression (Rodríges-Rodero et al., 2007).

Post-transcriptional mechanisms have been shown to control NKG2DL expression. A number of human microRNAs have been identified by Stern-Ginossar et al. collectively regulating MICA and MICB expression (Stern-Ginossar et al., 2008). Based on their data the authors suggested that these microRNAs set up a threshold to prevent the expression of MICA and MICB proteins and consequently the killing of healthy self cells. During short-term stresses, such as heat shock and viral infection, although microRNA amounts do not change much, higher MICA and MICB mRNA expression stimulated by stress may “saturate” the microRNA suppressive capacity and, ultimately, result in MICA and MICB protein expression. MICB has a fivefold longer 3’ untranslated region (3’ UTR) than MICA, which may have other so far not identified seed sequences for microRNAs distinct from those targeting MICA 3’ UTR and retaining MICB translation.

The discrete patterns of MICA and MICB expression might be also caused by epigenetic regulation. In fact, we found that in melanoma cells the MICB promoter region is bound to mono-ubiquitinated histone H2A operating as a gene expression silencer and proteotoxic stress facilitates the release of the MICB promoter region from this repression. The mechanism of this regulation will be discussed below.

5.4.1 HSF-1 dependent induction of MICB expression upon proteasome inhibition

According to our data short-term proteasome inhibitor drug treatment caused a strong up-regulation of MICB mRNA, while MICA and ULBP mRNA levels were not significantly influenced. The combined treatment of melanoma cells with Actinomycin D, which is an inhibitor of transcription and proteasome inhibitor, abrogated the induction of MICB mRNA, suggesting that transcription is essential for the up-regulation of MICB mRNA under proteotoxic stress, and that stabilization of mRNA is not a major event. We have found that the treatment with MG132 was able to activate the MICB promoter. To better understand the

mechanism and to define the factors responsible for transcriptional stimulation under proteasome inhibition, several MICB promoter constructs were generated. The longest promoter fragment consisted of 470 bp upstream of the start codon and contained a known HSE sequence and a putative binding site for NRF1. A second fragment of 225 bp contained only the HSE, while the shortest promoter fragment (115 bp) lacked this element. As control the MICA promoter construct of 455 bp was generated. Promoters were cloned into pGL4.10 a promoterless vector, upstream of the Firefly luciferase gene. The first promoter construct and the second one, containing HSE, were strongly activated when proteotoxic stress was applied. The shortest MICB promoter failed to drive luciferase gene expression in melanoma cells both under normal culture conditions and under proteotoxic stress.

Proteasome inhibitors have been also reported to cause a heat shock response (Bush et al 1997). We proposed that proteotoxic stress may activate HSF1, which is a member of the heat shock transcription factor family regulating heat shock genes. The heat shock response is an evolutionary conserved process, which defends the organism from environmental stress. It is very rapid and mostly acts on heat shock responsive genes via induction of transcription, but not mRNA stabilization (Shamovsky and Nudler, 2008). Heat shock responses are executed by heat shock transcription factors, such as HSF1 and HSF2. The latter has been mainly reported to participate in development, but recently growing body of evidence suggests that it is capable to cooperate with the key player of the heat shock response, with HSF1 (Shamovsky and Nudler, 2008). Transcription factor HSF1 is constitutively expressed in the cell under the normal conditions and where it is present both in the cytoplasma and in the nucleus in an inactive form. It is known to form inhibitory complexes with HSP70/HSP40, but the main negative regulator of HSF1 is believed to be the abundant chaperon HSP90. Heat shock stress rapidly converts HSF1 to its active form via post-translational modifications. HSF1 is released from complexes with chaperones, becomes phosphorylated and activated. The activation event is associated with the transition of the monomer form to a trimer, which acquires a strong DNA-binding activity (Shamovsky and Nudler, 2008). HSF1 trimers bind to an extremely conserved sequence, the heat shock responsive element (HSE), which is present within promoter region of heat shock responsive genes. Interestingly, a number of different stressors, such as hypoxia, peroxides, alcohols, and transition metal ions, leading to an accumulation of proteins, operate via the heat shock responsive machinery (Shamovsky and Nudler, 2008).

To analyze the role of HSF1 in the induction of MICB promoter activity, site-directed mutagenesis of the HSE sequence within the MICB promoter was performed. HSE mutation

led to a loss of promoter responsiveness under proteotoxic stress pointing out the essential role of HSE and HSF1 in the implication of a stress response. Moreover, Fionda et al. showed that the inhibition of HSP90, a negative regulator of HSF1, led to the rapid activation of the latter and also stimulated transcription and surface expression of MICA and MICB in multiple myeloma cells and sensitizing them to NK cell recognition (Fionda et al., 2009). The next step to make sure that HSF1 is the key factor triggering MICB up-regulation under proteotoxic stress was to knockdown its expression by siRNA. Indeed, cells with silenced HSF1 did not respond to proteotoxic stress and did not up-regulate MICB protein expression as compared to the cells transfected with control siRNA or to non-transfected cells. Taken together, the data underline the essential role of HSF1 in the regulation of MICB expression by proteasome inhibition. In accordance to our study, Venkataraman et al. demonstrated that the HSE element is important to induce MIC expression under heat shock (Venkataraman et al., 2007).

In order to confirm the essential role of HSF1 in the regulation of MICB expression in response to proteotoxic stress induced by MG132 treatment we over-expressed a constitutive active HSF1 in melanoma cells by transient transfection. Expression of active HSF1 in cells co-transfected with MIC promoter constructs led to a strong induction of both MICA and MICB promoter activity, while co-transfection of empty control vectors with MICA and MICB promoter constructs did not cause their activation. However, transient expression of active HSF1 did not influence the endogenous MIC expression of the cell. Surface expression, total protein level as well as mRNA level of MIC molecules remained unchanged after the transfection of melanoma cells with plasmids encoding constitutively active HSF1, while HSP70 mRNA, a direct target of HSF1, was strongly increased, which confirms functional activity of HSF1. We suggest that activated HSF1 can only get the access to the endogenous cellular MICB promoter, when the promoter region is opened by additional regulatory events. Thus, the MICB promoter might be epigenetically silenced in the absence of proteotoxic stress induced by proteasome inhibition.

5.4.2 Depletion of free ubiquitin under proteasome inhibition influences MICB expression

Within this study it has been shown that proteotoxic stress strongly increased MICB expression. We speculated that blockade of the proteasome may lead to a depletion of the free ubiquitin pool in the cell because of a blockade in ubiquitin turn-over.

Free ubiquitin is important to maintain the ubiquitination of histones such as H2A. DNA is organized in a compact chromatin structure consisting of nucleosoms controlling DNA accessibility. A nucleosome is composed of four histones H2A, H2B, H3 and H4, which are

organized in octamers and consists of 147 bp DNA wrapped around each octamer. The structure is very stable because of the multiple interactions of DNA and histones, which prevents unnecessary transcription. Accessibility of DNA to factors initiating transcription can be controlled by a number of different covalent modifications of histones, which can in turn either facilitate or repress transcription. So far, the following histone modifications have been identified: acetylation, methylation, monoubiquitynation, sumoylation, ADP-ribosylation and phosphorylation (Li et al., 2007). Mostly, histone modifications have been mapped to the upstream region of the core promoter, the 5' or the 3' region of the open reading frames of the genes. The modifications, which silence genes or chromosome regions, are found predominantly in the heterochromatin. On the contrary, the modifications facilitating transcription localize in euchromatin regions. This system is able to fine tune gene transcription. In most cases covalent modifications result in a change of the nucleosome charge that could loosen DNA-histone association. Moreover, histone modifications can be recognized by other proteins influencing chromatin dynamics and function like chromatin remodeling enzymes or transcription factor complexes, which can even displace histone dimers of H2A and H2B, or the entire octamer (Li et al., 2007).

One of the most important modifications is histone monoubiquitynation. So far only H2A and H2B have been described to be ubiquitinated. The ubiquitination process is well characterized and consists of three steps. Ubiquitin is first activated by an ATP-dependent reaction involving a ubiquitin activating enzyme (E1), followed by its conjugation via a thioester bond to a cysteine residue in a ubiquitin-conjugating enzyme (E2). In the final enzymatic step, ubiquitin is transferred from the E2 enzyme to a target lysine residue in a particular substrate protein by an ubiquitin-protein isopeptide ligase (E3). E3 enzymes are often characterized by the presence of a C3HC4 (RING) finger motif, which binds zinc and is required for ubiquitin ligase activity (Weake et al., 2008). To date, a number of histone Ub-ligases have been identified. In mammals histone H2B is monoubiquitynated at lysine 120 by the E3 ubiquitin ligase hBRE1 or RNF20/RNF40 (Zhu et al., 2005). Only 1% of H2B has been fount to be monoubiquitynated and its function has been related to transcription initiation. H2A ubiquitination that occurs at lysine 119 has been estimated to comprise between 5% and 15% of the available H2A and is a relatively abundant modification. While some studies have pointed to an association of uH2A with transcriptionally active chromatin (Nickel et al., 1989), others have failed to demonstrate this (Kallin et al., 2009). Recent studies show that RING2/Ring1b in the Polycomb repressive complex 1 (PRC1) monoubiquitynates nucleosomal histone H2A at lysine 119 and links H2A ubiquitination to

Polycomb silencing (Wang et al., 2004) as well as to X chromosome inactivation (de Napoles et al., 2004). More recent studies suggested that both Ring1A and another component of PRC1, Bmi-1, play an important role in H2A ubiquitination and Hox gene silencing and demonstrate the sequential events of H3-K27 methylation by methyltransferase EZH2 and H2A-K119 ubiquitination (Cao et al., 2005). Although, the mechanism of H2A ubiquitination leading to gene repression is mostly unknown, there are evidences that histone H2A monoubiquitination represses transcription of the RANTES gene via blocking of FACT (facilitates transcription) complex recruitment to the promoter region of the gene (Zhou et al., 2008). We found that the MICB promoter is associated with monoubiquitinated histone H2A, which may block transcription initiation under normal conditions. This might explain why the constitutively active HSF1 (Nakai A, Widlak W, see Materials) failed to stimulate endogenous MICB expression in transfected melanoma cells. The situation is different when cells were co-transfected with HSF1 and opened-structured MICB promoter reporter gene constructs. In this case HSF1 could easily access the MICB promoter and stimulate transcription of the luciferase reporter gene.

During proteotoxic stress caused by proteasome inhibition, the accumulation of ubiquitinated substrates takes place, which in turn leads to the depletion of the free ubiquitin pool. Dantuma et al. showed that this coincides with the depletion of ubiquitinated histone H2A and chromatin remodeling (Dantuma et al., 2006). Proteasome inhibition does not alter the rate of histone deubiquitination, but depletes the pool of free ubiquitin, which may result in a rising competition between ubiquitin substrates – proteasome substrates and histones. This assumption was confirmed for melanoma cells. When treated with proteasome inhibitor for 4 hrs the level of ubiqutinantion of H2A at the MICB promoter clearly decreased. Depletion of free ubiquitin under MG132 treatment is reflected in a decrease of H2A ubiquitination, the subsequent release of the promoter DNA for transcription factor binding. We also demonstrated that under proteotoxic stress binding of HSF1 to the MICB promoter region is enhanced. However, in the absence of proteotoxic stress the MICB promoter region seems not to be locked in a way that prevents efficient binding of HSF1 (Venkataraman et al., 2007; Rodríguez-Rodero et al., 2007).

5.4.3 Stabilisation of MIC surface expression under proteasome inhibition

We confirmed that inhibition of translation via Cycloheximide treatment led to a rapid reduction of total MIC protein levels, pointing out that MIC molecules are short-lived proteins. It has been described that most MICA and MICB alleles encode proteins with a long

cytoplasmic domain containing a number of ubiquitination sites (lysines) located close to the transmembrane domain of the proteins (Thomas et al., 2008). This seems to be important for the internalization of the proteins and the redistribution in intracellular compartments. In general, the regulation of the membrane residence of stress markers like MIC molecules is extremely important as the long presence of the stress ligands at the cell surface might be harmful for the cells and lead to autoimmune disturbances.

Interestingly, some viruses such as the Kaposi sarcoma associated herpes virus evolved mechanisms to escape NK cell surveillance by down-regulating NKG2DL from the surface of virus-infected cells. The viral genome encodes the ubiquitin ligase K5, which has been shown to ubiquitinate the lysine residues of the cytoplasmic domain of the MIC molecules, leading to their rapid internalization. Moreover, K5 failed to retain the surface expression of MICA*008 with a truncated cytoplasmic domain lacking ubiquitination sites (Thomas et al., 2008).

Also cellular ubiquitin ligases exist that are involved in the regulation of the membrane persistence of proteins (Lehner et al., 2005) and that trigger internalization of transmembrane molecules by mono- or diubiquitination of lysine residues within the cytoplasmic domains. Thus, we speculated that the activity of such ligases might be disturbed also by depletion of the free ubiquitin pool upon proteasome inhibition. To analyse this melanoma cells were treated with Brefeldin A (BFA), an inhibitor of the vesicular transport from the Golgi to the surface membrane and BFA in combinantion with MG132. Blocking by BFA strongly interfered with the surface expression of both MICA and MICB suggesting that trafficking through the cellular compartment is relevant for an effective surface expression. Thus, blocking of the vesicular transport interrupts the delivery of the newly synthesized NKG2DL to the cell surface. BFA treatment together with proteasome inhibition stabilized MICA and MICB molecues on the melanoma cell lines studied. Hence, we suggest that inhibition of the proteasome might stabilize MIC molecules at the cell surface via abrogation of endocytosis. On the other hand, proteasome inhibition might prolong the membrane residence time of the MIC molecules by blocking the degradation of endocytosed proteins which then recycle back to the membrane. The exact mechanism facilitating the prolonged residence of MIC molecules on the cell surface under proteotoxic stress needs to be elucidated and was beyond the scope of the thesis.

6 Conclusions

Taken together we found that proteotoxic stress elicited by inhibition of the proteasome strongly up-regulates MICB expression in human melanoma cells. The mechanism of this induction is rather complex and involves different levels of regulation such as transcriptional, epigenetic, and post-translational regulation. We first showed that proteasome inhibition intensively induces MICB transcription, which is mediated by HSF1. Silencing of HSF1 *in vitro* interfered with MICB up-regulation under proteotoxic stress as well as mutation of the HSF1 binding site (HSE) within the MICB promoter led to the abrogation of MICB promoter activation in cells incubated with a proteasome inhibitor. Over-expression of a constitutively active HSF1 in the melanoma cells was found to stimulate only the MICB promoter cloned in the reporter gene plasmids, but not the cellular endogenous MICB promoter, suggesting that other mechanisms controlling the accessibility of the MICB promoter for HSF1 have to be involved. We showed that the MICB promoter is associated with ubiquitinated histone H2A (uH2A), which is known to be involved in gene silencing. Proteasome inhibition resulted in a loss of H2A ubiquitination. Along with this we showed in CHIP experiments that proteasome inhibition decreased the levels of uH2A at the MICB promoter wile increasing the binding of HSF1 which in turn triggers MICB transcription. Moreover, we found that MG132 not only transcriptionally regulates MICB, but also prolongs the residence of MICB protein on melanoma cell surface.

The uncovered mechanism might be relevant for novel melanoma treatment strategies including proteasome inhibitors not only as inducers of apoptosis and sensitizers of chemotherapy, but also as agents to modulate the immunogenicity of melanoma.

7 Literature

Adams J. 2004. The proteasome: a sutable antineoplastic target. Nature Reviews 4:349-60.

Agarwala SS. 2010. Novel immunotherapies as potential therapeutic partners for traditional or targeted agents: cytotoxic T-lymphocyte antigen-4 blockade in advanced melanoma. Melanoma Research 20:1–10.

Agüera-González S, Boutet P, Reyburn HT, Valés-Gómez M. 2009. Brief residence at the plasma membrane of the MHC class I-related chain B is due to clathrin-mediated cholesterol-dependent endocytosis and shedding. The Journal of Immunology 182:4800–4808.

Almond JM, Cohen GM. 2002. The proteasome: a novel target for cancer chemotherapy. Leukemia 16:433–443.

Ames E, Hallett WHD, Murphy WJ. 2008. Sensitization of human breast cancer cells to natural killer cell-mediated cytotoxicity by proteasome inhibition. Clinical and Experimental Immunology 155:504–513.

Andresen L, Jensen H, Pedersen MT, Hansen KA, Skov S. 2007. Molecular regulation of MHC class I chain-related protein A expression after HDAC-inhibitor treatment of Jurkat T cells. The Journal of Immunology 179:8235–8242.

Armeanu S, Bitzer M, Lauer UM, Venturelli S, Pathil A, Krusch M. 2005. Natural killer cell-mediated lysis of hepatoma cells via specific induction of NKG2D ligands by the histone deacetylase inhibitor sodium valproate. Cancer Research 65:6321-6329.

Armeanu S, Krusch M, Baltz KM, Weiss TS, Smirnow I, Steinle A, Lauer UM, Bitzer M, Salih HR. 2008. Direct and Natural Killer cell-mediated antitumor effects of low-dose bortezomib in hepatocellular carcinoma. Clinical Cancer Research 14(11):3520-3528.

Aziz SA, Pick-Golan E, McCarthy MM, Flaherty KT, Camp RL, Rimm DL. 2007. ASCO annual meeting proceedings Part I. Journal of Clinical Oncology 25:8521.

Bloethner S, Chen B, Hemminki K, Müller-Berghaus J, Ugurel S, Schadendorf D, Kumar R. 2005. Effect of common B-RAF and N-RAS mutations on global gene expression in melanoma cell lines. Carcinogenesis 26(7):1224-1232.

Bloethner S, Hemminki K, Thirumaran RK, Chen B, Mueller-Berghaus J, Ugurel S, Schadendorf D, Kumar R. 2006. Differences in global gene expression in melanoma cell lines with and without homozygous deletion of the CDKN2A locus genes. Melanoma Research 16:297–307.

Boissel N, Rea D, Tieng V, Dulphy N, Brun M, Cayuela JM, Rousselot P, Tamouza R, Bouteiller PL, Mahon FX, Steinle A, Charron D, Dombret H, Toubert A. 2006. BCR／ABL oncogene directly controls MHC class I chain-related molecule A expression in chronic myelogenous leukemia. The Journal of Immunology 176:5108–5116.

Borissenko L, Groll M. 2007. Diversity of proteasomal missions: fine tuning of the immune response. Biological chemistry 388(9):947-955.

Bryceson YT, March ME, Ljunggren H-G, Long EO. 2006. Activation, coactivation, and costimulation of resting human natural killer cells. Immunological Reviews 214:73–91.

Burke S, Lakshmikanth T, Colucci F, Carbone E. 2010. New views on natural killer cell-based immunotherapy of melanoma treatment. Trends in Immunology 31(9):339-345.

Bush KT, Goldberg AL, Nigam SK. 1997. Proteasome inhibition leads to a heat-shock response, induction of endoplasmic reticulum chaperones, and thermotolerance. The Journal of Biological Chemistry 272(14):9086–9092.

Butler JE, Moore MB, Presnell SR, Chan HW, Chalupny NJ, Lutz CT. 2009. Proteasome regulation of ULBP1 transcription. The Journal of Immunology 182:6600-6609.

Cao R, Tsukada Y, Zhang Y. 2005. Role of Bmi-1 and Ring1A in H2A ubiquitylation and Hox gene silencing. Molecular Cell 20:845–854.

Cervenka A, Baron JL, Lanier LL. 2001. Ectopic expression of retinoic acid early inducible-1 gene (RAE-1) permits natural killer cell-mediated rejection of a MHC class I-bearing tumor *in vivo*. Proceedings of the National Academy of Science USA 98:11521-111526.

Cerwenka A, Lanier LL. 2001. Natural killer cells, viruses and cancer. Nature Reviews Immunology 1:41-49.

Champsaur M, Lanier LL. 2010. Effect of NKG2D ligand expression on host immune responses. Immunological Reviews 235:267–285.

Chauhan D, Hideshima T, Mitsiades C, Richardson P, Anderson KC. 2005. Proteasome inhibitor therapy in multiple myeloma. Molecular Cancer Therapy 4(4):686–92.

Chin L, Garraway LA, Fisher DE. 2006. Malignant melanoma: genetics and therapeutics in the genomic era. Genes & Development 20:2149-2182.

Concannon CG, Koehler BF, Reimertz C, Murphy BM, Bonner C, Thurow N, Ward MW, Villunger A, Strasser A, Kögel D, Prehn JHM. 2006. Apoptosis induced by proteasome inhibition in cancer cells: predominant role of the p53/PUMA pathway. Oncogene 2006:1-12.

Coudert JD, Held W. 2006. The role of the NKG2D receptor for tumor immunity. Seminars in Cancer Biology 16:333–343.

Croghan GA, Suman VJ, Maples WJ, Albertini M, Linette G, Flaherty L, Eckardt J, Ma C, Markovic SN, Erlichman C. 2010. A study of paclitaxel, carboplatin, and bortezomib in the treatment of metastatic malignant melanoma: a phase 2 Consortium study. Cancer 116(14):3463-3468.

Dahl C, Guldberg P. 2007. The genome and epigenome of malignant melanoma. APMIS 115(10):1161–1176.

Danson S, Lorigan P, Arance A, Clamp A, Ranson M, Hodgetts J. 2003. Randomized phase II study of temozolomide given every 8 hours or daily with either interferon alfa-2b or thalidomide in metastatic malignant melanoma. Journal of Clinical Oncology 21:2551–7.

Dantuma NP, Groothuis TAM, Salomons FA, Neefjes J. 2006. A dynamic ubiquitin equilibrium couples proteasomal activity to chromatin remodelling. The Journal of Cell Biology 173(1):19–26.

Dohment RJ. 2003. The Ubiquitin proteasome system. Obtained from web site www.genetik.uni-koeln.de.

Dudley ME, Wunderlich JR, Robbins PF, Yang JC, Hwu P, Schwartzentruber DJ; Topalian SL, Sherry R, Restifo NP, Hubicki AM, Robinson MR, Raffeld M, Duray P, Seipp CA, Rogers-Freezer L, Morton KE, Mavroukakis SA, White DE, Rosenberg SA. 2002. Cancer regression and autoimmunity in patients after clonal repopulation with antitumor lymphocytes. Science 298:850-854.

Dunn C, Chalupny NJ, Sutherland CL, Dosch S, Sivakumar PV, Johnson DC, Cosman D. 2003. Human cytomegalovirus glycoprotein UL16 causes intracellular sequestration of NKG2D ligands, protecting against Natural Killer cell cytotoxicity. The Journal of Experimental Medicine 197(11):1427–1439.

Eagle RA, Traherne JA, Ashiru O, Wills MR, Trowsdale J. 2006. Regulation of NKG2D ligand gene expression. Human Immunology 67:159–169.

Eagle RA, Trowsdale J. 2007. Promiscuity and the single receptor: NKG2D. Nature Reviews Immunology 7:737-744.

Eagle RA, Jafferji I, Barrow AD. 2009. Beyond stressed self: evidence for NKG2D ligand expression on healthy cells. Current Immunology Reviews 5(1):22–34.

Ebihara T, Masuda H, Akazawa T, Shingai M, Kikuta H, Ariga T, Matsumoto M, Seya T. 2007. Induction of NKG2D ligands on human dendritic cells by TLR ligand stimulation and RNA virus infection. International Immunology 19(10):1145–1155.

Eigentler TK, Caroli UM, Radny P, Garbe C. 2003. Palliative therapy of disseminated malignant melanoma: a systematic review of 41 randomised clinical trials. Lancet Oncology 4:748–59.

Eisele G, Wischhusen J, Mittelbronn M, Meyermann R, Waldhauer I, Steinle A, Weller M, Friese MA. 2006. TGF-β and metalloproteinases differentially suppress NKG2D ligand surface expression on malignant glioma cells. Brain 129:2416–2425.

Empson VG, McQueen FM, Dalbeth N. 2010. The natural killer cell: a further innate mediator of gouty inflammation? Immunology and Cell Biology 88:24–31.

Fionda C, Soriani K, Malgarini G, Iannitto ML, Santoni A Cippitelli M. 2009. Heat shock protein-90 inhibitors increase MHC Class I-related chain A and B ligand expression on multiple myeloma cells and their ability to trigger NK cell degranulation. The Journal of Immunology 183:4385-4394.

Friese MA, Platten M, Lutz SZ, Naumann U, Aulwurm S, Bischof F, Bühring HJ, Dichgans J, Rammensee HG, Steinle A, Weller M. 2003. MICA／NKG2D-mediated immunogene therapy of experimental gliomas. Cancer Research 63:8996–9006.

Gasser S, Orsulic S, Brown EJ, Raulet DH. 2005. The DNA damage pathway regulates innate immune system ligands of the NKG2D receptor. Nature 436(7054):1186–1190.

Gogas HJ, Kirkwood JM, Sondak VK. 2007. Chemotherapy for metastatic melanoma: time for a change? Cancer 109(3):455–464.

Guerra N, Tan YX, Joncker NT, Choy A, Gallardo F, Xiong N, Knoblaugh S, Cado D, Greenberg NR, Raulet DH. 2008. NKG2D-deficient mice are defective in tumor surveillance in models of spontaneous malignancy. Immunity 28:571–580.

Haluska FG, Tsao H, Wu H, Haluska FS, Lazar A, Goel V. 2006. Genetic Alterations in Signaling Pathways in Melanoma. Clinical Cancer Research 12(7 Suppl):2301s-2307s.

Hamerman JA, Ogasawara K, Lanier LL. 2004. Cutting edge: Toll-like receptor signaling in macrophages induces ligands for the NKG2D receptor. The Journal of Immunology 172:2001–2005.

Hocker TL, Singh MK, Tsao H. 2008. Melanoma genetics and therapeutic approaches in the 21st century: moving from the benchside to the bedside. Journal of Investigative Dermatology 128:2575–2595.

Jinushi[1] M, Takehara T, Tatsumi T, Kanto T, Groh V, Spies T, Kimura R, Miyagi T,

Mochizuki K, Sasaki Y, Hayashi N. 2003. Expression and role of MICA and MICB in human hepatocellular carcinomas and their regulation by retinoic acid. International Journal of Cancer 104:354–361.

Jinushi[2] M, Takehara T, Kanto T, Tatsumi T, Groh V, Spies T, Miyagi T, Suzuki T, Sasaki T, Hayashi N. 2003. Critical role of MHC class I-related chain A and B expression on IFN-α-stimulated dendritic cells in NK cell activation: impairment in chronic hepatitis C virus infection. The Journal of Immunology 170:1249–1256.

Jinushi M, Vanneman M, Munshi NC, Tai Y-T, Prabhala RH, Ritz J, Neuberg D, Anderson KC, Carrasco DR, Dranoff G. 2008. MHC class I chain-related protein A antibodies and shedding are associated with the progression of multiple myeloma. Proceedings of the National Academy of Science USA 105(4):1285–1290.

Kallin EM, Cao R, Jothi R, Xia K, Cui K, Zhao K, Zhang Y. 2009. Genome-wide uH2A localization analysis highlights Bmi1-dependent deposition of the mark at repressed genes. PLoS Genetics 5(6):e1000506.

Kato N, Tanaka J, Sugita J, Toubai T, Miura Y, Ibata M, Syono Y, Ota S, Kondo T, Asaka M, Imamura M. 2007. Regulation of the expression of MHC class I-related chain A, B (MICA, MICB) via chromatin remodeling and its impact on the susceptibility of leukemic cells to the cytotoxicity of NKG2D-expressing cells. Leukemia 21:2103–2108.

Khammari A, Labarrière N, Vignard V, Nguyen J-M, Pandolfino M-C, Knol AC. 2009. Treatment of metastatic melanoma with autologous Melan-A/MART-1-specific cytotoxic T lymphocyte clones. Journal of Investigative Dermatology 129:2835–42.

Lara PN Jr, Koczywas M, Quinn DI, Lenz HJ, Davies AM, Lau DH, Gumerlock PH, Longmate J, Doroshow JH, Schenkein D, Kashala O, Gandara DR. 2006. Bortezomib plus docetaxel in advanced non-small cell lung cancer and other solid tumors: a phase I California Cancer Consortium trial. Journal of Thoracic Oncology 1(2):126-134.

Lecis D, Drago C, Manzoni L, Seneci P, Scolastico C, Mastrangelo E, Bolognesi M, Anichini A, Kashkar H, Walczak H, Delia D. 2010. Novel SMAC-mimetics synergistically stimulate melanoma cell death in combination with TRAIL and bortezomib. British Journal of Cancer 102:1707 – 1716.

Lee JA. 2010. The determination of melanoma stage at diagnosis. Dermatology Research and Practice 2010(839829):1-3.

Lehner PJ, Hoer S, Dodd RB, Duncan LM. 2005. Downregulation of cell surface receptors by the K3 family of viral and cellular ubiquitin E3 ligases. Immunological Reviews 207:112–125.

Li B, Carey M, Workman JL. 2007. The role of chromatin during transcription. Cell 128:707–719.

Livak KJ, Schmittgen TD. 2001. Analysis of relative gene expression data using real-time quantitative PCR and the $2^{-\Delta\Delta C}_{T}$ method. Methods 25(4):402-408.

Ljunggren H-G, Karre K. 1990. In search of the ‘‘missing self’’: MHC molecules and NK cell recognition. Immunology Today 11:237–244.

López-Larrea C, Suárez-Alvarez B, López-Soto A, López-Vázquez1 A, Gonzalez S. 2008. The NKG2D receptor: sensing stressed cells. Trends in Molecular Medicine 14(4):179-189.

Mackensen A, Meidenbauer N, Vogl S, Laumer M, Berger J, Andreesen R. 2006. Phase I study of adoptive T-cell therapy using antigenspecific CD8+ T cells for the treatment of patients with metastatic melanoma. Journal of Clinical Oncology 24:5060–5069.

Meier F, Busch S, Lasithiotakis K, Kulms D, Garbe C, Maczey E, Herlyn M, Schittek B. 2007. Combined targeting of MAPK and AKT signalling pathways is a promising strategy for melanoma treatment. British Journal of Dermatology 156:1204–1213.

Mistry AR, O’Callaghan CA. 2007. Regulation of ligands for the activating receptor NKG2D Immunology 121:439–447.

Młynarczuk-Biały I, Roeckmann H, Kuckelkorn U, Schmidt B, Umbreen S, Goła J, Ludwig A, Montag C, Wiebusch L, Hagemeier C, Schadendorf D, Kloetzel PM, Seifert U. 2006. Combined effect of proteasome and calpain inhibition on cisplatin-resistant human melanoma cells. Cancer Research 66(15):7598-7605.

Molhoek KR, Brautigan DL, Slingluff CL. 2005. Synergistic inhibition of human melanoma proliferation by combination treatment with B-Raf inhibitor BAY43-9006 and mTOR inhibitor Rapamycin. Journal of Translational Medicine 3(39):1-11.

Mooi WJ, Peeper DS. 2006. Oncogene-induced cell senescence – halting on the road to cancer. The New England Journal of Medicine 355:1037–1046.

Nakai A, Suzuki M, Tanabe M. 2000. Arrest of spermatogenesis in mice expressing an active heat shock transcription factor 1. EMBO Journal 19(7):1545-1554.

Nandi D, Tahiliani P, Kumar A, Chandu D. 2006. The ubiquitin-proteasome system. Journal of Biosciences 31:137–155.

de Napoles M, Mermoud JE, Wakao R, Tang YA, Endoh M, Appanah R, Nesterova TB, Silva J, Otte AP, Vidal M. 2004. Polycomb group proteins Ring1A/B link ubiquitylation of histone H2A to heritable gene silencing and X inactivation. Developmental Cell 7:663–676.

Nausch N, Cerwenka A. 2008. NKG2D ligands in tumor immunity. Oncogene 27:5944–5958.

Nice TJ, Coscoy L, Raulet DH. 2009. Posttranslational regulation of the NKG2D ligand Mult1 in response to cell stress. The Journal of Experimental Medicine 206:287–298.

Nickel BE, Allis CD, Davie JR. 1989. Ubiquitinated histone H2B is preferentially located in transcriptionally active chromatin. Biochemistry 28:958–963.

Obeng EA, Carlson LM, Gutman DM, Harrington WJ, Lee KP, BoiseLH. 2006. Proteasome inhibitors induce a terminal unfolded protein response in multiple myeloma cells. Blood 107(12):4907–4916.

Page TJ, Sikder D, Yang L, Pluta L, Wolfinger RD, Kodadek T, Thomas RS. 2006. Genome-wide analysis of human HSF1 signaling reveals a transcriptional program linked to cellular adaptation and survival. Molecular Biosystems 2:627–639.

Panka DJ, Atkins MB, Mier JW. 2006. Targeting the mitogen-activated protein kinase pathway in the treatment of malignant melanoma. Clinical Cancer Research 12(7 Suppl):2371s-2375s.

Paschen A, Méndez RM, Jimenez P, Sucker A, Ruiz-Cabello F, Song M, Garrido F, Schadendorf D. 2003. Complete loss of HLA class I antigen expression on melanoma cells: a result of successive mutational events. International Journal of Cancer 103(6):759-67.

Paschen A, Arens N, Sucker A, Greulich-Bode KM, Fonsatti E, Gloghini A, Striegel S, Schwinn N, Carbone A, Hildenbrand R, Cerwenka A, Maio M, Schadendorf D. 2006. The coincidence of chromosome 15 aberrations and β2-microglobulin gene mutations is causative for the total loss of human leukocyte antigen class I expression in melanoma. Clinical Cancer Research 12(11):3297-3305.

Paschen A, Sucker A, Hill B, Moll I, Zapatka M, Nguyen XD, Sim GJ, Gutmann I, Hassel J, Becker JC, Steinle A, Schadendorf D, Ugurel S. 2009. Differential clinical significance of individual NKG2D ligands in melanoma: soluble ULBP2 as an indicator of poor prognosis superior to S100B. Clinical Cancer Research 15(16):5208-5215.

Pende D, Rivera P, Marcenaro S, Chang CC, Biassoni R, Conte R, Kubin M, Cosman D, Ferrone S, Moretta L, Moretta A. 2002. Major histocompatibility complex class I-

related chain A and UL16-binding protein expression on tumor cell lines of different histotypes: analysis of tumor susceptibility to NKG2D-dependent natural killer cell cytotoxicity. Cancer Research 62:6178-6186.

Pickart C M, Cohen R E. 2004. Proteasomes and their kin: proteases in the machine age. Molecular Cell Biology 5:177–187.

Quintana E, Shackleton M, Sabel MS, Fullen DR, Johnson TM, Morrison SJ. 2008. Efficient tumour formation by single human melanoma cells. Nature 456:593-599.

Rodríguez-Rodero S, González S, Rodrigo L, Fernández-Morera JL, Martínez-Borra J, López-Vázquez A, López-Larrea C. 2007. Transcriptional regulation of MICA and MICB: a novel polymorphism in MICB promoter alters transcriptional regulation by Sp1. European Journal of Immunology 37(7):1938-1953.

Russo A, Bronte G, Fulfaro F, Cicero G, Adamo V, Gebbia N, Rizzo S. 2010. Bortezomib: a new pro-apoptotic agent in cancer treatment. Current Cancer Drug Targets 10(1):55-67.

Salih HR, Rammensee HG, Steinle A. 2002. Cutting edge: down-regulation of MICA on human tumors by proteolytic shedding. The Journal of Immunology 169:4098-4102.

Salih HR, Antropius H, Gieseke F, Lutz SZ, Kanz L, Rammensee HG, Steinle A. 2003. Functional expression and release of ligands for the activating immunoreceptor NKG2D in leukemia. Blood 102:1389–1396.

Schadendorf D, Algarra SM, Bastholt L, Cinat G, Dreno B, Eggermont AMM, Espinosa E, Guo J, Hauschild A, Petrella T, Schachter J, Hersey P. 2009. Immunotherapy of distant metastatic disease. Annals of Oncology 20(Suppl. 6):41–50.

Schwinn N, Vokhminova D, Sucker A, Textor S, Striegel S, Moll I, Nausch N, Tuettenberg J, Steinle A, Cerwenka A, Schadendorf D, Paschen A. 2009. Interferon-gamma downregulates NKG2D ligand expression and impairs the NKG2D-mediated cytolysis of MHC class I-deficient melanoma by natural killer cells. International Journal of Cancer 124:1594–1604.

Seeger JM, Schmidt P, Brinkmann K, Hombach AA, Coutelle O, Zigrino P, Wagner-Stippich D, Mauch C, Abken H, Krönke M, Kashkar H. 2010. The proteasome inhibitor bortezomib sensitizes melanoma cells toward adoptive CTL attack. Cancer Research 70(5):1825-34.

Shamovsky I, Nudler E. 2008. New insights into the mechanism of heat shock response activation. Cellular and Molecular Life Sciences 65:855-861.

Soengas MS, Lowe SW. 2003. Apoptosis and melanoma chemoresistance. Oncogene 22(20):3138–3151.

Stern-Ginossar N, Gur C, Biton M, Horwitz E, Elboim M, Stanietsky N, Mandelboim M, Mandelboim O. 2008. Human microRNAs regulate stress-induced immune responses mediated by the receptor NKG2D. Nature Immunology 9(9):1065-1073.

Straten P, Becker JC. 2009. Adoptive Cell Transfer in the Treatment of Metastatic Melanoma. Journal of Investigative Dermatology 129:2743–2745.

Su Y, Amiri KI, Horton LW, Yu Y, Ayers GD, Koehler MC, Puzanov I, Richmond A, Sosman JA. 2010. A phase I trial of bortezomib with temozolomide in patients with advanced melanoma: toxicities, antitumor effects, and modulation of therapeutic targets. Clinical Cancer Research 16(1):348-357.

Thomas M, Boname JM, Field S, Nejentsev S, Salio M, Cerundolo V, Wills M, Lehner PJ. 2008. Down-regulation of NKG2D and NKp80 ligands by Kaposi's sarcoma-associated herpesvirus K5 protects against NK cell cytotoxicity. Proceedings of the National Academy of Science USA 105(5):1656–1661.

Unno M, Mizushima T, Morimoto Y, Tomisugi Y, Tanaka K, Yasuoka N, Tsukihara T. 2002. The structure of the mammalian 20S proteasome at 2.75 Å resolution. Structure 10:609–618.

Valés-Gómez M, Chisholm SE, Cassady-Cain RL, Roda-Navarro P, Reyburn HT. 2008. Selective induction of expression of a ligand for the NKG2D receptor by proteasome inhibitors. Cancer Research 68(5):1546–1554.

Venkataraman GM, Suciu D, Groh V, Boss JM, Spies T. 2007. Promoter region architecture and transcriptional regulation of the genes for the MHC class I-related chain A and B ligands of NKG2D. The Journal of Immunology 178:961–969.

Vetter CS, Groh V, Straten Pt P, Spies T, Brocker EB, Becker JC. 2002. Expression of stressinduced MHC class I related chain molecules on human melanoma. Journal of Investigative Dermatology 118:600–605.

Vetter CS, Lieb W, Bröcker EB, Becker JC. 2004. Loss of nonclassical MHC molecules MIC-A/B expression during progression of uveal melanoma. British Journal of Cancer 91(8):1495-1499.

Wang H, Wang L, Erdjument-Bromage H, Vidal M, Tempst P, Jones RS, Zhang Y. 2004. Role of histone H2A ubiquitination in Polycomb silencing. Nature 431:873–878.

Wang H, Ruan Z, Wang Y, Han J, Fu X, Zhao T, Yang D, Xu W, Yang Z, Wang L, Chen Y, Wu Y. 2008. MHC class I chain-related molecules induced on monocytes by IFN-gamma promote NK cell activation. Molecular Immunology 45:1548–1556.

Watson NF, Spendlove I, Madjd Z, McGilvray R, Green AR, Ellis IO, Scholefield JH, Durrant LG. 2006. Expression of the stress-related MHC class I chain-related protein MICA is an indicator of good prognosis in colorectal cancer patients. International Journal of Cancer 118(6):1445-1452.

Weake VM, Workman JL. 2008. Histone ubiquitination: triggering gene activity. Molecular Cell 29:653-663.

Yadav D, Ngolab J, Lim RS-H, Krishnamurthy S, Bui JD. 2009. Cutting edge: down-regulation of MHC class I-related chain A on tumor cells by IFN-γ-induced microRNA. The Journal of Immunology 182:39–43.

Yee C, Thompson JA, Byrd D. 2002. Adoptive T cell therapy using antigen-specific $CD8^+$ T cell clones for the treatment of patients with metastatic melanoma: *in vivo* persistence, migration, and antitumor effect of transferred T cells. Proceedings of the National Academy of Science USA 99:16168-16173.

Zhou W, Zhu P, Wang J, Pascual G, Ohgi KA, Lozach J, Glass CK, Rosenfeld MG. 2008. Histone H2A monoubiquitination represses transcription by inhibiting RNA polymerase II transcriptional elongation. Molecular Cell 29:69-80.

8 Appendix

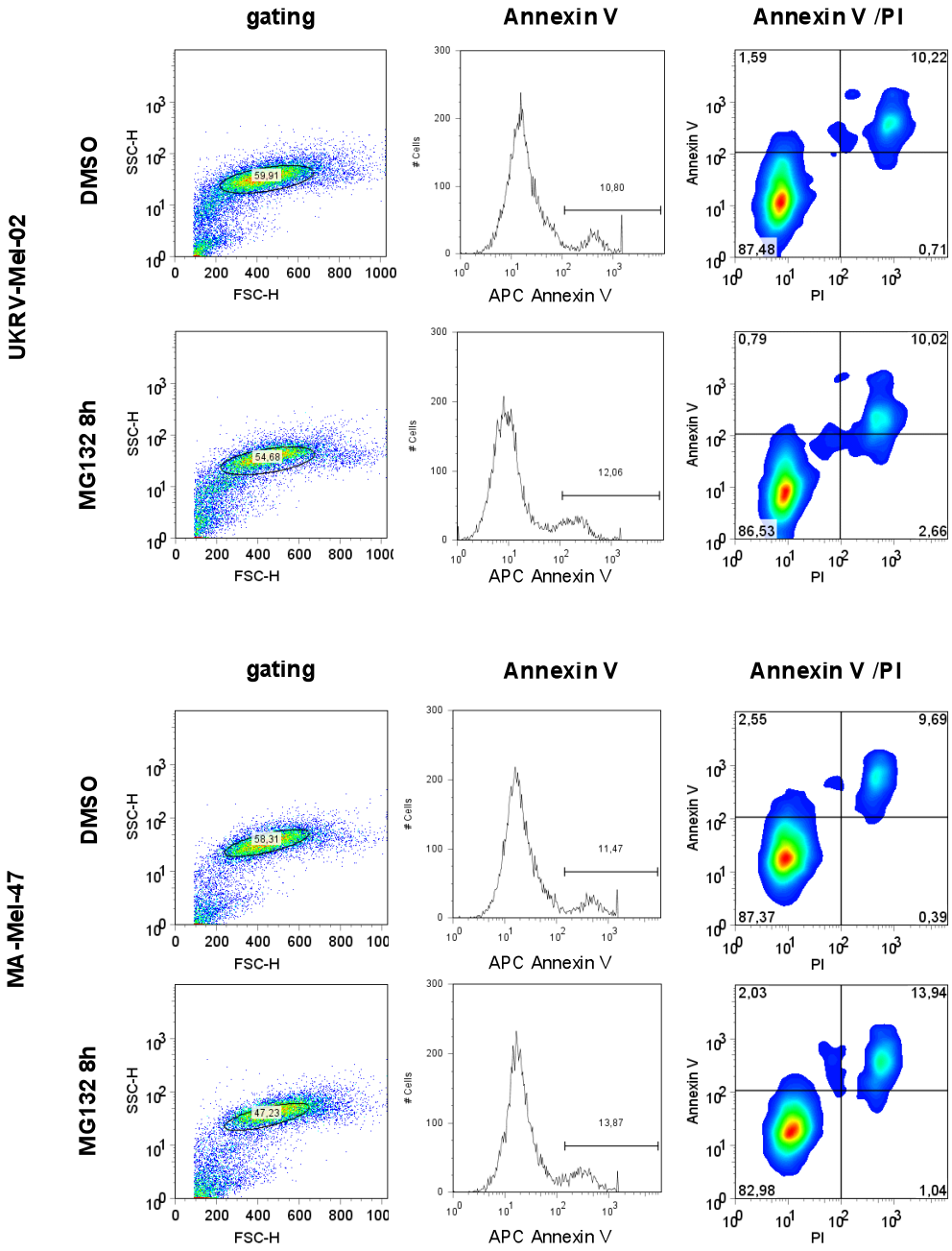

Figure A1. Annexin/PI staining of melanoma cells treated with proteasome inhibitor

UKRV-Mel-02 and MA-Mel-47 cell lines were treated with 10 µM MG132 or with DMSO as a solvent control for 8 hrs, harvested and stained with APC-Annexin V and Propidium iodide (PI) to ascertain the fraction of the cells which undergo apoptosis (Annexin V /PI). "Gating" dotplots represent the strategy used to gate on living cells. Annexin V positive population represent cells undergoing apoptosis. Double positive populations represent dead cells. For both cell lines there was no significant difference in the number of cells, which undergo apoptosis, between controls or MG132 treated cells. Data are representative of two independent experiments for each cell line.

9 List of abbreviations

A

Ab	antibody
ACT	adoptive cell transfer
Act.D.	Actinomycin D
ADP	adenosine 5'-diphosphate
AKT	serine/threonine kinase B (PKB)
ALL	acute lymphatic leukemia
AML	acute myeloid leukemia
ATM	ataxia telangiectasia, mutated
ATR	ATM and Rad3-related
ATP	adenosine 5'-trihosphate

B

Bcl	B-cell lymphoma
BCR/ABL	breakpoint cluster region/c-abl oncogene 1, non-receptor tyrosine kinase
BFA	Brefeldin A
bp	base pairs
BPB	bromphenol blue
B-RAF	B-Raf proto-oncogene serine/threonine-protein kinase
BSA	bovine serum albumin

C

CD	cluster of differentiation
CDK4	cyclin dependent kinase 4
CDKN2A	cyclin-dependent kinase inhibitor 2A
cDNA	coding DNA
ChIP	chromatin immunoprecipitation
CHX	Cycloheximide
CML	chronic myeloid leukemia
CMV	cytomegalovirus
CLL	chronic lymphatic leukemia
conc	concentration

Ct	threshold cycle by RT-PCR
CTLA-4	cytotoxic T-lymphocyte antigen 4

D

DC	dendritic cell
dNTP	deoxyribonucleotide triphosphate
DMSO	dimethyl sulfoxide
DTIC	Dimethyl-trizeno-imidazol-Carboxamid (also called Dacarbazine)

E

ECL	enhanced chemiluminescence
EDTA	ethylenediaminetetraacetic acid
ER	endoplasmic reticulum
ERK	extracellular-signal-regulated kinase

F

F_{ab}	fragment antigen binding
6-FAM	6-Carboxy->Fluorescein
FACS	fluorescence activated cell sorting
FACT	facilitates chromatin transcription
FDA	U.S. Food and Drug Administration

G

g	gram
GAPDH	glyceraldehyde-3-phosphate dehydrogenase
gp100	glycoprotein 100, a melanoma antigen
GPI	glycosylphosphatidylinositol
GTP	guanosine-5'-triphosphate

H

H2A	histone H2A
HDAC	histone deacetylase
HCC	hepatocellular carcinoma
HLA	human leukocyte antigen

HNSCC	head and neck squamous cell carcinoma
HRP	horseradish peroxidase
hrs	hours
HSE	heat shock responsive element
HSF1	heat shock factor 1
HSP	heat shock protein
HSV-TK	herpes simplex virus thymidine kinase

I

IFN	interferon
Ig	immunoglobulin
IκB	IkappaB kinase, inhibitor of NF-kappaB kinase
IL	interleukin

K

kb	kilobase
kD	kilodalton
K_D	dissociation constant
KIR	killer cell immunoglobulin-like receptor

L

l	liter
LPS	lipopolysaccharides
LUC	luciferase

M

µl	microliter
µM	micromolar
ml	milliliter
mM	millimolar
µg	microgram
mg	milligram
min	minute
mAb	monoclonal antibody

MAPK mitogen activated protein kinase
MDM2 negative regulator of p53, E3 ubiquitin ligase
MEK MAP-ERK kinase
Melan-A/MART-1 Melanoma-associated antigen recognized by T cells
MHC major histocompatibility complex
MICA/B MHC class I chain-related sequence A/B
MIC MICA and MICB
miRNA microRNA
MMP matrix metalloproteinases
mRNA messenger ribonucleic acid
mTOR mammalian target of rapamycin

N

NCR natural cytotoxicity receptor
NF-κB nuclear factor kappa-B
NK Natural killer cell(s)
NKG2D Natural-killer group 2, member D
NKG2DL NKG2D ligand(s)
NKT Natural killer T cell(s)
NOD/SCID Non-obese diabetic/severe immunodeficiency genetic disorder mice
NOXA phorbol-12-myristate-13-acetate-induced protein 1, a pro-apoptotic member of the Bcl-2 protein family
NRAS neuroblastoma RAS viral (v-ras) oncogene homolog
NRF1 nuclear respiratory factor 1

O – P

OD optical density
p53 protein 53, a tumor suppressor
PCR polymerase chain reaction
PE phycoerythrin
PFA PBS/formaldehyde
PI3K phosphatidylinosytol 3-kinase
PMSF phenylmethylsulfonyl fluoride
PRC polycomb repressive complex

PTEN	phosphatase and tensin homolog
PUMA	p53 upregulated modulator of apoptosis, a pro-apoptotic member of the Bcl-2 protein family

R

Rae1	retinoic acid early inducible gene-1
RAS	specific guanine nucleotide-releasing factor 1
RING	really interesting new gene domain
RNA Pol II	RNA polymerase II
rpm	rotations per minute
RT	room temperature
RT-PCR	reverse transcription polymerase chain reaction

S

SD	standard deviation
SDS	sodium dodecyl sulfate
sNKG2DL	soluble NKG2D ligand(s)
siRNA	small interfering RNA
SMAC	second mitochondria-derived activator of caspase
STAT	signal transducer and activator of transcription
SV40	Simian vacuolating virus 40

T

Taq	*Thermus aquaticus*
TBS	Tween/PBS
TEB	triton extraction buffer
TGF	transforming growth factor
TLR	toll-like receptor
TMZ	Temozolomide
TNF	tumor necrosis factor
TRAMP	mouse prostate adenocarcinoma model
TRIS	tris (hydroxymethyl) aminomethane

U

Ub	ubiquitin
uH2A	monoubiquitinated histone H2A
ULBP	UL16-binding proteins
UMP1	proteasome maturation protein
UPS	ubiquitin-proteasome system
UTR	untranslated region
UV	ultraviolet

W – Z

WB	western blot

Aknowlegment

It is a pleasure to thank those who made this thesis possible.

I owe my deepest gratitude to my supervisor PD Dr. Annette Paschen whose encouragement, supervision and support from the preliminary to the concluding level enabled me to develop an understanding of the subject. I am heartily thankful to her for the invaluable personal support and understanding.

I am grateful to Prof. Dr. Dirk Schadendorf for the opportunity to perform my work in his group.

I would like to thank Prof. Dr. Viktor Umansky for his support and help as well as for the fruitfull discussions about my work.

I would like to show my gratitude to Dr. Anne Régnier-Vigouroux. I am grateful for the helpful advices from her side.

My deepest gratitude goes to PD Dr. Christine S. Falk for her support and optimism, as well as for the invaluable scientific input.

It is an honour for me to thank Prof. Dr. Alexander Steinle for the insights and comments on my work. I also grateful for creative ideas he shared with me and for the materials he kindly provided.

This thesis would not have been possible without our great lab team. I want to thank all my colleagues and especially Antje Sucker and Iris Moll for their friendly support and the great friendly atmosphere in the lab and outside.

Lastly, I am heartily thankful to my parents, who supported and inspired me during this time.